NOTE TO USERS

Page(s) not included in the original manuscript are
unavailable from the author or university. The
manuscript was microfilmed as received

IX, XII, XIV-XVIII

This reproduction is the best copy available.

UMI®

ON THE ADAPTIVE CONTROLS OF NONLINEAR SYSTEMS WITH DIFFERENT HYSTERESIS MODEL REPRESENTATIONS

Jun Fu

A Thesis

in

The Department

of

Mechanical and Industrial Engineering

Presented in Partial Fulfillment of the Requirements
for the Degree of Doctor of Philosophy (Mechanical Engineering) at
Concordia University
Montreal, Quebec, Canada

August 2009

ABSTRACT

On the Adaptive Controls of Nonlinear Systems with Different Hysteresis Model Representations

Jun Fu, Ph.D.

Concordia Univeristy, 2009

The hysteresis phenomenon occurs in diverse disciplines ranging from physics to biology, from material science to mechanics, and from electronics to economics. When the hysteresis nonlinearity precedes a controlled system, the nonlinearity usually causes the overall closed-loop system to exhibit inaccuracies or oscillations, even leading to instability. Control techniques to mitigate the unwanted effects of hysteresis have been studied for decades and have recently once again attracted significant attention. In this thesis, several adaptive control strategies are developed for systems with different hysteresis model representations to guarantee the basic stability requirement of the closed-loop systems and to track a desired trajectory with a certain precision.

These proposed strategies to mitigate the effects of hysteresis are as follows:

i). With the classical Duhem model, an observer-based adaptive control scheme for a piezoelectric actuator system is proposed. Due to the unavailability of the hysteresis output, an observer-based adaptive controller incorporating a pre-inversion neural network compensator is developed for the purpose of mitigating the hysteretic effects;

ii). With the Prandtl-Ishlinskii model, an adaptive tracking control approach is developed for a class of nonlinear systems in p-normal form by using the technique of adding a power integrator to address the challenge of how to fuse this hysteresis model with the control techniques to mitigate hysteresis, without necessarily constructing a hysteresis inverse;

iii). With a newly proposed hysteresis model using play-like operators, two control strategies are proposed for a class of nonlinear systems: one with sliding mode control and the other with backstepping techniques.

ACKNOWLEDGEMENTS

I am sincerely grateful to my supervisors, **Dr. W. F. Xie** and **Dr. C. -Y. Su**, for their initiation of the research project, their guidance and efforts, as well as their support throughout this research. Their supervision and encouragement were essential to my completing this work.

I would like to thank my committee members for their time and helpful suggestions during the course of my PhD studies.

I also thank my colleagues and friends at Concordia who have offered help in various ways.

Last, but certainly not least, I would like to express special thanks to my wife, Ying Jin, and to my family for their encouragement and support. I dedicate this thesis to my daughter, Emma Fu.

TABLE OF CONTENTS

LIST OF FIGURES

x

NOMENCLATURE

SYMBOL	DESCRIPTION
$\mu(\alpha,\beta)$	Density function of α,β
P	Preisach plane
$\hat{\gamma}_{\alpha,\beta}[v](t)$	Relay hysteresis with switching threshold α,β
$C^{(n)}[R]$	The n-dimensional space of continuous functions defined on R
$C[0,t_E]$	The space of continuous functions defined on the time interval $[0,t_E]$
$C_m[0,t_E]$	The space of piecewise monotone continuous functions defined on the time interval $[0,t_E]$
r	Threshold in play and stop operators
$F_r[v]$	The play hysteresis operator
$f_r(v,w)$	$f_r(v,w) = \max(v-r,\min(v+r,w))$
$E_r[v]$	The stop hysteresis operator
$e_r(v,w)$	$e_r(v,w) = \min(r,\max(-r,v))$
$p(r)$	The density function of the Prandtl-Ishlinskii hysteresis model
p_0	The parameter $p_0 = \int_0^R p(r)dr$
$d[v](t)$	The term describing the nonlinear hysteretic behavior
$v(t)$	The system input
$w(t)$	The output of the hysteresis operator

$p_{0\min}$	The lower bound of p_0
$p_{\max}(r)$	The upper bound of $p(r)$
$\widetilde{p}(t,r)$	The estimation of $p(r)$
$\widetilde{p}(t,r)$	The error between $\hat{p}(t,r)$ and $p(r)$
k_p	Kernel function which gives output values of each KP kernel defined by a pair of parameters $p(p_1,p_2)$ in Preisach plane
$\mu(p_1,p_2)$	Density distribution of KP model
$\xi_p(t)$	Memory variable depending on the kernel k_p
$r(v(t))$	The ridge function of kernel k_p
$a_{\min}$	The lower bound of a
$a_{\max}$	The upper bound of a
χ_i	Indicator functions
$H(\cdot)$	The representation of the Duhem model
$proj(x,y)$	The projection operator
$V(t)$	The Lyapunov function
X	The plant state vector
X_d	The desired trajectory vector
$\widetilde{X}$	Tracking error vector
$s(t)$	The filtered tracking error
s_ε	A tuning error
Ω_θ	The space $\Omega_\theta=\{\theta|\ \theta_{i\min}\le\theta_i\le\theta_{i\max},i=1,...k\}$

Ω_ϕ The space $\Omega_\phi = \{\phi \mid 1/(b_{\max} p_{0\max}) \leq \phi \leq 1/(b_{\min} p_{0\min})\}$

Ω_s The space $\Omega_\varepsilon = \{\widetilde{X}(t) \mid \| \widetilde{X}_i \mid \leq 2^{i-1} \lambda^{i-n} \varepsilon, i = 1, \ldots, n\}$

Ω_d A compact set

$\mathrm{sgn}(\cdot)$ Sign function

$sat(\cdot)$ Saturation function

CHAPTER 1

INTRODUCTION

1.1 Hysteresis and Control

The hysteresis phenomenon occurs in diverse disciplines, ranging from physics to biology, from material science to mechanics, and from electronics to economics [1-5]. Some examples are hysteresis switching in synthetic gene networks [3], hysteresis curves in ferromagnetism, backlash in mechanical systems, and hysteresis effects in smart materials such as piezoelectrics and shape memory alloys [5]. Although hysteresis can be explored in positive ways in engineering applications, such as the fundamental mechanism in magnetic data storage and emerging computer memory technologies, it is typically viewed as an undesirable, detrimental effect in physical, biological and engineering systems [5]. The major drawback of hysteresis is that it usually results in inaccuracies or oscillation and even instability when it precedes the system to be controlled. Hence, it is necessary to mitigate the effect of hysteresis by using control techniques.

However, the non-smoothness of the hysteresis, resulting from the relationship between input and output, usually in the form of multi-valued loops, as shown in Figure 1.1, makes traditional control approaches insufficient. Thus, the development of some new, effective control strategies to mitigate the effect of hysteresis is required, which is a quite challenging task in the control community.
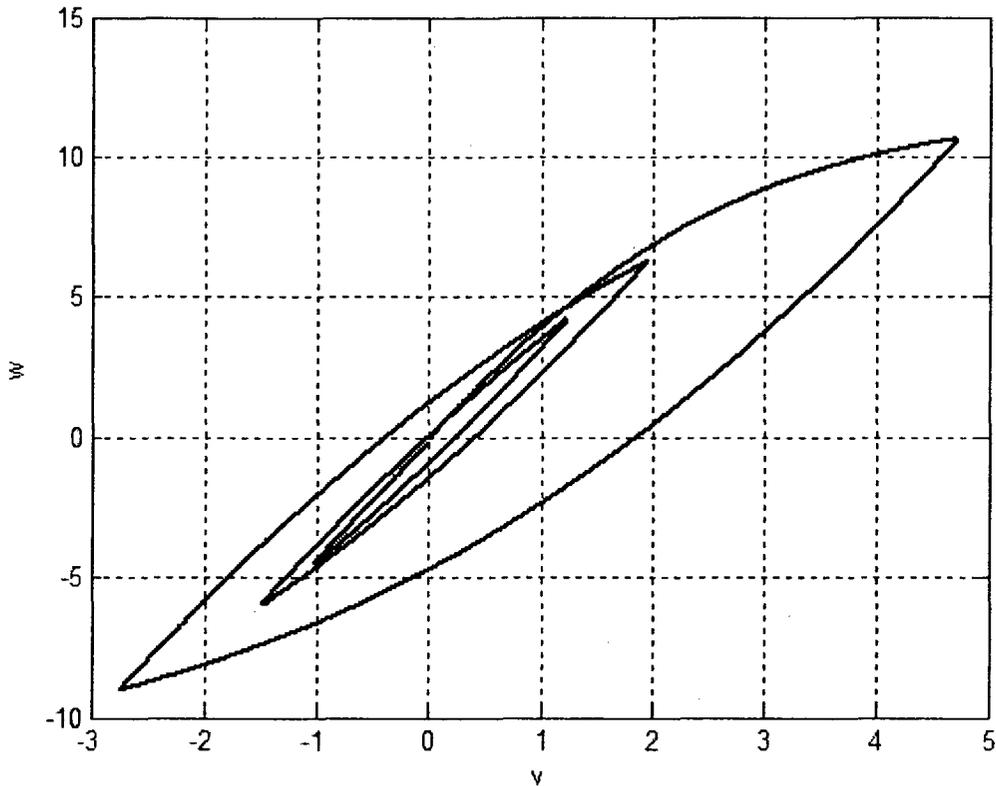
Figure 1.1 Hysteresis loops

To control hysteretic systems, it is necessary to first study the hysteresis model. Hysteresis models can be roughly classified into two categories: physics-based models such as the Jiles-Atherton model [6, 7] and phenomenology-based models such as the Preisach operator [8-10]. Physics-based models are built on the principles of physics, while phenomenology-based models are used to produce behaviours similar to those of the physical systems, without necessarily considering their physical peroperties in the problems [6]. This thesis will mainly focus on phenomenology-based hysteresis models.

With the available hysteresis models, there are some interesting and important results in the literature [5, 7 and 11]. However, to our best knowledge, how to fuse hysteresis models with available control techniques to mitigate the hysteresis effects

2

while, from the point of view of engineering applications, taking the unavailability of a hysteresis output and the stability of the overall hysteretic dynamic systems into account, is still an open problem. In this thesis, several typical hysteresis models are chosen and, at the same time, a new hysteresis model is developed to address the challenge of developing control methods to mitigate the hysteresis effects of the hysteretic systems subject to the two aforementioned practical limitations. Several adaptive control frameworks are therefore developed to meet the challenge.

1.2 Scopes and Contributions of the Thesis

1.2.1 Scopes of the Thesis

In the literature, some main challenges in the control of systems with hysteresis nonlinearities are as follows:

(1) How to fuse hysteresis models with available control techniques to mitigate the unwanted effects of hysteresis nonlinearities is largely open.

(2) As far as current hysteresis models and control methods are concerned, it is generally difficult to analyze the stability properties of the closed-loop systems due to the multi-valued and non-smoothness features of hysteresis.

(3) Apart from the available hysteresis models which can be fused with the available control methods, whether new hysteresis models can be constructed, which is specifically suitable for controller designs to mitigate the effects of hysteresis.

Hence, the scope of this thesis is to propose several adaptive control strategies to fuse control techniques with typical hysteresis models or newly constructed hysteresis

3

models, in order to address the above challenges and to achieve stability of the hysteretic system, while tracking a desired trajectory with a certain precision.

1.2.2 Contributions of the Thesis

This thesis focuses on the adaptive controls of nonlinear systems with different hysteresis model presentations. It successfully provides the solutions to the challenging problems above.

The contributions of this thesis are specifically listed as follows.

- *An observer-based adaptive control scheme for nonlinear systems with the Duhem hysteresis model representation*

  An observer-based adaptive control scheme for nonlinear systems is proposed. In the developed method, the classical Duhem model is adapted to describe the hysteresis exhibited in the piezoelectric actuators. Due to the unavailability of the hysteresis output, an observer-based adaptive controller incorporating a pre-inversion neural network compensator to mitigate the hysteretic effects is designed to guarantee the stability of the adaptive system and to track the error between the position of the piezoelectric actuator and the desired trajectory with a certain precision. Simulation studies illustrate the effectiveness of the proposed method.

- *Practical tracking control of nonlinear systems in p-normal form with Prandtl-Ishlinskii hysteresis model representation*

Focusing on a class of inherently nonlinear systems and using available mathematical models of hysteresis nonlinearities, this work addresses the challenge of how to fuse available hysteresis models with the adaptive control techniques for inherently nonlinear systems to achieve practically adaptive output tracking control. Such a possibility is shown by combining the recently developed framework of Immersion and Invariance (I&I) tools, adding a power integrator technique, and the Prandtl-Ishlinskii hysteresis model.

- *Construction a new hysteresis model with play-like operators*

    A new class of hysteresis models is constructed, where the play-like operators play the role of building blocks. From the point of view of an alternative one-parametric representation of the Preisach operator, the constructed model mathematically falls into PKP-type operators, as the Prandtl-Ishilinskii model falls into Preisach model. This provides a possibility to mitigate the effects of hysteresis without necessarily constructing an inverse, which is the unique feature of this subclass model compared to the SSSL-PKP hysteresis model of general class in the literature.

- *Sliding mode control design for nonlinear systems with play-like operators-based hysteresis model representation*

    With the constructed class of hysteresis models based on play-like operators, for the first time in this thesis, an attempt is made to fuse this model of hysteresis with the available control techniques without constructing a complicated hysteresis

inverse. A sliding mode control based scheme is therefore developed to guarantee the stability of the adaptive system and to track the desired trajectory with a desired precision.

- *Backstepping control design for nonlinear systems with play-like operators-based hysteresis model representation*

Two backstepping schemes are proposed to accomplish robust adaptive control tasks for a class of nonlinear systems with the constructed models. Such control schemes not only ensure the stabilization and tracking of the hysteretic dynamic nonlinear systems, but also derive the transient performance in terms of L_2 norm of tracking error as an explicit function of design parameters.

1.3 Organization of the Thesis

This dissertation is organized into seven chapters together.

In Chapter 2, a detailed literature review is conducted for hysteresis models and control methods, followed by how the present research advances the knowledge in the literature;

In Chapter 3, with the classical Duhem model, an observer-based adaptive scheme for nonlinear systems incorporating of a pre-inversion neural network compensator for the purpose of mitigating the hysteretic effects is presented;

With the Prandtl-Ishlinskii hysteresis model, Chapter 4 addresses the challenge of how to fuse this hysteresis model with those results for the inherently nonlinear systems

in the literature to achieve practically adaptive output tracking control without necessarily constructing an inverse operator of hysteresis model;

Chapter 5 deals with the adaptive control of nonlinear systems with a newly constructed hysteresis model with play-like operators. A sliding mode based control scheme is developed to deal with the hysteresis effects, stability and tracking issues;

Following the Chapter 5, in Chapter 6, two backstepping schemes are proposed to accomplish adaptive control tasks for the same class of nonlinear systems, with a newly constructed hysteresis model with play-like operators;

Chapter 7 presents the major conclusions of this dissertation and recommendations for future work.

CHAPTER 2

LITERATURE REVIEW

2.1 Hysteresis

When speaking of hysteresis, one usually refers to the input-output relationship between two time-dependent quantities which cannot be expressed as a single-value function. Instead, the relationship usually is in the form of loops which are traversed along a certain orientation [10]. As Mayergoyz [9] pointed out, this may be misleading and may create an impression that looping is the essence of hysteresis. Hence, it is necessary to introduce the definition of hysteresis. Although the specific meanings of hysteresis vary from one discipline to another, and there is no agreement in the literature regarding the definition of hysteresis, the mathematical definition in the monographs [10, 13] is adopted for the purpose of this research.

Definition of Hysteresis

Mathematically, a hysteresis relationship between two functions u and v that are defined on some time interval $[0,t]$, attaining their values in some sets U and V, respectively, can be expressed as an operator equation $v = F[u]$, where F is an operator characterized by memory effect and rate-independence.

Suppose a system is described by the input-output pair u and v. Memory effect means that, at any instant t, the value of the output v is not simply determined by the value u of the input at the same instant, but it also depends on the previous evolution of

the input u. The rate independence means that the path (u, v) is invariant with respect to any increasing time homeomorphism [79].

From a nonlinearity point of view, hysteresis can also be viewed as a multi-branch nonlinearity. To be clear on this point, an alternative definition of hysteresis in [9] is presented below.

Consider a transducer which is characterized by an input $u(t)$ and an output $v(t)$, as in Figure 2.1. This transducer is said to be hysteretic if its input-output relationship is a multi-branch nonlinearity for which branch-branch transitions occur at input extremes [9]. Figure 2.2 shows a typical multi-branch nonlinearity.
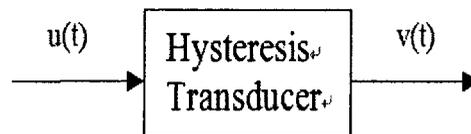
Figure 2.1 Hysteresis transducer
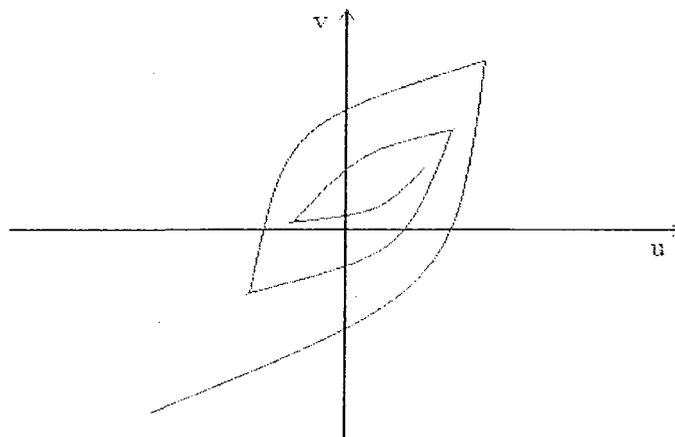
Figure 2.2 Multi-branch nonlinearity

As stated in [9] by Mayergoyz, the above definition emphasizes the fact that branching constitutes the essence of hysteresis, although in the existing literature, the hysteresis phenomenon is by and large linked with the formation of hysteresis loops (looping) which may mislead to the impression that looping is the essence of hysteresis. In fact, looping is a particular case of branching. Looping occurs when one applies an input that varies back and forth between two consecutive extremum values, while branching takes place for arbitrary input variations.

Besides the branching of hysteresis, other characteristics of hysteresis such as rate-independence, memory, and major and minor loops can also be briefly described as follows with respect to the multi-branch nonlinearity accordingly. The more precise descriptions can be found in [9, 10].

Hysteresis is rate-independent if the branches of the hysteresis, as defined above, are determined only by the past extremum values of input, while the rate of change of input variation between extreme points has no influence on branching.

Memory implies that at any instant of time τ, output $v(\tau)$ depends not only on input $u(\tau)$ but also on the previous evolution of input u. Hysteresis can be interpreted as a nonlinearity with a memory which reveals itself through branching [9].

The major loop encloses the hysteresis region and minor loops exist inside the region, as shown in Figure 2.3. Not every hysteresis model can produce minor loop(s), like Relay.
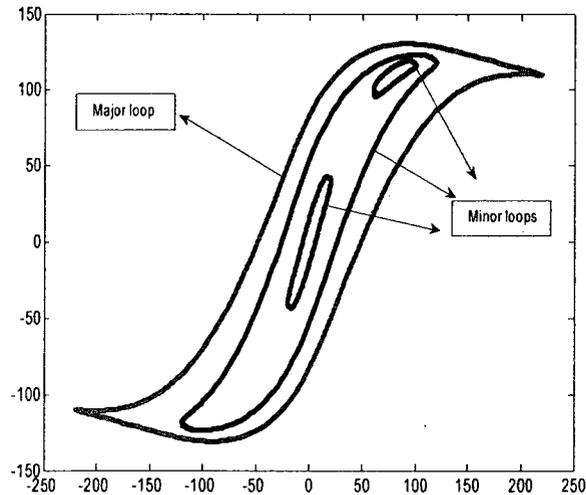
Figure 2.3 Illustration of a major hysteresis loop containing several minor loops

After this brief introduction of the general hysteresis concept, it is necessary to review several classes of hysteresis models important for this study.

2.2 Hysteresis Models

Hysteresis models will be reviewed from two classes of mathematical descriptions: differential-equation-based hysteresis models and operator-based hysteresis models.

2.2.1 Differential-equation-based Hysteresis Models

Three main differential-equation-based hysteresis models are reviewed: the Duhem model, the Bouc-Wen model and the Chua-Stromsmoe (C-S) model.

<u>Duhem Model</u>

The Duhem model focuses on the fact that the output can only change its characteristics when the input changes direction. The input-output relationship is expressed by the following differential equation [14]:

$$\dot{v}(t) = f_1(v(t),u(t))\dot{u}(t)^+ - f_2(v(t),u(t))\dot{u}(t)^-,$$
$$v(0) = v_0,$$

(2.1)

where $\dot{u}^\pm = \dfrac{|\dot{u}| \pm \dot{u}}{2}$, $f_1, f_2 \in C^0(R^2)$ and the input $u(t)$ and the output $v(t)$ are continuous and differentiable functions on $[0,T]$. An increase in input $u(t)$ causes the output $v(t)$ to increase along a particular path. Under a decreasing input, the output tends to decrease along a different path. The output is governed in terms of slope functions f_1, f_2 by

$$\frac{dv}{du} = \begin{cases} f_1(u(t),v(t)) & if \quad \dot{u} > 0, \\ f_2(u(t),v(t)) & if \quad \dot{u} < 0. \end{cases}$$

(2.2)

Hodgdon and Coleman [14, 15] have extensively studied this model by setting the input magnetic field (H) and the level of magnetization of the medium (B) to characterize magnetic hysteresis. This model is presented analytically by the following differential equation:

$$\frac{dB}{dt} = \alpha \left| \frac{dH}{dt} \right| [f(H) - B] + \frac{dH}{dt} g(H)$$

(2.3)

where $\alpha > 0$ is a constant, $f(H)$ and $g(H)$ are prescribed real-valued functions on $(-\infty, +\infty)$. They proved that the solutions of (2.3) move on the curves defined by

12

$$\frac{dB}{dH} = \alpha \cdot \text{sgn}(\dot{H})[f(H) - B] + g(H),$$

and this can be solved explicitly for H piecewise monotone:

$$B = f(H) + [B_0 - f(H_0)]e^{-\alpha(H-H_0)\text{sgn}\,\dot{H}} + e^{-\alpha H\,\text{sgn}\,\dot{H}} \int_{H_0}^{H} [g(\xi) - f'(\xi)]e^{\alpha\xi\,\text{sgn}\,\dot{H}} d\xi,$$

for $\dot{H}$ constant, $B(H_0) = B_0$, sgn is sign function and provided that:

(1) f is piecewise smooth, monotone increasing, odd, with $\lim_{H\to\infty} f'(H)$ finite;

(2) g is piecewise continuous, even, with $\lim_{H\to\infty}[f'(H) - g(H)] = 0$;

(3) $f'(H) > g(H) > \alpha e^{\alpha H} \int_{H}^{\infty} [f'(\xi) - g(\xi)]e^{-\alpha\xi} d\xi$ for all $H > 0$.

It has been shown that the Duhem model can describe a large class of rate-independent hysteresis in various smart materials, such as ferromagnetically soft material, or a piezoelectric actuator [14-16], as shown in Figure 2.4 where τ and v is the output and input of the Duhem model, respectively.
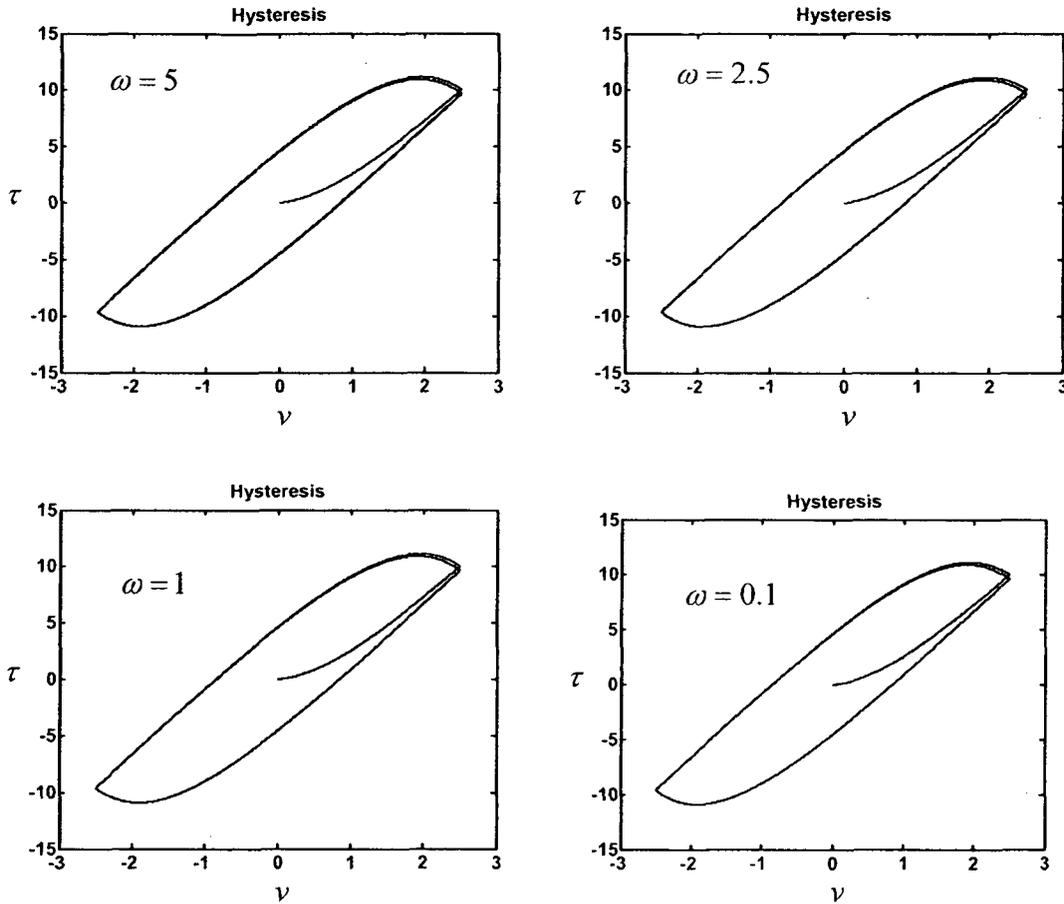
Figure 2.4 The loops of a ferromagnetically soft material of isoperm type described by

the Duhem model

It is worth noting that Su et al. [17] proposed a backlash-like model based on Duhem model and [18] refers to the backlash-like model as the SSSL model, then extends the SSSL model to the n-th order case, called a play-like operator.

Bouc-Wen model

The Bouc-Wen model of hysteresis [19] is mathematically simple and is able to represent a large class of hysteretic behaviour [20, 21]. This model can be applied to

14

describe the hysteresis in a single degree of freedom oscillator [20] and a magnetorheological damper attached to a scaled, three-degree-of-freedom building [21]. Suppose x is the position of an oscillator system given by

$$\ddot{x} = f(x, \dot{x}, z, u),$$ (2.4)

where z is the hysteretic variable proportional to the restoring force acting on the oscillator, described by the first order differential equation

$$\dot{z} = A\dot{x} - \beta\dot{x}|z|^n - \gamma|\dot{x}||z|^{n-1}z,$$ (2.5)

where the parameters $n, A, \beta,$ and γ are the shape parameters of the hysteresis curves, which can also be functions of time. Please note that, in this model, $\dot{x}$ acts as an input, and the equation is not involved in x although the hysteresis phenomenon is observed between x and z. When $n = 1$, (2.5) becomes a linear ordinary differential equation which can be solved according to the signs of $\dot{x}$ and z. The hysteresis loop will converge to a bilinear curve governed by $\dot{z} = \dot{x}[\text{sgn}(z + A) - \text{sgn}(z - A)]/2$ as n goes to ∞.

Chua-Stromsmoe Model

[22] first proposed the Chua-Stromsmoe (C-S) model to represent nonlinear inductors. But being a phenomenological model, it can be applied to a wide variety of physical systems. The C-S model can be defined by the differential equation

$$\frac{dv}{dt} = k(v)g \circ [u(t) - f(v)], \quad \forall t \in (0, T),$$
$$v(0) = v_0,$$ (2.6)

15

where $f,g,k \in C^1(R)$, $f' > 0, g' > 0$, on R, $f,g : R \rightarrow R$ onto, and there exist α, β such that $0 < \alpha \le k \le \beta < \infty$ on R. $u,v \in C^1(0,T)$ and a bound on input guarantees the existence and uniqueness of a solution [22].

The function g is referred to as the dissipation function, and the function f as the restoring function, while k is called the weighting function. Physically, the function g is responsible for energy dissipation, f for energy storage. A simple geometrical algorithm to construct suitable f,g,h functions can be found in [22].

Chua and Bass [23] modified (2.6) as follows by introducing a frequency function $w(\dot{u})$, such that the generalized model not only provides for hysteresis loops at frequencies down to the direct current, but also allows for extensive control over higher frequency behaviour.

$$\frac{dv}{dt} = w(\dot{u})k(v)g \circ [u(t) - f(v)], \quad \forall t \in (0,T),$$
$$v(0) = v_0,$$
(2.7)

It is easy to see that for $w(\dot{u}) = |\dot{u}|$, (2.7) becomes rate-independent and a special case of the Duhem model.

To save space, other hysteresis models based on differential equations are omitted here, such as the Jiles-Atherton model and the Maxwell model. One may refer to [24, 25] and references therein for the details.

2.2.2 Operator-based Hysteresis Models

16

The operator-based hysteresis models mainly include the Preisach, Prandtl-Ishilinskii and Krasnosel'skii-Pokrovskii models [8-10, 26-29].

Preisach model

The most popular hysteresis model is certainly the Preisach model. It was first proposed by Weiss and De Freundenreichin in 1916 [26]. In 1935, Preisach suggested a geometrical interpretation, which is now one of the main features of the model [27]. The Preisach model [9] has been most widely applied to characterize the hysteresis properties of electromagnetic materials, smart actuators. However, the success of this model has to be ascribed to Krasnosel'skii and other Russian mathematicians [8] having elucidated the phenomenological characteristics of the Preisach model. They proved that the model can be considered as a superposition of elementary hysteretic relay operators

$$W(t) = \iint_P \mu(\alpha,\beta)\hat{\gamma}_{\alpha,\beta}[v](t)d\alpha d\beta, \tag{2.8}$$

where $\mu(\alpha,\beta)$ is the Preisach function, P is the Preisach plane, often referred to as the density function of α and β and identified from measured data, and $\hat{\gamma}_{\alpha,\beta}[v](t)$ is a relay hysteresis shown in Figure 2.5 and defined by

$$\hat{\gamma}_{\alpha,\beta}[v](t) = \begin{cases} +1 & if\ v(t) > \alpha \\ -1 & if\ v(t) < \beta \\ remains\ unchanged & if \alpha < v(t) < \beta \end{cases}$$
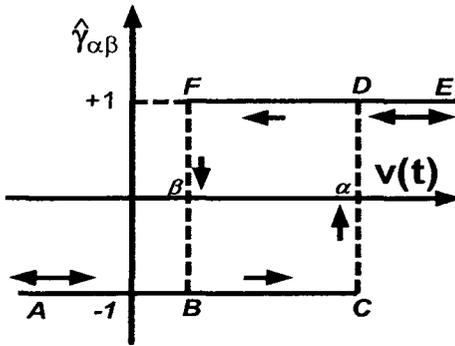
Figure 2.5 Relay hysteresis operators

The parameters α and β correspond to "on" and "off" switches, respectively, for the thresholds of input applied on the relay. It is assumed that each relay has only two saturated output values: $\hat{\gamma}_{\alpha\beta}[v(t)] = +1$ and $\hat{\gamma}_{\alpha\beta}[v(t)] = -1$. Suppose the output of the relay remains in its negative saturation state ($\hat{\gamma}_{\alpha\beta}[v(t)] = -1$). If the input $v(t)$ of the relay is continuously increased from $v_0 < \beta$, the output of the relay switches to its positive saturation state ($\hat{\gamma}_{\alpha\beta}[v(t)] = +1$) when $v(t) = \alpha$, and remains in this state while $v(t) > \alpha$.

Thus, the monotonic increases of $v(t)$ form the ascending branch *ABCDE* of the relay (see Fig.2.5). Similarly, while the input monotonically decreases, the descending branch *EDFBA* is traced. Hence, (2.8) can be interpreted as a parallel connection of infinite weighted relays with positive/negative saturation values $+1/-1$ (see Fig.2.6).
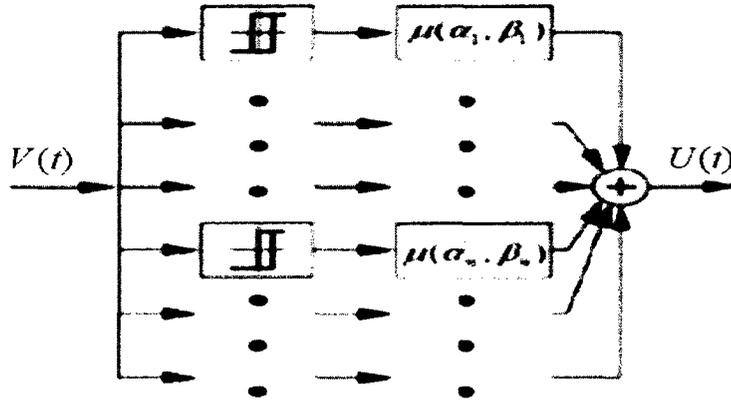
Figure 2.6 Structural interpretation of the Preisach model [9]

An extensive investigation of this model can be found in the monograph [9], where a detailed geometric interpretation based on the Preisach plane was given. Many experimental setups have shown that this model can be used to describe the hysteresis behaviour in smart material-based actuators and sensors, like magnetostrictive [6], piezoceramic in a stacked form [28], and SMA actuators [10].

Prandtl-Ishlinskii (PI) model

The Prandtl-Ishlinskii model relies on the building blocks: play and stop operators. Let's introduce these operators before reviewing the Prandtl-Ishlinskii model. One can find a detailed discussion in [10].

Stop Operator

The stop operator, shown in Fig 2.7, has been proposed to characterize elastic-plastic behaviour in continuum mechanics. The figure illustrates the linear stress-strain (w-v) relationship as Hook's law, when the stress is below the yield stress (threshold) r.
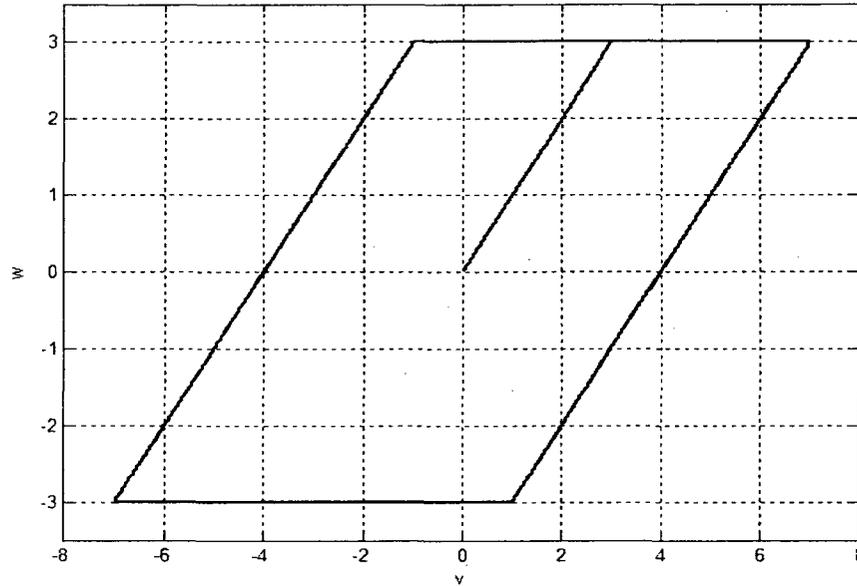
Figure 2.7 Stop operator (where the threshold $r = 3$)

Analytically, let $C_m[0, t_E]$ represent the space of piecewise monotone continuous functions. For any input $v(t) \in C_m[0, t_E]$, the stop operator $w = E_r[v](t)$ is defined by:

$$E_r[v](0) = e_r(v(0))$$

$$E_r[v](t) = e_r(v(t) - v(t_i) + E_r[v](t_i)),$$

$$\text{for } t_i < t < t_{i+1} \text{ and } 0 \le i \le N - 1 \tag{2.9}$$

where $e_r(v) = \min(r, \max(-r, v))$.

Play Operator

Figure 2.8 illustrates the play operator. The one dimensional play operator has been described by the motion of a piston within a cylinder of length $2r$. The position of the center of the piston is represented by coordinate v, while the cylinder position is given by w[10].

For any input $v(t) \in C_m[0,t_E]$, the play operator $w = F_r[v](t)$ is defined by:

$$F_r[v](0) = f_r(v(0),0) = w(0) \text{ ,}$$

$$F_r[v](t) = f_r(v(t),F_r[v](t_i)) ; t_i < t < t_{i+1} \text{ and } 0 \le i \le N-1 \qquad (2.10)$$

where $f_r(v,w) = \max(v-r,\min(v+r,w))$,
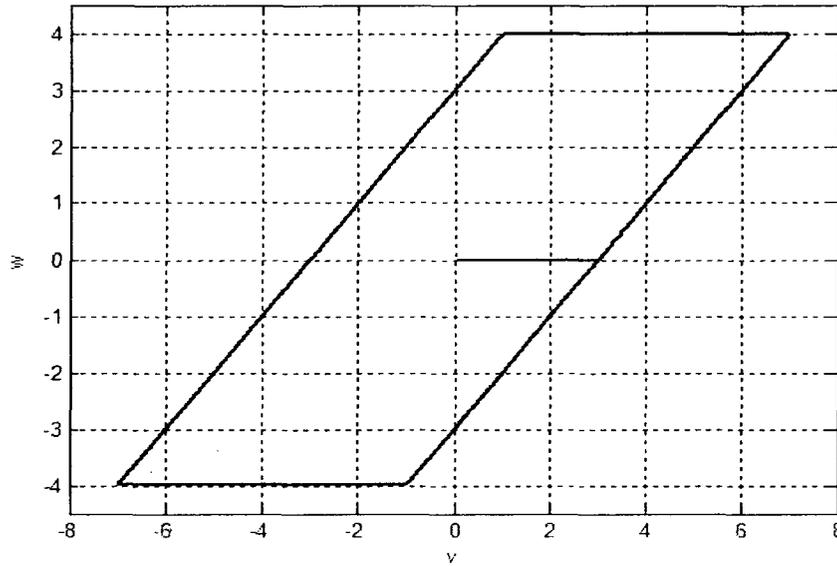
Figure 2.8 Play hysteresis operator (where the threshold $r = 3$)

where $0 = t_0 < t_1 < \ldots < t_N = t_E$ is a partition of $[0,t_E]$ such that the function v is monotone on each of the sub-intervals $[t_i,t_{i+1}]$. The argument of the operator is written in square brackets to indicate the functional dependence, as it maps a function onto another function.

The play and stop operators are characterized by input v and the threshold r. The maximum value of the stop operator is determined by threshold r in the (v, w) plane. From definitions (2.9) and (2.10), it can be proven that operator $F_r[v]$ is the complement

21

of operator $E_r[v]$ [10], and that they are related in the following manner for any piecewise monotone input function $v(t) \in C_m[0, t_E]$ and threshold $r \geq 0$:

$$F_r[v](t) + E_r[v](t) = v(t) \,. \tag{2.11}$$

Using the stop operator $E_r[v](t)$, the Prandtl-Ishlinskii model is defined by [10]:

$$y_s = \int_0^R p(r) E_r[v](t) dr \,, \tag{2.12}$$

where $p(r)$ is a density function, satisfying $p(r) \geq 0$, and is expected to be identified from experimental data.

The Prandtl-Ishlinskii model is also defined using the play operator $F_r[v](t)$ by:

$$y_P = qv(t) + \int_0^R p(r) F_r[v](t) dr \,, \tag{2.13}$$

as shown in Figure 2.9. The Prandtl-Ishlinskii model with the density function maps $C[t_o, \infty)$ onto $C[t_o, \infty)$. In other words, Lipschitz continuous inputs will yield Lipschitz continuous outputs [8]. Since the density function $p(r)$ vanishes for large values of r, the choice of $R = \infty$ as the upper limit of integration is widely used in the literature just for convenience [10]. In the above model, q is a positive constant. As a special case, this constant can be expressed by:

$$q = \int_0^R p(r) dr \tag{2.14}$$

Since the play and stop hysteresis operators and the density function defined above are rate independent, the Prandtl-Ishlinskii model is applicable for characterizing only rate independent hysteresis.
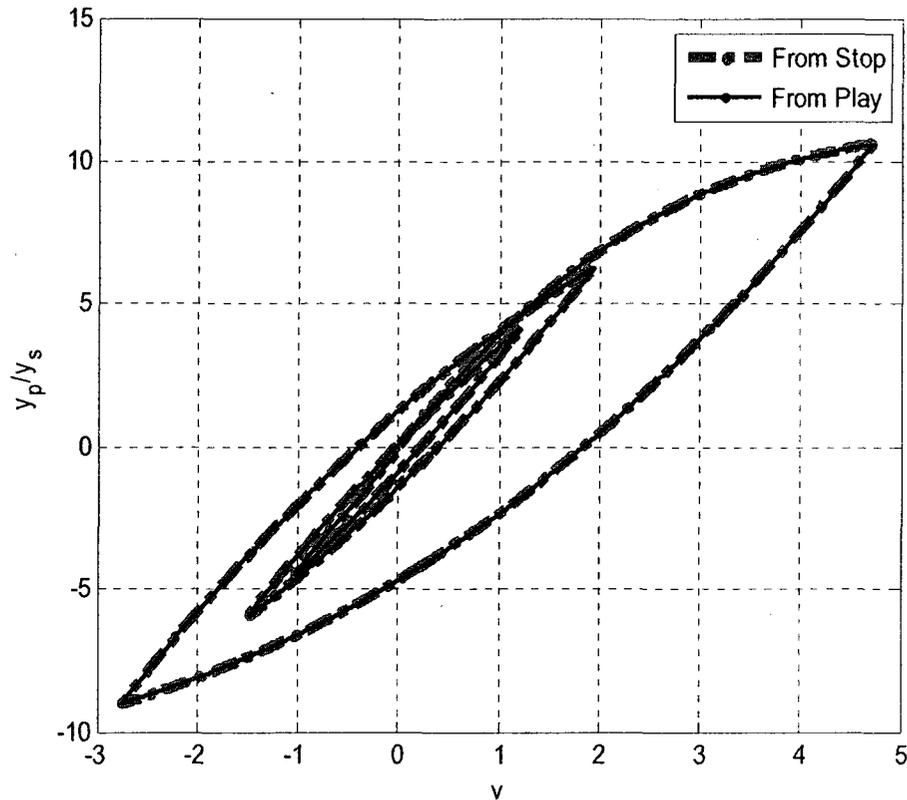
Figure 2.9 Hysteresis loops

Krasnosel'skii-Pokrovskii (KP) model

In the 1970's, M. Krasnosel'skii and A. Pokrovskii [8] systematically investigated the hysteresis phenomenon from a purely mathematical point of view. They presented a hysteresis operator called the KP model in reference [8]. The KP model has the same

integral form of weighted elementary operators as the Preisach model. But, unlike the Preisach relay which is a discontinuous function on the Preisach Plane and has only two saturation output states (+1,-1), the KP kernel, the element of the KP model, is a continuous function on the Preisach plane, and has minor loops within its major loop.
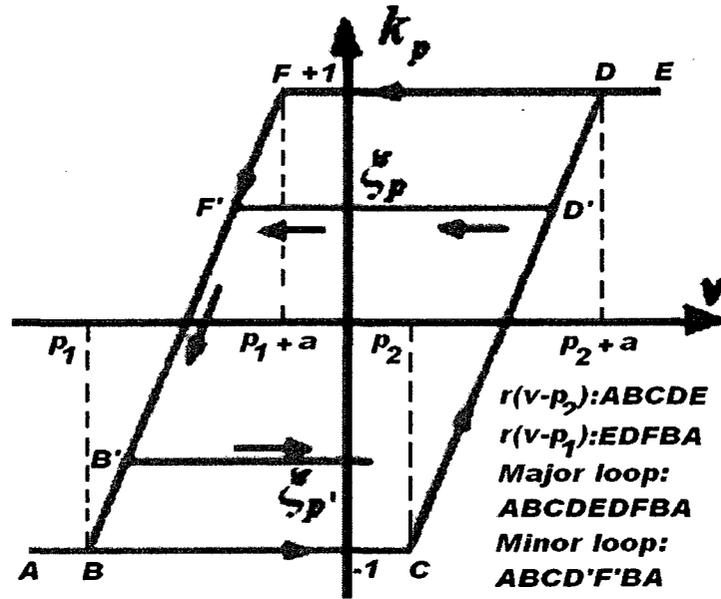
Figure 2.10 KP kernel [29]

As presented in reference [29], the Krasnosel'skii – Pokrovkii (KP) hysteresis model can be expressed as an integral of kernels (see Fig.2.10) over a specific domain by

$$u(t) = H[v](t) = \int_P k_p[v, \xi_p](t)\mu(p)dp, \qquad (2.15)$$

where $v(t)$ is the input of the hysteresis, $u(t)$ is the output; $H(\cdot)$ is an operator to transform the input $v(t)$ into the output $u(t)$; P is the Preisach Plane (see Fig.2.11) over which hysteresis occurs. P is defined by

$$P = \{p(p_1, p_2) \in R^2 : v^+ - a \geq p_2 \geq p_1 \geq -v^-\}, \tag{2.16}$$

where v^- and v^+ represent input values of negative and positive saturation states of hysteresis, respectively. a is the rise-constant of the kernel k_p, which will be explained later. The range of $v(t) \in [v^-, v^+]$ represents the hysteresis input domain. If the input exceeds the range, the output of hysteresis remains at its saturation states. k_p is the kernel function that gives the output values of each KP kernel defined by a pair of parameters $p(p_1, p_2) \in P$ (see Fig.2.11), as it is subjected to the input $v(t)$; $\xi_p(t)$ is a variable to memorize the previous extreme output of the kernel parameterized by p; $\mu(p)$ is the density of the kernel k_p, which is utilized to weight the output of the kernel k_p.

Each point $p(p_1, p_2)$ in the Preisach plane P is associated with a kernel k_p and has its specific density value $\mu(p_1, p_2)$. The function to describe the densities $\mu(p_1, p_2)$ of all points in the Preisach plane P is called the density function or density distribution of the KP model. Please note that the density function of the KP model is different from the density of the Preisach hysteresis model for modeling a particular hysteresis.
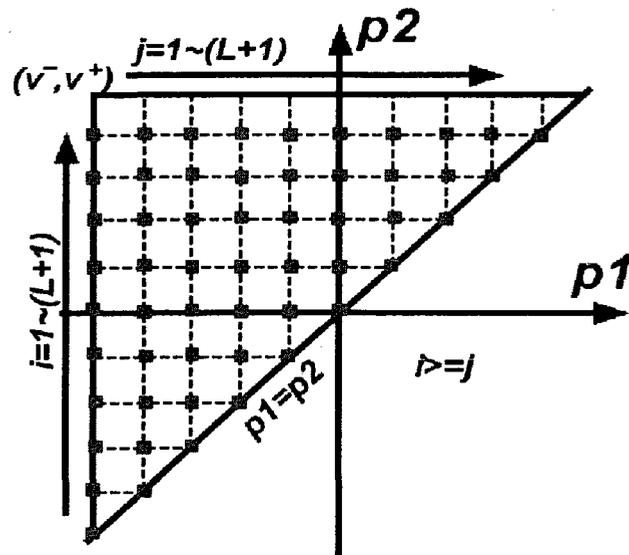
Figure 2.11 The Preisach plane P [29]

The integral KP model given by equation (2.15) can be interpreted as a parallel connection of an infinite number of weighted kernels (see Fig.2.12).
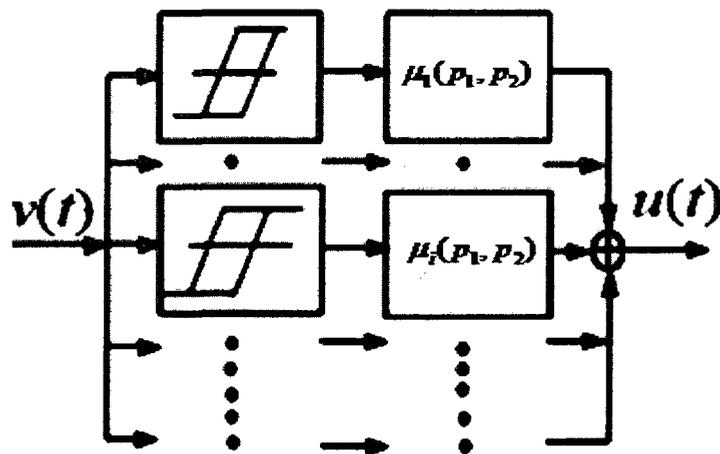
Figure 2.12 Parallel connections of weighted kernels [29]

The kernel function $k_p[v,\xi_p](t)$(see Fig.2.10) with parameters (p_1,p_2,a) is expressed by

$$k_p[v,\xi_p](t) = \begin{cases} \max \ \{\xi_p(t), r(v(t)-p_2)\} & for \quad \dot{v} \geq 0 \\ \\ \min \ \{\xi_p(t), r(v(t)-p_1)\} & for \quad \dot{v} \leq 0 \end{cases} \tag{2.17}$$

where the value of the memory variable $\xi_p(t)$ depends on the kernel k_p and is updated whenever the rate of $v(t)$ changes sign. For example, if the input $v(t)$ starts from a value less than v^-, i.e. $v(t_0) < v^-$, both initial values of $\xi_p(t_0)$ and output $k_p[v(t_0),\xi_p(t_0)]$ will equal -1. As the input $v(t)$ monotonically increases from $v(t_0)$ to a value $v(t_1)$ and then tends to decrease at time t_1, $\dot{v}(t)$ switches sign at the time t_1, i.e. $sign(\dot{v}(t_1^+)) = -sign(\dot{v}(t_1^-))$. Each $\xi_p(t_1)$ updates to $k_p[v(t_1),\xi_p(t_0)]$ and retains this value until the input $v(t)$ increases again at a time t_2, i.e., $sign \ (\dot{v}(t_2^+)) = -sign \ (\dot{v}(t_2^-)) = -sign \ (\dot{v}(t_1^+))$. Thus, the memory variable $\xi_p(t)$ is expressed as

$$\xi_p(t) = \begin{cases} -1 & if \quad t = t_0 \\ \\ k_p[v(t),\xi_p(t_{i-1})] & if \quad t = t_i > t_{i-1} \ and \ sign \ (\dot{v}(t^+)) = -sign \ (\dot{v}(t^-)) \\ \\ \xi_p(t_{i-1}) & if \quad t_i \geq t > t_{i-1} \ and \ sign \ (\dot{v}(t^+)) = sign \ (\dot{v}(t^-)) \end{cases} \tag{2.18}$$

for $i = 1,2,....$ representing the i th turning point. In equation (2.17), the boundary functions $r(v(t)-p_1)$ and $r(v(t)-p_2)$ form the major loop $(ABCDEDFBA)$ of the kernel k_p between -1 and +1(see Fig.2.10). Any other loops which are located inside the major loop and are not enveloped by the boundaries $r(v(t)-p_1)$ and $r(v(t)-p_2)$ are called minor loops of the kernel k_p, for example, $(ABCD'F'BA)$. It can be seen that the width of the

kernel is determined by the switching input values, p_1 and p_2, while the transfer slope

between -1 and $+1$ is determined by the rise-constant a. The ridge function $r(v(t))$ is

defined as follows:

$$r[v](t) = \begin{cases} -1 & v(t) < 0, \\ -1 + 2v(t)/a & 0 \leq v(t) \leq a, \\ +1 & v(t) > a, \end{cases}$$

and it is shown by the Fig. 2.13:
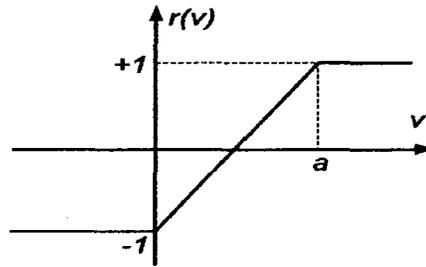
Figure 2.13 Ridge function of KP kernel k_p [29]

Banks et al. [30] used this model to characterize hysteresis in the SMA actuator, while

Galinaities [31] investigated Krasnosel'skii-Pokrovskii model focusing on the properties

of inverse and approximation.

2.3 Control Methods

After the review of hysteresis models, the control techniques for a plant preceded by

a hysteresis actuator are reviewed below. In the literature, different control schemes for

systems with hysteresis have been developed. The most common approach to mitigate the

effects of hysteresis is inversion compensation, which was pioneered by Tao and

Kokotovic [32]. For hysteresis with major and minor loops, they used a simplified linear parameterized model to develop an adaptive hysteresis inverse model with parameters updated online by adaptive laws. Model-based compensation of hysteresis has been addressed in [5, 11], and the references therein. The main issue is how to find the inverse of the hysteresis models.

The compensation of hysteresis effects in smart material actuation systems using Preisach model-based control architectures has been studied by many researchers [5, 11, 31-37]. Ge and Jouaneh [33] proposed a static approach to reduce the hysteresis effects in the problem of tracking control for a piezoceramic actuator and a desired sinusoidal trajectory. The relationship between the input and the output of the actuator was first initialized by a linear approximation model of a specific hysteresis. The Preisach model of the hysteresis was then used to reduce the corresponding input signals for the desired output of the actuator displacements. A PID feedback controller was used to adjust tracking errors. The developments worked for both specific trajectories and required resetting for different inputs. Galinaitis [31] analytically investigated the inverse properties of the general Preisach model and proved that a general Preisach operator can only be locally invertible. He gave a closed form inverse formula when the weight function of the Preisach model took a very particular form. Mittal and Meng [34] developed a method of hysteresis compensation in an electromagnetic actuator through the inversion of numerically expressed Preisach models in terms of the first-order reversal curves and the input history. Instead of modeling the forward hysteresis in piezoceramic actuators and then finding the inverse, Croft et al. and Bernard et al. [35] directly formulated the inverse hysteresis effects using the Preisach model. Tan and

Iyer's work proposed an approximate inverse for the Preisach operators, but in a numerical way or by assuming that the density function has a specific feature, like with a piecewise constant density, as shown in [5]. The latest paper [11] proposed a new Preisach modelling approach for feed-forward compensation of complex hysteresis and creep effects in a threshold-discrete way. Methods based on the inverse of the KP model can be found in [31, 36]. Galinaitis mathematically investigated the properties and the discrete approximation method of the KP operators [31]. Webb defined a parameterized discrete inverse KP model, combined with adaptive laws to adjust the parameters online to compensate hysteresis effects [36]. Recently, a feed-forward control design based on the inverse of the Prandtl-Ishlinskii model was also applied to reduce hysteresis effects in piezoelectric actuators [37].

In addition to the above mentioned model-based inverse methods, neural networks and fuzzy systems were also developed to deal with hysteresis control. It is well known that the universal approximation property is one of the most important properties of neural networks and fuzzy systems. However, this property is generally proven for continuous and one-to-one functions. Wei and Sun [38] studied the rate-independent memory property. After analyzing multi-layer feed-forward, recurrent and reinforcement learning networks, they found that networks with only computational nodes and links cannot function as hysteresis simulators. They proposed a propulsive neural unit to construct hysteretic memory. Several propulsive neural units with distinct sensible ranges were used to form a model. These can be trained to follow the loops given by the Preisach model. Selmic [39] gave a neural network structure to approximate piecewise continuous functions appearing in friction, or functions with jumps. Hwang [40, 41]

developed a neuro-adaptive control method for unknown piezoelectric actuator systems. The proposed neural network (NN) included two different nonlinear gains according to the change rate of the input signal and a linear dynamic system to learn the dynamics of the piezoelectric actuators. A feed-forward control based on the inverse of the learned model was used to achieve an acceptable trajectory tracking. Because the tracking performance by the controls in [40, 41] could not be guaranteed as the system was subject to uncertainties, a discrete-time variable-structure control was synthesized to improve performances [42, 43].

Essentially, inversion methods usually treat hysteresis and the structure response function separately, that is, they use the inverse model in the feed-forward loop to cancel hysteresis behaviour, and then they design a feedback controller to compensate the structural dynamic effects. However, it is difficult to decouple the effects from the hysteresis and those from the structural dynamics in experimental measurements. It would be better to develop an approach that can consider both effects simultaneously [44]. Due to the multi-valued and non-smoothness feature of hysteresis, it is usually difficult to analyze the stability of the hysteretic systems, except for certain special cases [32].

Passivity-based stability and control of hysteresis in smart actuators were attempted by Pare [45], who considered hysteresis as uncertainties, as well as by Gorbet [46]. In [46], the energy properties of the Preisach hysteresis model were investigated, and the passivity was demonstrated for the relationship between the input and the derivative of the output. But in smart actuator applications like motion control in nanopositioning, the output of the hysteretic system is more concerned. Also, there are some results based on the Bouc-Wen models for control purposes, mainly by F. Ikhouane and his colleagues,

31

and published in the book [47], where the hysteresis nonlinearities are connected to plants in a parallel manner.

From the above analysis, it is, to our best knowledge, still unclear how to fuse these models with available control techniques to mitigate the hysteresis effects, while, from the point of view of engineering applications, taking the unavailability of hysteresis output and the stability of the overall hysteretic dynamics systems into account. In this research interest, there are some pioneer results by Su [17, 48, and 49]. The research in this thesis further addresses the challenges in this direction by presenting several original contributions.

2.4 Summary

This chapter presents the literature review on hysteresis models and the control methods to mitigate the effects of the hysteresis. This thesis addresses the challenges seen above from the research area of control systems with hysteresis.

CHAPTER 3

ADAPTIVE CONTROL OF NONLINEAR SYSTEMS WITH DUHEM HYSTERESIS MODEL REPRESENTATIONS

3.1 Introduction

A typical differential equation based hysteresis model is the Duhem model [8, 14-16, 19, 24, 47, 50-52] since it can describe a large class of hysteresis in various smart materials, such as ferromagnetically soft materials or piezoelectric actuators. Many variations of the Duhem model have been studied in different contexts. For instance, the Bouc-Wen model [16, 24, and 50], the Madelung model [19], the Dahl friction model [47], the LuGre friction model [8], and the presliding friction model [50] are special cases of Duhem models. This chapter will deal with the adaptive control of systems with Duhem hysteresis model representation.

To mitigate the hysteresis nonlinearity, a neural network (NN) based inversion compensation is proposed because of its ability to approximate the universal function of nonlinearities [53, 54]. However, only a few results using NN to tackle hysteresis in the literature are available [55-57]. In [55, 56], a NN model is used to describe the hysteresis behaviour at different frequencies with the knowledge of some properties of magnetic materials, such as the loss separation property, to allow the separate treatment of quasi-static and dynamic hysteresis effects. In [57], a modified Luenberger observer and an NN are used to identify a general model of hysteresis. To our best knowledge, NN has not

been explored to construct an inverse of any hysteresis models, which is one of our motivations for this chapter.

On the other hand, measuring the output of hysteresis is not practical in applications, which discourages applying the available adaptive control technique to the control of systems with hysteresis nonlinearities. Taking the unavailability of the output of hysteresis into account, an observer has to be developed to estimate the output for the application of the adaptive control.

Stemming from our motivations, an observer-based adaptive control scheme for systems with Duhem hysteresis model representation is proposed. In the developed method the classical Duhem model is adapted to describe the hysteresis nonlinearity. With the incorporation of a pre-inversion neural network compensator for the purpose of mitigating the hysteretic effects, an observer-based adaptive controller is designed to guarantee the stability of the adaptive system and tracking error between the position of the piezoelectric actuator and the desired trajectory with a desired precision. Simulation studies illustrate the effectiveness of the proposed method.

3.2 An Explicit Solution of the Duhem Model and Preliminaries

3.2.1 Duhem Model of Hysteresis

Many different mathematical models are built to describe hysteresis behavior, such as the Preisach, Prandtl-Ishlinkiil and Duhem models [24, 16, 30, and 31]. Considering its capability of providing a finite-dimensional differential model of hysteresis, the classical Duhem model is adapted here to develop the adaptive controller for the piezoelectric actuator.

The Duhem model is a rate independent operator, with input signal $v, \dot{v}$ and output signal τ. The Duhem model describes hysteresis $H(t)$ by the following mathematical model [14, 15]:

$$\frac{d\tau}{dt} = \alpha \cdot \left| \frac{dv}{dt} \right| \cdot [f(v) - \tau] + \frac{dv}{dt} \cdot g(v) \tag{3.1}$$

where α is a positive number, $f(v)$ and $g(v)$ are prescribed real-valued functions on $(-\infty, +\infty)$.

It can also be represented as [14, 15]:

$$\frac{d\tau}{dv} = \begin{cases} \alpha \cdot [f(v) - \tau] + g(v), & \dot{v} > 0 \\ -\alpha \cdot [f(v) - \tau] + g(v), & \dot{v} < 0 \end{cases} \tag{3.2}$$

where α is the same positive number in (3.1), $g(v)$ is the slope of the model, and $f(v)$ is the average value of the difference between the upward and downward sides.

Property 1[14, 15]: $f(v)$ is a piecewise smooth, monotone increasing, odd function with a derivative $f'(v)$, which is not identical to zero. For large values of input $v(t)$, there exists a finite limit $f'(\infty)$;

$$f(v) = -f(-v), \quad \lim_{v \to \infty} f'(v) < \infty .$$

Property 2[14, 15]: $g(v)$ is a piecewise continuous, even function with

$$g(v) = g(-v), \quad \lim_{v \to \infty} g(v) = \lim_{v \to \infty} f'(v) .$$

It has been shown that the Duhem model can describe a large class of hysteresis in various smart materials, such as ferromagnetically soft materiala or piezoelectric actuators by appropriately choosing $f(v)$ and $g(v)$ [14-16]. One widely used pair of functions of $f(v)$ and $g(v)$ are

$$f(v) = \begin{cases} a_1 v_s + a_2(v - v_s) & for \quad v > v_s \\ a_1 \cdot v & for \quad |v| \le v_s \\ -a_1 v_s + a_2(v + v_s) & for \quad v < -v_s \end{cases} \tag{3.3}$$

$$g(v) = a_3$$

where $v_s > 0$, $a_1 > 0$, $a_2 > 0$, $1 > a_3 > 0$, a_1 and a_2 satisfy $a_1, a_2 \in [a_{min} \quad a_{max}]$, a_{min} and a_{max} are known constants.

Substituting the $f(v)$ and $g(v)$ into (3.2), one has

$$\dot{\tau} = \begin{cases} \alpha \cdot \dot{v}[a_1 \cdot v_s + a_2(v - v_s) - \tau] + a_3 \cdot \dot{v} & v > v_s, \dot{v} > 0 \\ \alpha \cdot \dot{v}[a_1 \cdot v - \tau] + a_3 \cdot \dot{v} & 0 < v \le v_s, \dot{v} > 0 \\ \alpha \cdot \dot{v}[\tau - a_1 \cdot v] + a_3 \cdot \dot{v} & -v_s \le v < 0, \dot{v} < 0 \\ \alpha \cdot \dot{v}[a_1 \cdot v_s - a_2(v + v_s) + \tau] + a_3 \cdot \dot{v} & v < -v_s, \dot{v} < 0 \end{cases} \tag{3.4}$$

The above equation can be solved for τ

$$\tau = \begin{cases} a_2 \cdot v - f_{21} & v > v_s, \dot{v} > 0 \\ a_1 \cdot v - f_{22} & 0 < v \le v_s, \dot{v} > 0 \\ a_1 \cdot v - f_{23} & -v_s \le v < 0, \dot{v} < 0 \\ a_2 \cdot v - f_{24} & v < -v_s, \dot{v} < 0 \end{cases}$$

with

$$
\begin{cases}
f_{21} = (a_2 v_0 - \tau_0) \cdot e^{-\alpha(v-v_0)} - e^{-\alpha v} \int_{v_0}^{v} (a_3 - a_2) \cdot e^{\alpha \xi} d\xi - (a_1 - a_2) \cdot v_s \\[4mm]
f_{22} = (a_1 v_0 - \tau_0) \cdot e^{-\alpha(v-v_0)} - e^{-\alpha v} \int_{v_0}^{v} (a_3 - a_1) \cdot e^{\alpha \xi} d\xi \\[4mm]
f_{23} = (a_1 v_0 - \tau_0) \cdot e^{\alpha(v-v_0)} - e^{\alpha v} \int_{v_0}^{v} (a_3 - a_1) \cdot e^{-\alpha \xi} d\xi \\[4mm]
f_{24} = (a_2 v_0 - \tau_0) \cdot e^{\alpha(v-v_0)} - e^{-\alpha v} \int_{v_0}^{v} (a_3 - a_2) \cdot e^{-\alpha \xi} d\xi + (a_1 - a_2) \cdot v_s
\end{cases}
$$

In order to describe the piezoelectric actuator, the same functions $f(v)$ and $g(v)$ as those in [16] are chosen, which is a special case of the above choice of $f(v)$ and $g(v)$, i.e. $a_1 = a$, $a_2 = 0$ and $a_3 = \bar{b}$ when $|v| \leq v_s$.

$$
f(v) = \begin{cases}
a \cdot v_s & for & v > v_s \\
a \cdot v & for & |v| \leq v_s \\
-a \cdot v_s & for & v < -v_s
\end{cases}
\tag{3.5}
$$

$$
g(v) = \begin{cases}
0 & for & v > v_s \\
\bar{b} & for & |v| \leq v_s \\
0 & for & v < -v_s
\end{cases}
\tag{3.6}
$$

where $v_s > 0$, $a > 0$, $\bar{b} > 0$ and $a > \bar{b} \geq a/2$.

Suppose the parameter a satisfies $a \in [a_{min} \quad a_{max}]$, a_{min} and a_{max} are known constants.

Substituting (3.5) and (3.6) into (3.1), one has

37

$$
\dot{\tau} =
\begin{cases}
\alpha \cdot \dot{v}[a \cdot v_s - \tau] & v > v_s, \dot{v} > 0 \\
\alpha \cdot \dot{v}[a \cdot v - \tau] + \overline{b} \cdot \dot{v} & 0 < v \leq v_s, \dot{v} > 0 \\
\alpha \cdot \dot{v}[\tau - a \cdot v] + \overline{b} \cdot \dot{v} & -v_s \leq v < 0, \dot{v} < 0 \\
\alpha \cdot \dot{v}[a \cdot v_s + \tau] & v < -v_s, \dot{v} < 0
\end{cases}
\tag{3.7}
$$

Equation (3.7) can be solved for τ

$$
\tau =
\begin{cases}
-f_{21} & v > v_s, \dot{v} > 0 \\
a \cdot v - f_{22} & 0 < v \leq v_s, \dot{v} > 0 \\
a \cdot v - f_{23} & -v_s \leq v < 0, \dot{v} < 0 \\
-f_{24} & v < -v_s, \dot{v} < 0
\end{cases}
\tag{3.8}
$$

where

$$
\begin{cases}
f_{21} = -\tau_0 e^{-\alpha(v-v_0)_1} - a v_s \\
f_{22} = (a \cdot v_0 - \tau_0) \cdot e^{-\alpha(v-v_0)} - e^{-\alpha \cdot v} \cdot \int_{v_0}^{v} (\overline{b} - a) \cdot e^{\alpha \zeta} d\zeta \\
f_{23} = (a \cdot v_0 - \tau_0) \cdot e^{\alpha(v-v_0)} - e^{-\alpha \cdot v} \cdot \int_{v_0}^{v} (\overline{b} - a) \cdot e^{-\alpha \zeta} d\zeta \\
f_{24} = -\tau_0 e^{-\alpha(v-v_0)_1} + a v_s
\end{cases}
\tag{3.9}
$$

Equation (3.8) can be also expressed as:

$$
\tau = a \cdot \chi_1 \cdot v - (f_{21} \cdot \chi_2 \cdot \chi_3 + f_{22} \cdot \chi_1 \cdot \chi_3 + f_{23} \cdot \chi_1 \cdot \chi_4 + f_{24} \cdot \chi_2 \cdot \chi_4)
\tag{3.10}
$$

where $\chi_i (i = 1, 2 \cdots 4)$ are indicator functions defined as:

$$
\chi_1 =
\begin{cases}
1 & |v| \leq v_s \\
0 & |v| > v_s
\end{cases}, \quad
\chi_2 =
\begin{cases}
0 & |v| \leq v_s \\
1 & |v| > v_s
\end{cases}, \quad
\chi_3 =
\begin{cases}
1 & \dot{v} \geq 0 \\
0 & \dot{v} < 0
\end{cases}, \quad
\chi_4 =
\begin{cases}
0 & \dot{v} \geq 0 \\
1 & \dot{v} < 0
\end{cases}.
$$

Following the definition of the indicator functions, one gets

$$
\chi_1 \cdot \chi_2 = 0, \quad \chi_1 + \chi_2 = 1, \quad \chi_3 \cdot \chi_4 = 0, \quad \chi_1 + \chi_2 = 1, \quad \chi_k^2 = \chi_k, \quad k = 1, 2, 3, 4
\tag{3.11}
$$

By defining $\dot\chi_1 = \dot\chi_2 = 0$, one has

$$\dot\tau = a \cdot \chi_1 \cdot \dot{v} - (\dot{f}_{21} \cdot \chi_2 \cdot \chi_3 + \dot{f}_{22} \cdot \chi_1 \cdot \chi_3 + \dot{f}_{23} \cdot \chi_1 \cdot \chi_4 + \dot{f}_{24} \cdot \chi_2 \cdot \chi_4)$$

Let

$$F_2 = \dot{f}_{21}\chi_2 \cdot \chi_3 + \dot{f}_{22}\chi_1 \cdot \chi_3 + \dot{f}_{23}\chi_1 \cdot \chi_4 + \dot{f}_{24}\chi_2 \cdot \chi_4$$

and

$$K_a = a\chi_1$$

Thus, $\dot\tau$ can be rewritten as

$$\dot\tau = K_a \dot{v} - F_2. \tag{3.12}$$

3.2.2 Augmented Multilayer Perceptron (MLP) Neural Network

The MLP NN has been explored to approximate any function with an arbitrary degree of accuracy [61]. However, it needs a large number of NN nodes and training iterations to approximate non-smooth functions (i.e. piecewise continuous), such as friction, hysteresis, backlash and other hard nonlinearities. For these piecewise continuous functions, the MLP needs to be augmented to work as a function approximator. Results for the approximation of piecewise continuous functions or functions with jumps are given in [39]. The augmented NN is used here to approximate the piecewise continuous function in the hysteresis model.

Let S be a compact set of R^n and define $C^n(S)$ as the space, such that the map $f(x) : S \to R^n$ is piecewise continuous. The NN can approximate a

function $f(x) \in C^n(S)$, $x \in R^n$, which has a jump at $x = c$ and is continuous from the right as

$$f(x) = W^T \sigma(V^T x) + W_f^T \varphi[V_f^T \cdot x - c] + \varepsilon(x) \qquad (3.13)$$

where $\varepsilon(x)$ is a functional restructuring error vector, W, W_f and V, V_f are nominal constant weight matrices, T represents the matrix transpose, and $\sigma(\cdot)$ and $\varphi(\cdot)$ are activation functions for hidden neurons.

The structure of the augmented MLPNN is shown by Fig. 3.1. For the hysteresis model (3.12), the piecewise continuous function F_2 is approximated by the augmented NN. In this paper, it is assumed that there exist weight matrices W such that $\|\varepsilon(x)\| \leq \varepsilon_N$ with constant $\varepsilon_N > 0$, for all $x \in R^n$, and that the Frobenius norm of each matrix is bounded by a known constant $\|W\| \leq W_N$ with $W_N > 0$.
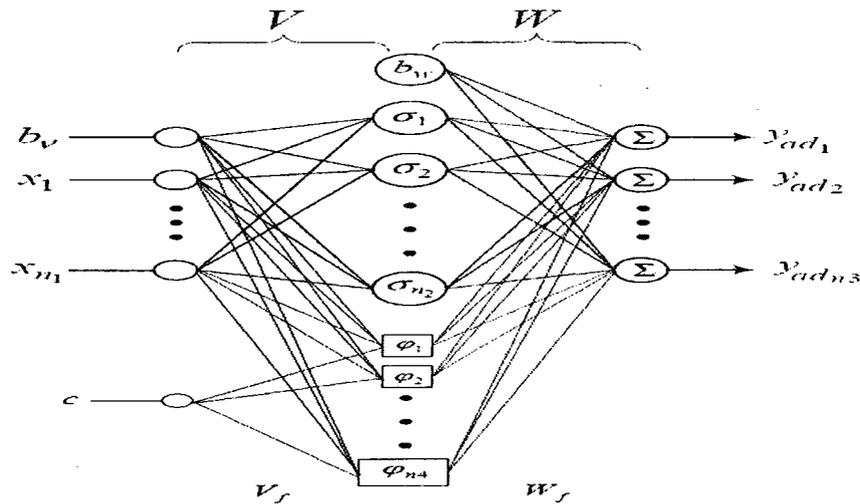
Figure 3.1 The structure of the augmented MLPNN

3.3 Robust Adaptive Control Design

Given the augmented MLP NN and hysteresis model, a NN-based pre-inversion compensator for the hysteresis is needed to cancel out the effect of hysteresis. In this section, a systematic approach is developed to compensate for the hysteretic nonlinearity and to guarantee the stability of the integrated piezoelectric actuator control system.

Consider a piezoelectric actuator subject to hysteresis nonlinearities described by the Duhem model. It can be identified as a second-order linear model preceded by hysteretic nonlinearity:

$$m \cdot \ddot{y}(t) + b \cdot \dot{y}(t) + k \cdot y(t) = k \cdot c \cdot \tau_{pr}(t)$$
$$\tau_{pr}(t) = H[v(t)]$$

(3.14)

where $v(t)$ is the input to the piezoelectric actuator, $y(t)$ denotes the position of the piezoelectric actuator, m, b, k denote the mass, damping and stiffness coefficients, respectively, τ_{pr} is the output of the hysteresis model, and $H(\cdot)$ represents the Duhem model (3.1).

In order to eliminate the effect of hysteresis on the piezoelectric actuator system, an NN-based hysteresis compensator is designed to make the output from the hysteresis model τ_{pr} approach the designed control signal τ_{pd}. After the hysteresis is compensated for by the NN, an adaptive control for the piezoelectric actuator is to be designed to ensure the stability of the overall system and that output tracking error of the piezoelectric actuator with unknown hysteresis is bounded.

The output of hysteresis is not normally measurable for the plant preceded by the unknown hysteresis. An observer will be designed to estimate the value of τ_{pr} based on the inputs and outputs of the plant in the Section 3.3.C. The goal of the subsequent Section 3.3.*A and B* is to show the theoretic possibility of applying the augmented MLP NN to deal with the system with unknown hysteresis under the assumption that the output of hysteresis is available.

The tracking problem is considered, in which $y(t)$ is to asymptotically track a reference signal $y_d(t)$ having the properties that $y_d(t)$ and its derivatives, up to the second derivative, are bounded, and $\ddot{y}_d(t)$ is piecewise continuous for all $t \geq 0$. The tracking error of the piezoelectric actuator is defined as

$$e_p(t) = y_d(t) - y(t). \tag{3.15}$$

A filtered error is defined as

$$r_p(t) = \dot{e}_p(t) + \lambda_p \cdot e_p(t) \tag{3.16}$$

where $\lambda_p > 0$ is a designed parameter.

Differentiating $r_p(t)$ and combining it with the system dynamics Eq. (3.14), one may obtain:

$$
\begin{aligned}
\frac{m}{k \cdot c} \cdot \dot{r}_p = {}& -\frac{b}{k \cdot c} \cdot r_p - \tau_{pr} + \frac{m}{k \cdot c} \cdot (\ddot{y}_d + \lambda_p \cdot \dot{e}_p) \\
& + \frac{b}{k \cdot c} \cdot (\dot{y}_d + (\lambda_p - \frac{k}{b}) \cdot e_p) + \frac{1}{c} \cdot y_d.
\end{aligned}
\tag{3.17}
$$

The tracking error dynamics can be written as

$$\frac{m}{k \cdot c} \cdot \dot{r}_p = -\frac{b}{k \cdot c} \cdot r_p - \tau_{pr} + Y_d^{\ T} \cdot \theta_p \qquad (3.18)$$

where

$$Y_d = \left[\ddot{y}_d + \lambda_p \dot{e}_p \quad \dot{y}_d + (\lambda_p - \frac{k}{b})e_p \quad y_d \right]^T$$

is a regression vector and

$$\theta_p = \left[\frac{m}{kc} \quad \frac{b}{kc} \quad \frac{1}{c} \right]^T \in R^3$$

is a unknown parameter vector with $\theta_{p\min} \le \theta_{pi} \le \theta_{p\max}$ $i = 1, 2, 3$ where $\theta_{p\min}$ and

$\theta_{p\max}$ are some known real numbers.

A. NN-based Compensator for Hysteresis

In the presence of an unknown hysteresis nonlinearity, the adaptive control signal

τ_{pd} to be designed for the piezoelectric actuator is different from the output of the

hysteresis model τ_{pr}. Defining the signal error as

$$\tilde{\tau}_p = \tau_{pd} - \tau_{pr}, \qquad (3.19)$$

and diferentiating (3.19) yields

$$\dot{\tilde{\tau}}_p = \dot{\tau}_{pd} - \dot{\tau}_{pr}. \qquad (3.20)$$

The output of hysteresis τ_{pr} satisfies (3.12). Substituting it into above equation, one has

$$\dot{\tilde{\tau}}_p = \dot{\tau}_{pd} - K_a \dot{v} + F_2 \tag{3.21}$$

Here, a second first-layer-fixed MLP [39] is utilized to approximate the nonlinear function F_2:

$$
\begin{aligned}
F_2 = {} & W_2^T \cdot \sigma(V_2^T \cdot h) + W_{f21}^T \cdot \varphi_{21}(V_{f21}^T \cdot h) \\
& + W_{f22}^T \cdot \varphi_{22}(V_{f22}^T \cdot h - v_s) \\
& + W_{f23}^T \cdot \varphi_{23}(V_{f23}^T \cdot h + v_s) + \varepsilon_1(h)
\end{aligned}
$$

where $h = \begin{bmatrix} \tau_{pd} & \tau_{p0} & v & \dot{v} & 1 \end{bmatrix}^T$, τ_{p0} is the initial value of the control signal, V_2^T, V_{f21}^T, V_{f22}^T, and V_{f23}^T are input-layer weight matrices, W_2^T, W_{f21}^T, W_{f22}^T, and W_{f23}^T are output-layer weight matrices, 0, v_s, and $-v_s$ are jump points on the output layer, $\sigma(\cdot)$, $\varphi_{21}(\cdot)$, $\varphi_{21}(\cdot)$, and $\varphi_{23}(\cdot)$ are the activation functions, and $\varepsilon_1(h)$ is the functional restructure error in which inversion error is included. Output-layer weight matrices W_2^T, W_{f21}^T, W_{f22}^T, and W_{f23}^T are trained so that the output of NN approximates the nonlinear function F_2.

Letting

$$\Theta(h, v_s) = [\sigma(V_2^T \cdot h) \quad \varphi_{21}(V_{f21}^T \cdot h) \quad \varphi_{22}(V_{f22}^T \cdot h - v_s) \quad \varphi_{23}(V_{f23}^T \cdot h + v_s)]^T$$

and

$$W_1^T = [W_2^T \quad W_{f21}^T \quad W_{f22}^T \quad W_{f23}^T],$$

the nonlinear function F_2 can be expressed as:

$$F_2 = W_1^T \Theta(h, v_s) + \varepsilon_1(h).$$

(3.22)

It is assumed that the Frobenius norm of weight matrix W_1 is bounded by a known constant $\|W_1\| \leq W_{1N}$ with $W_{1N} > 0$ and $\|\varepsilon_1(h)\| \leq \varepsilon_{1N}$ with constant $\varepsilon_{1N} > 0$, for all $x \in R^n$.

The estimated nonlinear function $\hat{F}_2$ is constructed by using the neural network with the weight matrix $\hat{W}_1$:

$$\hat{F}_2 = \hat{W}_1^T \Theta(h, v_s).$$

(3.23)

Hence, the restructure error between the nonlinear functions F_2 and $\hat{F}_2$ is derived as:

$$\tilde{F}_2 = F_2 - \hat{F}_2 = \tilde{W}_1^T \Theta(h, v_s) + \varepsilon_1(h).$$

(3.24)

Then, the hysteresis pre-inversion compensator is designed:

$$\dot{v} = \hat{\mu} \cdot \{ k_b \cdot \tilde{\tau}_p + \dot{\tau}_{pd} + \hat{W}_1^T \cdot \Theta(h, v_s) + r_p \}$$

(3.25)

where $\hat{\mu} = \dfrac{a_{\min}}{\hat{a}}$ is an estimated constant which satisfies $0 < \hat{\mu} \leq 1$ with the known boundary of $a \in [a_{\min} \quad a_{\max}]$. k_b is a positive constant, $\hat{a}$ is the estimated value of a, and $\hat{W}_1^T = [\hat{W}_2^T \quad \hat{W}_{f21}^T \quad \hat{W}_{f22}^T \quad \hat{W}_{f23}^T]$ is the estimated output-layer weight matrix W_1^T.

Defining the error matrix as

$$\tilde{W}_1^T = W_1^T - \hat{W}_1^T,$$

and inserting (3.23), (3.25) into (3.21), one obtains

$$
\begin{aligned}
\dot{\tilde{\tau}}_p &= -k_b \cdot \hat{\mu} \cdot K_a \cdot \tilde{\tau}_p + (1 - \hat{\mu} \cdot K_a) \cdot \dot{\tau}_{pd} \\
&+ (1 - \hat{\mu} \cdot K_a) \cdot \hat{W}_1^{\ T} \cdot \Theta(h, v_s) \\
&- \hat{\mu} \cdot K_a \cdot r_p + \tilde{W}_1^{\ T} \cdot \tilde{\Theta}(h, v_s) \\
&+ \varepsilon_1(h)
\end{aligned}
$$

and the weight matrix update rule as

$$
\dot{\hat{W}}_1 = \Gamma \Theta(h, v_s) \cdot \tilde{\tau}_p + k_{p1} \left| \tilde{\tau}_p \right| \cdot \hat{W}_1 \ , \tag{3.26}
$$

where Γ is a positive adaptation gain diagonal matrix, and k_{p1} is a positive constant.

The design of the updating rule of parameter $\hat{\mu}$ in the pre-inversion compensator $\dot{v}$

is taken as

$$
\dot{\hat{\mu}} = Proj(\hat{\mu}, \quad \eta \cdot \tilde{\tau}_p \cdot [\dot{\tau}_{pd} + \hat{W}_1^{\ T} \Theta(h, v_s) + r_p]) \tag{3.27}
$$

where η is a positive constant and *Proj(.)* is a projection operator defined as follows:

$$Proj(\hat{\mu}, \quad \eta \cdot \tilde{\tau}_p \cdot [\dot{\tau}_p + \hat{W}_1^T \Theta(h, v_s) + r_p]) =$$

$$\begin{cases} 0 & \hat{\mu}=1 \quad \& \quad \eta \cdot \tilde{\tau}_p \cdot [\dot{\tau}_{pd} + \hat{W}_1^T \Theta(h, v_s) + r_p] < 0 \\ \\ \eta \cdot \tilde{\tau}_p \cdot [\dot{\tau}_{pd} + \hat{W}_1^T \Theta(h, v_s) + r_p] & \begin{aligned} & \left(\frac{a_{\min}}{a_{\max}}\right)^2 < \hat{\mu} < 1 \quad or \\ & \hat{\mu}=1 \quad \& \eta \cdot \tilde{\tau}_p \cdot [\dot{\tau}_{pd} + \hat{W}_1^T \Theta(h, v_s) + r_p] \geq 0 \, or \\ & \hat{\mu}=\left(\frac{a_{\min}}{a_{\max}}\right)^2 \& \eta \cdot \tilde{\tau}_p \cdot [\dot{\tau}_{pd} + \hat{W}_1^T \Theta(h, v_s) + r_p] \leq 0 \end{aligned} \\ \\ 0 & \hat{\mu}=\left(\frac{a_{\min}}{a_{\max}}\right)^2 \& \eta \cdot \tilde{\tau}_p \cdot [\dot{\tau}_{pd} + \hat{W}_1^T \Theta(h, v_s) + r_p] > 0 \end{cases} \quad (3.28)$$

The adaptive NN-based pre-inversion compensator $\dot{v}$ is developed to drive the adaptive control signal τ_{pd} to approach the output of the hysteresis model τ_{pr} so that the hysteretic effect is counteracted.

B. Adaptive Robust Controller for the Integrated System

In this section, an adaptive robust controller for the piezoelectric actuator with the pre-inversion compensator is developed to drive the tracking error between the output of the actuator and the desired trajectory $y_d(t)$ to converge to a small neighbourhood around zero. A rigorous analysis is carried out to prove the stability of the overall system.

The adaptive controller is designed as

$$\tau_{pd} = k_{pd} \cdot r_p + Y_d^T \cdot \hat{\theta}_p. \quad (3.29)$$

The updating rule is designed as

$$\dot{\hat{\theta}}_p = Proj_{\hat{\theta}_p}(\hat{\theta}_p, \quad \beta \cdot Y_d \cdot r_p), \tag{3.30}$$

where β is a positive constant adaptation gain, and

$$\{Proj_{\hat{\theta}_p}(\hat{\theta}_p, \quad \beta \cdot Y_d \cdot r_p)\}_i =$$

$$\begin{cases} 0 & if \quad \hat{\theta}_{pi} = \theta_{p\max} \quad and \quad \beta \cdot (Y_d \cdot r_p)_i < 0 \\[2ex] & if \quad \theta_{p\min} < \hat{\theta}_{pi} < \theta_{p\max} \\ \beta \cdot (Y_d \cdot r_p)_i & or \quad \hat{\theta}_{pi} = \theta_{p\max} \quad and \quad \beta \cdot (Y_d \cdot r_p)_i \geq 0 \\ & or \quad \hat{\theta}_{pi} = \theta_{p\min} \quad and \quad \beta \cdot (Y_d \cdot r_p)_i \leq 0 \\[2ex] 0 & if \quad \hat{\theta}_{pi} = \theta_{p\min} \quad and \quad \beta \cdot (Y_d \cdot r_p)_i > 0 \end{cases} \tag{3.31}$$

The stability and convergence of the above integrated control system is summarized in Theorem 3.1.

Theorem 3.1 For a piezoelectric actuator system (3.14) with unknown hysteresis (3.1) and a desired trajectory $y_d(t)$, the adaptive robust controller (3.29) and the NN based compensator (3.24) are designed to make the output of the actuator track the desired trajectory $y_d(t)$. The parameters of the adaptive robust controller and the NN based compensator are tuned by the updating rules (3.26), (3.27), and (3.30). Then, the tracking error $e_p(t)$ between the output of the actuator and the desired trajectory $y_d(t)$ will converge to a small neighbourhood around zero by appropriately choosing suitable gains k_{pd} and k_b. The overall control system is guaranteed to be stable.

Proof: Define the Lyapunov function as

$$V_1 = \frac{1}{2} \cdot \frac{m}{k \cdot c} \cdot r_p{}^2 + \frac{1}{2} \tilde{\tau}_p{}^2 + \frac{1}{2} \cdot tr(\tilde{W}_1{}^T \Gamma^{-1} \tilde{W}_1)$$

$$+ \frac{1}{2 \cdot \eta K_a}(1 - \hat{\mu} K_a)^2 + \frac{1}{2\beta} \cdot (\theta_p - \hat{\theta}_p)^T \qquad (3.32)$$

$$\cdot (\theta_p - \hat{\theta}_p) > 0$$

Differentiating Equation (3.32) yields

$$\dot{V}_1 = \frac{m}{k \cdot c} \cdot r_p \ \dot{r}_p + \tilde{\tau}_p \dot{\tilde{\tau}}_p - tr(\tilde{W}_1{}^T \Gamma^{-1} \dot{\tilde{W}}_1)$$

$$- \frac{1}{\eta}(1 - \hat{\mu} K_a)\dot{\hat{\mu}} - \frac{1}{\beta} \cdot (\theta_p - \hat{\theta}_p)^T \cdot \dot{\hat{\theta}}_p . \qquad (3.33)$$

Introducing the control strategies (3.24), (3.29), and the updating rule (3.26), (3.27), (3.30) into the above equation, one obtains

$$\dot{V}_1 = -\frac{b}{k \cdot c} \cdot r_p^2 - k_{pd} \cdot r_p^2 - k_b \cdot \hat{\mu} \cdot K_a \cdot \tilde{\tau}_p{}^2$$

$$+ \tilde{\tau}_p \varepsilon_1(h) - k_{p1}\left|\tilde{\tau}_p\right| tr(\tilde{W}_1{}^T \hat{W}_1). \qquad (3.34)$$

With the assumption of neural network output weight matrix W_1 and the approximation error $\varepsilon_1(h)$, one has

$$\dot{V}_1 \leq -(\frac{b}{k \cdot c} + k_{pd}) \cdot r_p{}^2 - k_m \cdot \tilde{\tau}_p{}^2$$

$$+ \left|\tilde{\tau}_p\right| \cdot \varepsilon_{1N} - k_{p1} \cdot \left|\tilde{\tau}_p\right| \qquad (3.35)$$

$$\cdot \left\|\tilde{W}_1\right\|(W_{1N} - \left\|\tilde{W}_1\right\|)$$

where $k_m = K_a \cdot k_b \cdot a_{\max}$.

If one has

$$\left|\tilde{\tau}_p\right| > \frac{-k_{p1}\cdot W_{1N}{}^2 \big/ 4 + \varepsilon_{1N}}{k_m} \qquad (3.36)$$

and

$$\left\|\tilde{W}_1\right\| > W_{1N}/2 + \sqrt{W_{1N}^2/4 - \varepsilon_{1N}/k_{p1}}\ , \qquad (3.37)$$

$\dot{V}_1$ can be easily proven to be negative. Inequality (3.36) shows that if the control

parameters k_b are chosen large enough then the following inequality holds

$$\frac{-k_{p1}\cdot W_{1N}{}^2 \big/ 4 + \varepsilon_{1N}}{k_m} < b_r\ , \qquad (3.38)$$

where $b_r > 0$ represents the radius of a ball inside the compact set C_r of the tracking

error $\tilde{\tau}_p(t)$.

Thus, any trajectory $\tilde{\tau}_p(t)$ starting in compact set $C_r = \left\{r\big|\ \|r\| \le b_r\right\}$ converges

within C_r and is bounded. Then, the filtered error $r_p(t)$ of the system and the tracking

error $\tilde{\tau}_p(t)$ of the hysteresis converge to a small neighbourhood around zero. According

to the standard Lyapunov theorem extension [62], this demonstrates the UUB (uniformly

ultimately bounded) of $r_p(t)$, $\tilde{\tau}_p(t)$ and $\tilde{W}_1$.

C. Observer-based Control of the Integrated System

In this subsection, the same problem is considered in the situation where the output of hysteresis is not available for control.

It is observed that the output of hysteresis is usually not measurable for a plant subject to unknown hysteresis. However, considering the whole system as a dynamic model preceded by the Duhem model, an observer can be designed to estimate the output of hysteresis based on the input and output of the plant by using the method in [61], as illustrated in Figure 3.1.

Figure 3.2 Configuration of the closed-loop control system

We denote the observed output of hysteresis as $\hat{\tau}_{pr}$, and define the error between the actual output of actuator y and the estimated output of actuator $\hat{y}$:

$$e_1 = y - \hat{y} \tag{3.39}$$

Denote the error between the output of hysteresis τ_{pr} and the observed $\hat{\tau}_{pr}$ is defined as $e_2 = \tau_{pr} - \hat{\tau}_{pr}$. Then the observer is designed as:

$$\dot{\hat{y}} = \dot{y} + L_1 e_1 \tag{3.40}$$

$$\dot{\hat{\tau}}_{pr} = \hat{K}_a \dot{v} - \hat{F}_2 + L_2 e_1 - K_{pr} \hat{\tau}_{pr} \tag{3.41}$$

where $\dot{y}(t)$ is the assumed measurable velocity of the actuator. The error dynamics of the observer are obtained based on the actuator and hysteresis models.

$$\dot{e}_1 = -L_1 e_1$$

$$\dot{e}_2 = \widetilde{K}_a \dot{v} - \widetilde{F}_2 - L_2 e_1 + K_{pr} \hat{\tau}_{pr} \tag{3.42}$$

where the error parameter is defined as $\widetilde{K}_a = K_a - \hat{K}_a$.

By using the observed hysteresis output $\hat{\tau}_{pr}$, one may define the signal error between the adaptive control signal τ_{pd} and the estimated hysteresis output as:

$$\widetilde{\tau}_{pe} = \tau_{pd} - \hat{\tau}_{pr} \tag{3.43}$$

The derivative of the signal error is:

$$\dot{\widetilde{\tau}}_{pe} = \dot{\tau}_{pd} - \hat{K}_a \dot{v} + \hat{F}_2 - L_2 e_1 + K_{pr} \hat{\tau}_{pr} \tag{3.44}$$

A hysteresis pre-inversion compensator is designed:

$$\dot{v} = \hat{\mu} \cdot \{ k_b \cdot \widetilde{\tau}_{pe} + \dot{\tau}_{pd} + \hat{F}_2 + r_p \} . \tag{3.45}$$

By substituting the neural network output $\hat{F}_2 = \hat{W}_1^T \Theta(h, v_s)$ and pre-inversion

compensator output into the derivative of the signal error, one obtains:

$$
\begin{aligned}
\dot{\tilde{\tau}}_{pe} = &(1 - \hat{K}_a \hat{\mu}) \dot{\tau}_{pd} - \hat{K}_a \hat{\mu} \cdot k_b \tilde{\tau}_{pe} \\
&+ (1 - \hat{K}_a \hat{\mu}) \hat{W}_1^T \Theta(h, v_s) \\
&- \hat{K}_a \hat{\mu} \cdot r_p - L_2 e_1 + K_{pr} \hat{\tau}_{pr}.
\end{aligned}
\tag{3.46}
$$

The weight matrix updating rule is chosen as:

$$
\dot{\hat{W}}_1 = \Gamma \Theta(h, v_s) \cdot \tilde{\tau}_{pe} + k_{p1} |\tilde{\tau}_{pe}| \cdot \hat{W}_1.
\tag{3.47}
$$

Furthermore, the updating rule of parameter $\hat{\mu}$ in the pre-inversion compensator $\dot{v}$ is

designed with the same projection operator as (3.28):

$$
\dot{\hat{\mu}} = Proj(\hat{\mu}, \quad \eta \cdot \tilde{\tau}_{pe} \cdot [\dot{\tau}_{pd} + \hat{W}_1^T \Theta(h, v_s) + r_p])
\tag{3.48}
$$

The updating rule of parameter $\hat{K}_a$ in the observer (3.41) is designed with the same

projection operator as (3.28):

$$
\dot{\hat{K}}_a = Proj(\hat{K}_a, \quad \gamma \cdot \hat{\mu} \cdot \tilde{\tau}_{pe} \cdot [\dot{\tau}_{pd} + \hat{W}_1^T \Theta(h, v_s) + r_p] + \dot{v} \cdot \tilde{\tau}_{pe})
\tag{3.49}
$$

Hence, the adaptive controller and the updating rule of the control parameter are

designed as:

$$
\tau_{pd} = k_{pd} \cdot r_p + Y_d^T \cdot \hat{\theta}_p
\tag{3.50}
$$

$$\dot{\hat{\theta}}_p = Proj_{\hat{\theta}_p}(\hat{\theta}_p, \quad \beta \cdot Y_d \cdot r_p) \tag{3.51}$$

where the projection operator is

$$\{Proj_{\hat{\theta}_p}(\hat{\theta}_p, \quad \beta \cdot Y_d \cdot r_p)\}_i =$$

$$
\begin{cases}
0 & if \quad \hat{\theta}_{pi} = \theta_{p\max} \; and \quad \beta \cdot (Y_d \cdot r_p)_i < 0 \\
& if \quad \theta_{p\min} < \hat{\theta}_{pi} < \theta_{p\max} \\
\beta \cdot (Y_d \cdot r_p)_i \; or & \hat{\theta}_{pi} = \theta_{p\max} \; and \quad \beta \cdot (Y_d \cdot r_p)_i \geq 0 \\
or & \hat{\theta}_{pi} = \theta_{p\min} \; and \quad \beta \cdot (Y_d \cdot r_p)_i \leq 0 \\
0 & if \quad \hat{\theta}_{pi} = \theta_{p\min} \; and \quad \beta \cdot (Y_d \cdot r_p)_i > 0
\end{cases}
$$

The stability and convergence of the above integrated control system are summarized in Theorem 3.2.

Theorem 3.2 For a piezoelectric actuator system (3.14) with unknown hysteresis (3.1) and a desired trajectory $y_d(t)$, the adaptive robust controller (3.50), NN based compensator (3.45) and hysteresis observer (3.40) and (3.41) are designed for the output of the actuator to track the desired trajectory $y_d(t)$. The parameters of the adaptive robust controller and the NN-based compensator are tuned by the updating rules (3.47), (3.48), (3.49) and (3.51). Then, the tracking error $e_p(t)$ between the output of the actuator and the desired trajectory $y_d(t)$ converge to a small neighbourhood around zero by appropriately choosing suitable control gains k_{pd}, k_b and observer gains L_1, L_2 and K_{pr}.

Proof: Defining a Lyapunov function

$$V_2 = \frac{1}{2} \cdot \frac{m}{k \cdot c} \cdot r_p{}^2 + \frac{1}{2} \tilde{\tau}_{pe}{}^2 + \frac{1}{2} \cdot tr(\tilde{W}_1{}^T \Gamma^{-1} \tilde{W}_1)$$

$$+ \frac{1}{2 \cdot \eta K_a}(1 - \hat{\mu} K_a)^2 + \frac{1}{2 \cdot \gamma}(K_a - \hat{K}_a)^2$$

$$+ \frac{1}{2\beta} \cdot (\theta_p - \hat{\theta}_p)^T \cdot (\theta_p - \hat{\theta}_p)$$

$$+ \frac{1}{2} e_1^2 + \frac{1}{2} e_2^2,$$

the derivative of the Lyapunov function is obtained as

$$\dot{V}_2 = \frac{m}{k \cdot c} \cdot r_p \dot{r}_p + \tilde{\tau}_{pe} \cdot \dot{\tilde{\tau}}_{pe} - tr(\dot{\tilde{W}}_1{}^T \Gamma^{-1} \tilde{W}_1)$$

$$- \frac{1}{\eta}(1 - \hat{\mu} K_a)\dot{\hat{\mu}} - \frac{1}{\gamma}(K_a - \hat{K}_a)\dot{\hat{K}}_a$$

$$- \frac{1}{\beta} \cdot (\theta_p - \hat{\theta}_p)^T \cdot \dot{\hat{\theta}}_p$$

$$+ e_1 \dot{e}_1 + e_2 \dot{e}_2.$$

Introducing control strategies (3.45) and (3.50), and the updating rules (3.47), (3.48), (3.49), and (3.51) into the above equation, one obtains

55

$$\dot{V}_2 = \frac{m}{k \cdot c} \cdot r_p \dot{r}_p + \tilde{\tau}_{pe} \cdot \dot{\tilde{\tau}}_{pe} - tr(\dot{\hat{W}}_1^T \Gamma^{-1} \tilde{W}_1)$$

$$- \frac{1}{\eta}(1 - \hat{\mu} K_a)\dot{\hat{\mu}} - \frac{1}{\gamma}(K_a - \hat{K}_a)\dot{\hat{K}}_a$$

$$- \frac{1}{\beta} \cdot (\theta_p - \hat{\theta}_p)^T \cdot \dot{\hat{\theta}}_p + e_1(-L_1 e_1)$$

$$+ e_2(\tilde{K}_a \dot{v} - \tilde{F}_2 - L_2 e_1 + K_{pr} \hat{\tau}_{pr}).$$

$$= -(\frac{b}{k \cdot c} + k_{pd}) \cdot r_p^2 - k_b \cdot \hat{\mu} \cdot \hat{K}_a \cdot \tilde{\tau}_{pe}^2$$

$$+ \varepsilon_1(h)\tilde{\tau}_{pe} - k_{p1}|\tilde{\tau}_{pe}|tr(\tilde{W}_1^T \hat{W}_1)$$

$$- e_2 r_p - L_2 e_1 \tilde{\tau}_{pe} + K_{pr} \hat{\tau}_{pr} \tilde{\tau}_{pe}$$

$$- L_1 e_1^2 - (L_2 e_1 + \tilde{F}_2)e_2$$

$$+ K_{pr} \hat{\tau}_{pr} e_2$$

By using $\hat{\tau}_{pr} = \tau_{pr} - e_2$, $|\tilde{F}| \leq \varepsilon_{1N}$ and inequality $\pm ab \leq \frac{1}{2}a^2 + \frac{1}{2}b^2$ and noticing (3.25),

one has:

$$\dot{V}_2 = -(\frac{b}{k \cdot c} + k_{pd}) \cdot r_p^2 - k_b \cdot \hat{\mu} \cdot \hat{K}_a \cdot \tilde{\tau}_{pe}^2$$

$$+ \varepsilon_1(h)\tilde{\tau}_{pe} - k_{p1}|\tilde{\tau}_{pe}|tr(\tilde{W}_1^T \hat{W}_1)$$

$$+ \frac{1}{2}e_2^2 + \frac{1}{2}r_p^2 + \frac{1}{2}L_2^2 e_1^2 + \frac{1}{2}\tilde{\tau}_{pe}^2$$

$$+ \frac{1}{2}\tilde{\tau}_{pe}^2 + \frac{1}{2}K_{pr}^2 \tau_{pr}^2 + \frac{1}{2}K_{pr}^2 \tilde{\tau}_{pe}^2 \qquad (3.52)$$

$$+ \frac{1}{2}e_2^2 - L_1 e_1^2 + \frac{1}{2}(L_2 e_1 + \varepsilon_{1N})^2$$

$$+ \frac{1}{2}e_2^2 + K_{pr} \tau_{pr} e_2 - K_{pr} e_2^2.$$

Using the inequality $\frac{1}{2}(a+b)^2 \leq a^2 + b^2$, the following inequality can be derived:

$$\dot{V}_2 \leq -(\frac{b}{k \cdot c} + k_{pd} - \frac{1}{2}) \cdot r_p^2 - (k_b \cdot \hat{\mu} \cdot \hat{K}_a - \frac{1}{2} K_{pr}^2 - 1) \cdot \tilde{\tau}_{pe}^2$$
$$+ |\tilde{\tau}_{pe}| \cdot \varepsilon_{1N} - k_{p1} \cdot |\tilde{\tau}_{pe}| \cdot \|\tilde{W}_1\| (W_{1N} - \|\tilde{W}_1\|)$$
$$- (L_1 - \frac{3}{2} L_2^2) e_1^2 - (K_{pr} - 2) e_2^2$$
$$+ \varepsilon_{1N}^2 + K_{pr}^2 \tau_{pr}^2 .$$

From Property 1 of Chapter 2 in [47], one knows τ_{pr}^2 is bounded (say,

$\tau_{pr}^2 \leq M^2$ where M is a constant), and we then define a constant

$$\delta = \varepsilon_{1N}^2 + K_{pr}^2 M^2 > \varepsilon_{1N}^2 + K_{pr}^2 \tau_{pr}^2$$

such that

$$\dot{V}_2 \leq -(\frac{b}{k \cdot c} + k_{pd} - \frac{1}{2}) \cdot r_p^2 - (k_b \cdot \hat{\mu} \cdot \hat{K}_a - \frac{1}{2} K_{pr}^2 - 1) \cdot \tilde{\tau}_{pe}^2$$
$$+ |\tilde{\tau}_{pe}| \cdot \varepsilon_{1N} - k_{p1} \cdot |\tilde{\tau}_{pe}| \cdot \|\tilde{W}_1\| (W_{1N} - \|\tilde{W}_1\|) \qquad (3.53)$$
$$- (L_1 - \frac{3}{2} L_2^2) e_1^2 - (K_{pr} - 2) e_2^2 + \delta$$

Selecting the control parameters k_{pd}, k_b and observer parameters L_1, L_2 and K_{pr} to

satisfy the following inequalities

$$\frac{b}{k \cdot c} + k_{pd} - \frac{1}{2} > 0$$

$$K_{pr} > 2$$

$$k_b \cdot a_{max} \cdot \hat{K}_a - \frac{1}{2} K_{pr}^2 - 1 > 0$$

$$L_1 > \frac{3}{2} L_2^2 ,$$

we let $k_m = k_b \cdot a_{max} \cdot \hat{K}_a - \frac{1}{2} K_{pr}^2 - 1$ such that

$$\left| \tilde{\tau}_{pe} \right| > \frac{- k_{p1} \cdot W_{1N}^2 / 4 + \varepsilon_{1N}}{k_m} \qquad (3.54)$$

$$\left\| \tilde{W}_1 \right\| > W_{1N} / 2 + \sqrt{W_{1N}^2 / 4 - \varepsilon_{1N} / k_{p1}} \; . \qquad (3.55)$$

Hence, we can easily conclude that the closed-loop system is semi-globally bounded [63].

Therefore, the following inequality holds

$$\frac{- k_{p1} \cdot W_{1N}^2 / 4 + \varepsilon_{1N}}{k_m} < b_r$$

where $b_r > 0$ represents the radius of a ball inside the compact set C_r of the tracking error $\tilde{\tau}_{pe}(t)$.

Thus, any trajectory $\tilde{\tau}_{pe}(t)$ starting in compact set $C_r = \left\{ r \middle| \|r\| \le b_r \right\}$ converges within C_r and is bounded. Then, the filtered error $r_p(t)$ of the system and the tracking error $\tilde{\tau}_{pe}(t)$ of the hysteresis converge to a small neighborhood around zero. According to the standard Lyapunov theorem extension [62], this demonstrates the UUB (uniformly ultimately bounded) of $r_p(t)$, $\tilde{\tau}_{pe}(t)$, $\tilde{W}_1$, e_1 and e_2.

3.4 Simulation Studies

In this section, the effectiveness of the NN-based adaptive controller is demonstrated on a piezoelectric actuator described by (3.14) with unknown hysteresis. The coefficients of the dynamic system and hysteresis model for the simulation purpose

are adopted from [54]: $m = 0.016\text{kg}$, $b = 1.2\text{Ns/}\mu\text{m}$, $k = 4500\text{N/}\mu\text{m}$, $c = 0.9$ μm $/\text{V}$, $a = 6$, $\bar{b} = 0.5$, $v_s = 6$ μm $/\text{s}, \beta = 0.1$, $k_{pd} = 50$. The input reference signal is $y_d = 3 \cdot \sin(0.2\pi t)$.

The Neural Network has ten hidden neurons for the first part of the neural network and five hidden neurons for the remaining parts of the neural network, with three jumping points $(0, v_s, -v_s)$. The gains for updating the output weight matrix are all set as $\Gamma = diag\{10\}_{25 \times 25}$. The activation function $\sigma(\cdot)$ is a sigmoid basis function and activation function $\varphi(\cdot)$ has the definition $\varphi(\cdot) = \left(\dfrac{1 - e^{-\alpha x}}{1 + e^{-\alpha x}}\right)^k$ $x \geq 0$, otherwise zero. The parameters for the observer are $K_a = 20$, $k_b = 100$, $\eta = 0.1$, $\gamma = 0.1$, $K_{pr} = 10$, $L_1 = 100$, $L_2 = 1$ and initial conditions are $\hat{y}(0) = 0$, $\hat{\tau}(0) = 0$. Fig. 3.3 shows the tracking performance of the adaptive controlled piezoelectric actuator without the hysteretic compensator. Fig. 3.4 shows that the tracking performance is much better than that of the case without hysteretic compensator, as shown in Fig. 3.3. The input and output maps of the NN-based pre-inversion hysteresis compensator and of the hysteresis are given in Fig. 3.5. The desired control signal and real control signal map (Fig. 3.5c) shows that the curve is approximate to a line, which means the relationship between the two signals is approximately linear with some deviations. In order to show the effectiveness of the designed observer, we compare the observed hysteresis output $\hat{\tau}_{pr}$ and the real hysteresis output τ_{pr} in Fig. 3.6.

(a)

(b)
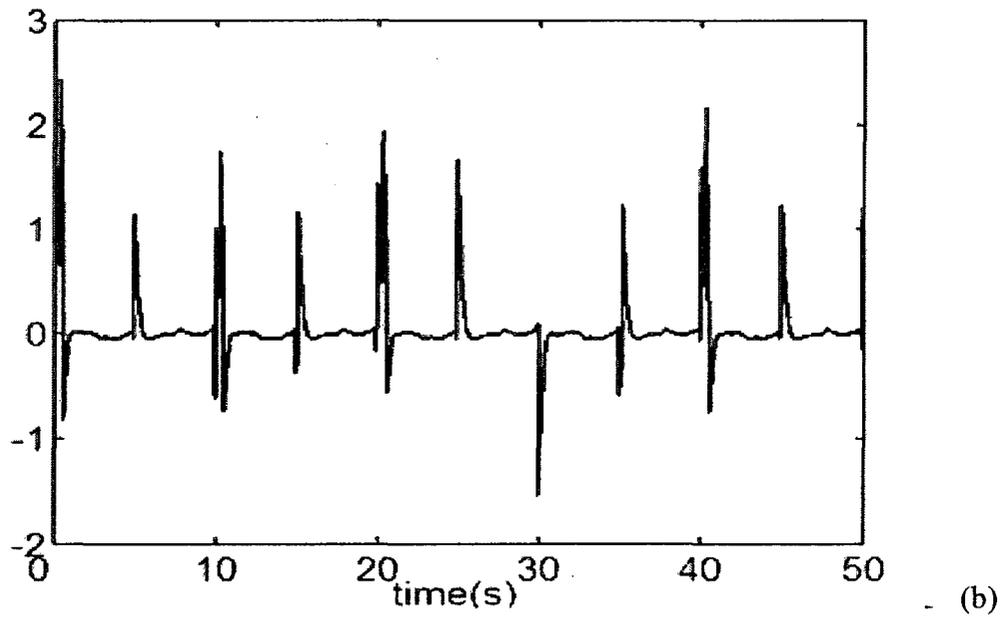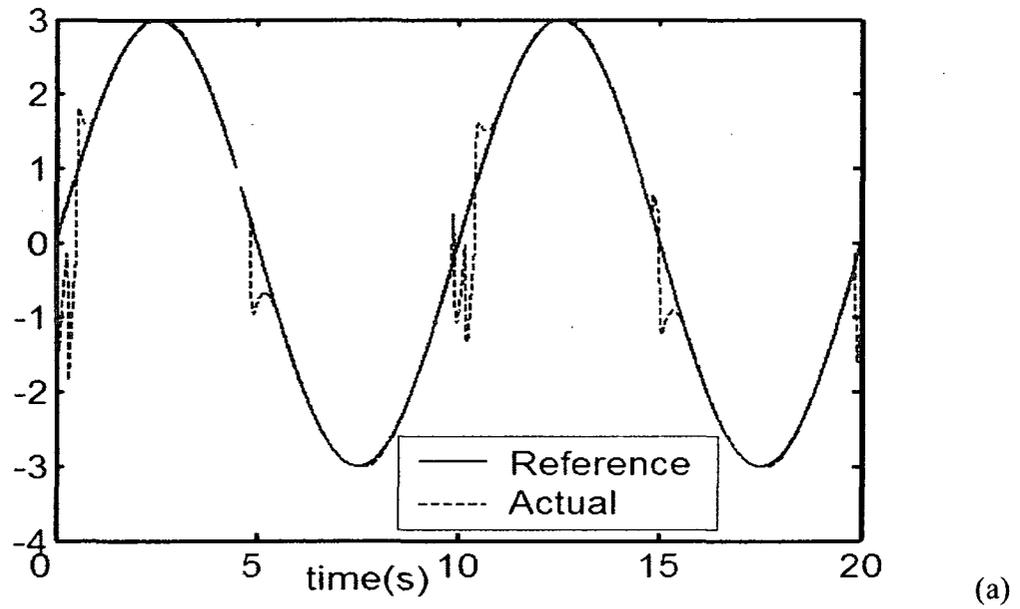
Figure 3.3 Performance of the NN controller without hysteretic compensator (a) The

actual control signal (dashed line) with reference signal (solid); (b) Error $y - y_d$;
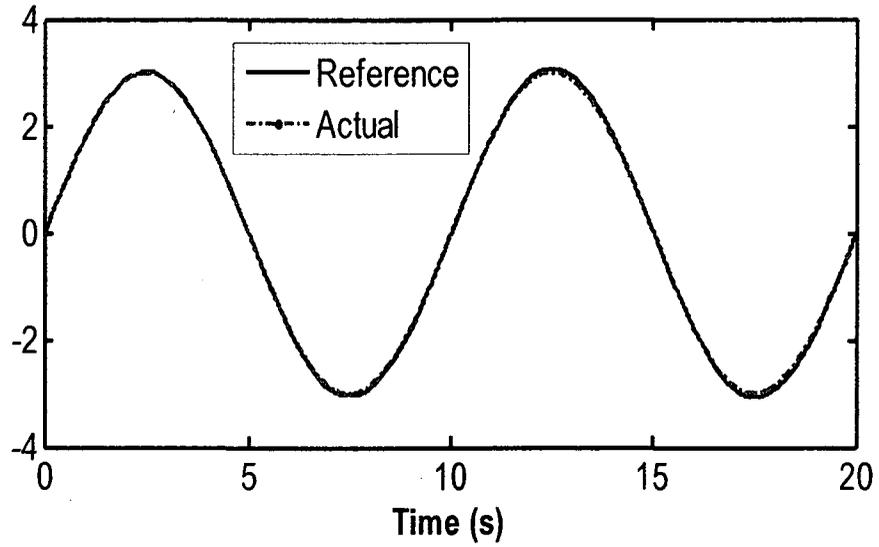
(a)
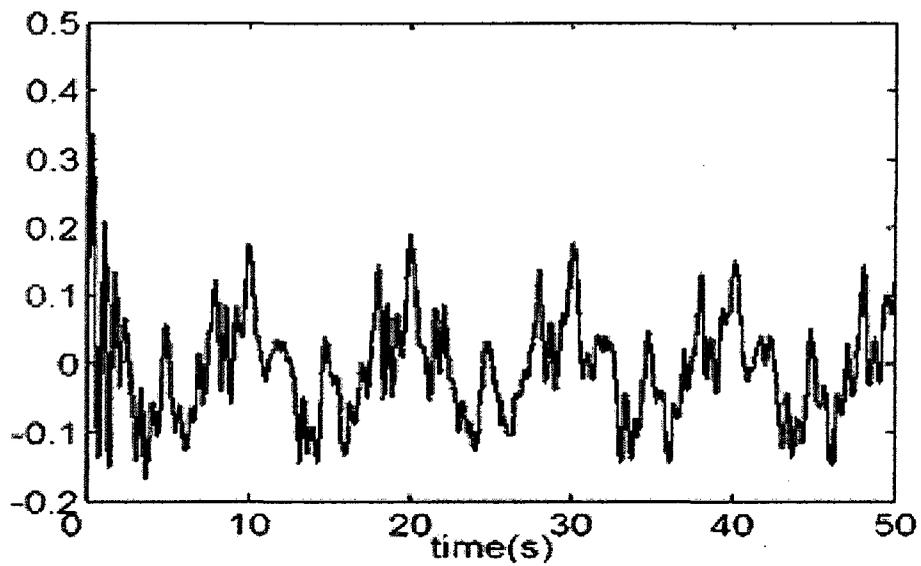
(b)

Figure 3.4 Performance of the NN controller with hysteresis, its compensator and

observer (a) The actual control signal (dashed line) with reference signal (solid); (b)

Error $y - y_d$
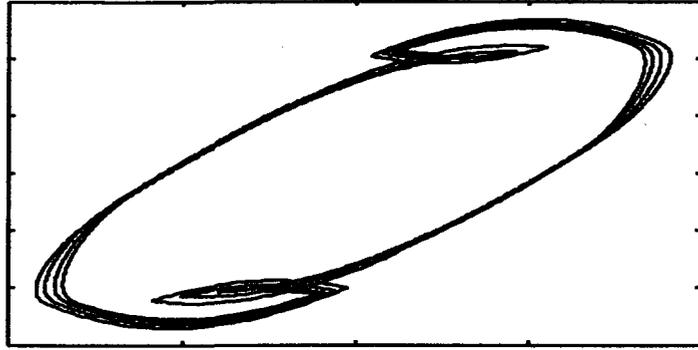
(a)
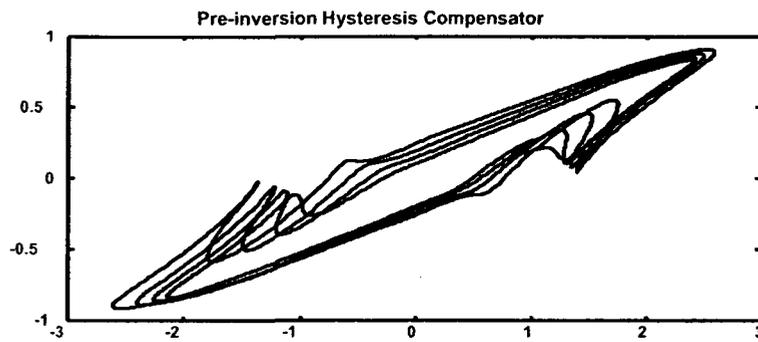
(b)
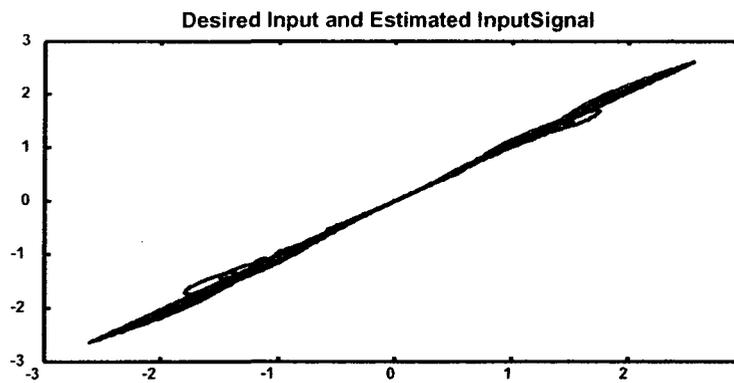
(c)

Figure 3.5 (a) Hysteresis's input and output map τ_{pr} vs. v ; (b) Pre-inversion

compensator's input and output map v vs. τ_{pd} ; (c) Desired input signal and Observed

input signal curve $\hat{\tau}_{pr}$ vs. τ_{pd} .
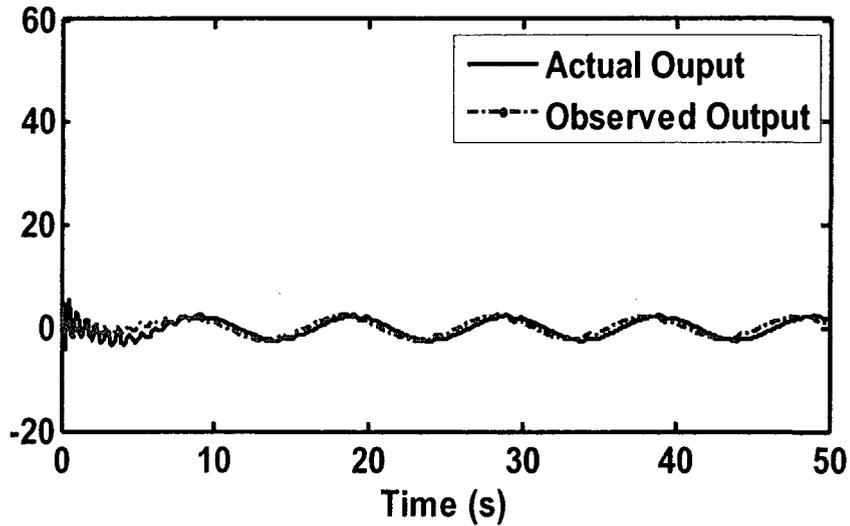
Figure 3.6 Observed hysteresis ouput $\hat{\tau}_{pr}$ and real hysteresis output τ_{pr}

3.5 Conclusion

In this chapter, an adaptive compensator was proposed for systems with Duhem hysteresis model representation. An augmented feed-forward MLP was used to approximate a complicated unknown piecewise continuous nonlinear function in the explicit solution to the differential equation of the Duhem model. The adaptive compensation algorithm and the weight matrix update rules for NN were derived to cancel out the effect of hysteresis. An observer was designed to estimate the value of the hysteresis output based on the input and output of the plant. With the designed pre-inversion compensator and observer, the stability of the integrated adaptive system and the boundedness of the tracking error were proved.

CHAPTER 4

ADAPTIVE CONTROL OF NONLINEAR SYSTEMS WITH

PRANDTL-ISHLINSKII HYSTERSIS MODEL REPRESENTATIONS

4.1 Introduction

In the literature, the most common approach to mitigate the effects of hysteresis is to construct an inverse operator, which was pioneered in [32], and recent progress can be found in [11, 12] and references therein. Essentially, constructing an inverse operator relies on the phenomenological modeling methods (say, using preisach models) and strongly influences the practical application of the design concept [75]. Because of the multi-valued and non-smoothness features of hysteresis, these methods are sometimes complicated, computationally costly and the model parameters are sensitive to unknown measurement errors. These issues are directly linked to the difficulties of stability analysis of these systems, except for certain special cases [32]. Thus, a question naturally rises: whether there is a possibility of mitigating the hysteresis nonlinearities, represented by appropriate hysteresis models, without necessarily constructing the inverse operators when the hysteresis nonlinearities precede general nonlinear systems, while taking into account the stability issue? This chapter will provide an affirmative answer to this question by selecting a typical operator-based Prandtl-Ishlinskii hysteresis model

representation and focusing on p-normal form systems, which have received much attention in the nonlinear control community [64-71].

The organization of this chapter is as follows. In Section 2, we recall the Prandtl-Ishlinskii model description based on play operators. Section 3 states the problem. The main results, including design of the parameter estimator, the re-treatment of the Prandtl-Ishlinskii model and the controller, are presented in Section 4. Conclusions are given in Section 5.

4.2 Review of the Prandtl-Ishlinskii Model

The Prandtl-Ishlinskii model can be defined by the stop or play hysteresis operators. The model defined by the stop operator is illustrated as follows:

$$w(t) = \int_0^R p(r)E_r[v](t)dr ,$$

where $p(r)$ is a given continuous density function, satisfying $p(r) > 0$ with $w(t) = \int_0^\infty rp(r)dr < \infty$; R is a constant such that $p(R)$ is close to zero.

As an alternative, the model can also be defined by the play operator as

$$w(t) = p_0 v(t) - \int_0^R p(r)F_r[v](t)dr \qquad (4.1)$$

where $p_0 = \int_0^R p(r)dr$ is a constant that only depends on the density function $p(r)$.

Remark 4.1: The treatment of the Prandtl-Ishlinskii model (4.1) as input signal $p_0 v(t)$, together with a shifting term $d[v](t)$, makes it possible to fuse the hysteresis with available control techniques to mitigate the hysteresis effects. This is our primary motivation for using the Prandtl-Ishlinskii model.

4.3 Problem Statement

The following inherently nonlinear system preceded by actuator hysteresis with Prandtl-Ishlinskii presentations is considered:

$$
\begin{aligned}
\dot{x}_1 &= x_2^{p_1} + \varphi_1(x_1)^T \theta_1 \\
\dot{x}_2 &= x_3^{p_2} + \varphi_2(x_1, x_2)^T \theta_2 \\
&\vdots \\
\dot{x}_i &= x_{i+1}^{p_i} + \varphi_i(x_1, \cdots, x_i)^T \theta_i \\
&\vdots \\
\dot{x}_n &= w(t) + \varphi_n(x_1, \cdots, x_n)^T \theta_n \\
y &= x_1,
\end{aligned}
\tag{4.2}
$$

where $(x_1, x_2, \cdots, x_n) \in R^n$ is the system state, $w(t)$ is the output of the Prandtl-Ishlinskii model (4.1) with $v(t)$ as an input, $\varphi_i(x_1, \cdots, x_i)$ is a smooth vector field, and θ_i is an unknown constant vector. For $i = 1, \cdots, n-1$, p_i is a positive odd integer.
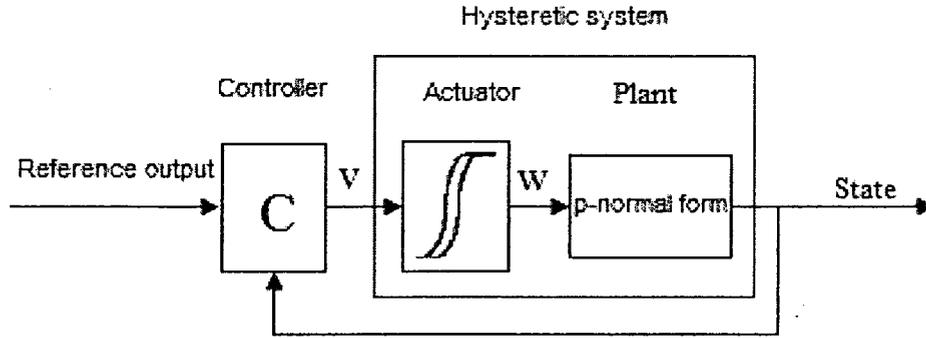
Figure 4.1 Configuration of the control system

The control objective is to design an adaptive feedback control law $v(t)$ that makes the output of system (4.2) follow a prescribed time varying reference signal, with an arbitrarily small tracking error and guarantees all signals of the closed-loop system are bounded, meanwhile mitigating the hysteretic effect without necessarily constructing a hysteresis inverse operator.

Global practically adaptive output tracking:

As [66] formulated, let $y_r(t)$ be a bounded C^1 reference signal whose derivative $\dot{y}_r(t)$ is also bounded. For any $\varepsilon > 0$, find, if possible, a dynamic controller of the form

$$v = \mu(x, \theta_1, \cdots, \theta_n, y_r(t))$$
$$\dot{\theta}_i = \eta_i(x_1, \cdots, x_{i+1}, \theta_1, \cdots, \theta_n),$$

(4.3)

where $\hat{\theta}_i$ is the estimation of system parameter θ_i, and $\beta_i(x_1, \cdots, x_i)$ is a smooth function to be designed later, such that:

67

(1). the states of closed-loop system (4.1), (4.2) and (4.3) are well-defined on $[0,+\infty)$ and globally bounded;

(2). for any $x(0) \in R^n$, there is a finite-time $T > 0$ such that the output of closed-loop system (4.1), (4.2) and (4.3) satisfies

$$|y(t) - y_r(t)| < \varepsilon, \quad \forall t \geq T > 0 \tag{4.4}$$

Before the end of this section, the first lemma is given here which is a consequence of Young's inequality.

Lemma 4.1[66]: For real numbers $a \geq 0$, $b > 0$, and $m \geq 1$, the following inequality holds:

$$a \leq b + \left[\frac{a}{m}\right]^m \cdot \left[\frac{m-1}{b}\right]^{m-1}. \tag{4.5}$$

4.4 Output Tracking Controller Design

In this section, a globally practical adaptive output tracking controller is designed for system (4.2) by combining I&I tools developed in [72] with the technique of adding a power integrator [64, 65]. The design procedure is mainly divided into the parameter estimator design, the particular treatment of the Prandtl-Ishlinskii model [10] and the controller design.

A. Parameter Estimator Design

Firstly, by I&I tools developed in [72], the error variable is defined as

$$z_i = \hat{\theta}_i - \theta_i + \beta_i(x_1, \cdots, x_i), \quad i = 1, 2, \cdots n \qquad (4.6)$$

where $\hat{\theta}_i$ is the estimate of θ_i, and $\beta_i(\cdot)$ is a smooth function yet to be defined.

Remark 4.2: It should be noted that the considered system (4.2) without considering actuator nonlinearity can be thought of as a special case of the systems considered in [65]. However, differing from [65], the proposed adaptive mechanism (4.6) does not need to follow the certainty equivalence principle. As it will be clarified later in the development, $\hat{\theta}_i$ is not directly used to update θ_i, instead, $\hat{\theta}_i + \beta_i(\cdot)$ is utilized to update θ_i.

Secondly, differentiating (4.6), the dynamics of z_i are given by the equation

$$\dot{z}_i = \dot{\hat{\theta}}_i + \sum_{k=1}^{i} \frac{\partial \beta_i}{\partial x_k} [x_{k+1}{}^{p_k} + \varphi_k(x_1, \cdots, x_k)^T$$
$$\cdot (\hat{\theta}_k + \beta_k(x_1, \cdots, x_k) - z_k)] \qquad (4.7)$$

with $x_{n+1} = w$.

The updating law can be selected as follows

$$\dot{\hat{\theta}}_i = -\sum_{k=1}^{i} \frac{\partial \beta_i}{\partial x_k} [x_{k+1} + \varphi_k(x_1, \cdots, x_k)^T (\hat{\theta}_k + \beta_k(x_1, \cdots, x_k)] \ . \qquad (4.8)$$

-Thus, the error dynamics are

$$\dot{z}_i = -\sum_{k=1}^{i} \frac{\partial \beta_i}{\partial x_k} \varphi_k(x_1, \cdots, x_k)^T z_k \ . \qquad (4.9)$$

Note that (4.9) is in lower triangular form.

In what follows, the selection of the functions $\beta_i(\cdot)$ and its assumption are adopted from [73].

In (4.9), the diagonal terms can be rendered negative semi-definite by selecting $\beta_i(\cdot)$ as

$$\beta_i(\cdots, x_i) = \int_0^{x_i} \kappa_i(\cdots, \chi_i)\varphi_i(\cdots, \chi_i)d\chi_i, \tag{4.10}$$

where $\kappa_i(\cdot)$ are positive functions.

The following assumption is needed [73].

Assumption 4.1: There exist a function $\kappa_i(\cdot)$ and a constant $\kappa_i(\cdot) \geq k_i > 0$ such that, for $j = 1, \cdots, i-1$,

$$\frac{\partial \beta_i}{\partial x_j} = \delta_{ij}(x_1, \cdots, x_i)\varphi_i(x_1, \cdots, x_i) \tag{4.11}$$

for some bounded functions $\delta_{ij}(\cdot)$, where $\beta_i(\cdot)$ is given by Equation (4.10).

In order to establish the stability properties of the estimator, the second lemma is given.

Lemma 4.2: Consider the system (4.9), with the functions $\beta_i(\cdot)$ given by (4.10), and suppose that Assumption 4.1 holds for all $i = 1, \cdots, n$. Then, there exist constants $\varepsilon_i > 0$ such that

$$\frac{d}{dt}(\sum_{i=1}^{n} \varepsilon_i z_i^{\mathrm{T}} z_i) \leq -\sum_{i=1}^{n} \left(\varphi_i(x_1, \cdots, x_i)^{\mathrm{T}} z_i \right)^2. \tag{4.12}$$

Proof: Similar to [73] and thus omitted here.

Remark 4.3: Since $\sum_{i=1}^{n} \varepsilon_i z_i^{\mathrm{T}} z_i$ is a decreasing function of time, $\sum_{i=1}^{n} \varepsilon_i z_i^{\mathrm{T}} z_i$ is upper

bounded by a constant (say M), i.e., $\sum_{i=1}^{n} \varepsilon_i z_i^{\mathrm{T}} z_i \le M$.

B. Special Treatment of the Prandtl-Ishlinskii Model

Here, the Prandtl-Ishlinskii model expressed through the play operator (4.1) is

considered. The hysteresis output $w(t)$ can be expressed as

$$w(t) = p_0 v(t) - d[v](t) , \qquad (4.13)$$

where

$$d[v](t) = \int_0^R p(r) F_r[v](t) dr .$$

Remark 4.4: The term $d[v](t)$ can be thought of as a shifting term or disturbance.

However, traditional methods for dealing with this shifting term cannot be directly

applied because it is an integral term and there is no conclusion on its boundedness. Since

the density function $p(r)$ is not a function of time, a special treatment is to be developed,

which is crucial for the fusion of the Prandtl-Ishlinskii model with the results of the

inherently nonlinear systems.

Remark 4.5: Since $p_0 = \int_0^R p(r)dr$ is a constant which depends only on the unknown

density function $p(r)$, it is an unknown constant. From (4.13), the hysteresis

nonlinearities also introduce the unknown control gain problem.

Hence, in order to develop the control law, the following assumption and definitions

are required, which are useful to derive the controller in the last step of the proposed

constructive approach.

Assumption 4.2: There exist known constants $p_{0\min}$, $p_{0\max}$ and $p_{\max}$, such that

$p_{0\min} < p_0 < p_{0\max}$ and $p(r) \leq p_{\max}$.

Remark 4.6: Based on the properties of the density function $p(r)$, it is reasonable to

set an upper bound $p_{\max}$ for $p(r)$. Here, $p_{0\min} > 0$ must be satisfied, otherwise

$p_0 = 0$ implies $w(t) = 0$.

We define

$$\tilde{p}(r,t) = p(r) - \hat{p}(r,t)$$
$$\tilde{\phi}(t) = \phi - \hat{\phi}(t)$$

where $\hat{p}(r,t)$ is an estimation of the density function $p(r)$ and $\hat{\phi}(t)$ is an estimation of

$\phi := 1/p_0$.

Letting

$$C(v(t)) := \int_0^R p(r)\left|F_r[v](t)\right|dr, \tag{4.14}$$

the estimation $\hat{C}(t)$ is described by

$$\hat{C}(t) := \int_0^R \hat{p}(r,t)|F_r[v](t)|dr, \tag{4.15}$$

which yields

$$\tilde{C}(t) = C(t) - \hat{C}(t) = \int_0^R [p(r) - \hat{p}(r,t)]|F_r[v](t)|dr. \tag{4.16}$$

C. Controller Design

In this subsection, we will first give a brief introduction to estimating solution trajectories from a differential inequality; then we propose a very useful lemma based on the abstract differential inequality estimation; finally, we design a global adaptively practical output tracking controller by combining the estimator design in the last subsection.

As proposed in [65], a sufficient condition for the existence of solutions to the practical control problem can be characterized by a Lyapunov-like inequality of the type

$$\frac{dV}{dt} \le -K(V) + \delta', \tag{4.17}$$

where δ' is a real constant, $K(\cdot)$ is a κ_∞ function and $V(\xi)$ is a C^1 function, and which is positive definite and proper. From (4.17), it is straightforward to conclude that there exists a finite time T such that

$$V(\xi(t)) < K^{-1}(2\delta'), \qquad \forall t \ge T > 0. \tag{4.18}$$

In fact, if we define $\Omega = \{\xi \mid V(\xi) \geq K^{-1}(2\delta')\}$, $\dot{V}(\xi)$ is strictly negative over Ω (particularly, on the boundary of Ω). As a result, $\xi(t)$ must enter the set $R^n - \Omega$ (described in Fig. 4.2) at a finite time and stay in the set for the future time. Namely, global boundedness of the state $\xi(t)$ is implied by (4.18). On the other hand, it is deduced from (4.18) that by tuning the parameter δ', $\|\xi(t)\|$ can be made arbitrarily small. This idea is the principle behind our adaptively practical output tracking, to be presented in this section.
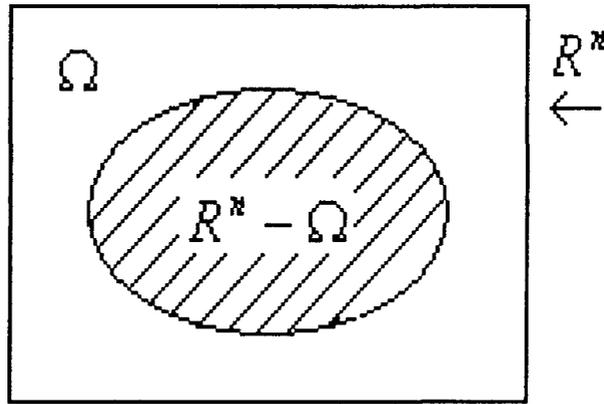
Figure 4.2 The set $R^n - \Omega$ entered by trajectories

Based on the above abstract estimation of the solution, we give the following lemma which estimates the state $\xi(t)$ explicitly.

Lemma 4.3: Let $p_i, i = 1,2,\cdots,n-1$ and $p_n = 1$ be odd positive integers and $p = \max\{p_i, i = 1, 2, \cdots, n\}$. Assume that there exist constants $\varepsilon_i, i = 1, 2, \cdots, n$, and a positive-definite and proper Lyapunov function

$$V = \sum_{i=1}^{n-1} \frac{\xi_i^{p-p_i+2}}{p-p_i+2} + \frac{\xi_n^{p+1}}{p+1} + \sum_{i=1}^{n} \frac{n+1-i}{2} \varepsilon_i z^T z + \frac{p_0}{2\eta} \tilde{\phi}^2 + \frac{1}{2q} \int_0^R \tilde{p}^2(t,r)dr \qquad (4.19)$$

which satisfies

$$\frac{dV}{dt} \le -\sum_{i=1}^{n} \xi_i^{p+1} + n\delta$$

where $0 < \delta < 1$ is a real constant, and $\xi_i(t)$ is a C^1 function of t. Then the following inequality holds after a finite time $T > 0$

$$\frac{\xi_i^{p-p_i+2}}{p-p_i+2} \le V \le 2\frac{\hat{c}\delta}{c(\delta)}$$

$$= \frac{2}{p+1}\left(\sum_{i=1}^{n} \frac{p_i-1}{p-p_i+2} + n + \frac{n\lambda}{2} \right) \cdot \delta^{2/(p+1)},$$

$$\forall t \ge T, i = 1, 2, \cdots, n.$$

Proof: Given any $\delta > 0$ and $i = 1, 2, \cdots, n$, defining $x = \delta^{1/(p+1)}$ and $y = \xi_i$, and using the well-known Young's inequality (i.e.,

$$x^{p_i-1}y^{p-p_i-1} \le \frac{p_i-1}{p+1} x^{p+1} + \frac{p-p_i+2}{p+1} y^{p+1}),$$

we have

$$-\xi_i^{p+1} \le -(p+1)\delta^{(p_i-1)/(p+1)} \frac{\xi_i^{p-p_i+2}}{p-p_i+2} + \frac{p_i-1}{p-p_i+2}\delta \qquad (4.20)$$

Using the same argument of [66] and inserting (4.20) into (4.19) can easily yield

$$\dot{V} \leq -c(\delta)V + \left(\sum_{i=1}^{n} \frac{p_i - 1}{p - p_i + 2} + n + \frac{n\lambda}{2} \right)\delta \tag{4.21}$$

$$= -c(\delta)V + \hat{c}\delta$$

where $c(\delta) = \min_{i=1,\cdots,n} \{(p+1)\delta^{(p-1)/(p+1)}, 1\} > 0$ and $\hat{c} = \left(\sum_{i=1}^{n} \frac{p_i - 1}{p - p_i + 2} + n + \frac{n\lambda}{2} \right)$.

By multiplying both sides of (4.21) with $e^{c(\delta)}$, we get

$$\frac{d}{dt}(e^{c(\delta)}V) \leq \hat{c}e^{c(\delta)} \tag{4.22}$$

Integrating both sides of (4.22) on interval $(0,t)$ yields

$$V \leq \frac{\hat{c}\delta}{c(\delta)} + e^{-c(\delta)}\left[V(0) - \frac{\hat{c}\delta}{c(\delta)} \right] \tag{4.23}$$

This implies that the states ξ are bounded and well defined on $[0,+\infty)$. Furthermore, we can get the conclusion from (4.23) that after a finite time T

$$\frac{\xi_i^{p-p_i+2}}{p - p_i + 2} \leq V \leq 2\frac{\hat{c}\delta}{c(\delta)}$$

hence, the conclusion is proved.

With the aid of lemmata 4.2 and 4.3, the adaptive controller is designed in an iterative manner by combining the adaptive mechanism with the modification of adding a power integrator. To this end, the main result of this paper is given below.

Theorem 4.1: Given a bounded smooth reference signal $y_r(t)$, whose derivative is also bounded, the global practically adaptive output tracking of system (4.2) can be achieved by a smooth state feedback adaptive controller of the form (4.3), if

$$\hat{\phi}(t_0) \in \Omega_\phi = \{\phi = 1/p_0 \mid 1/p_{0\max} \leq \phi \leq 1/p_{0\min}\} \tag{4.24}$$

76

$$\hat{p}(t_0, r) \in \Omega_p = \{\hat{p}(t_0, r) \mid 0 \leq \hat{p}(t, r) \leq p_{\max}, \forall r \in [0, R]\}$$

Proof: In what follows, the proof is given in a constructive way.

First, an odd positive integer is needed, i.e.

$$p = \max_{i=1,2,\cdots n-1} \{p_i\}.$$

Step 1: Given a bounded smooth reference signal $y_r(t)$, let $\xi_1 = x_1 - y_r$ be the error signal. Then its time derivative can be given as

$$\dot{\xi}_1 = \dot{x}_1 - \dot{y}_r$$
$$= x_2^{p_1} + \varphi_1(x_1)^T(\hat{\theta}_1 + \beta_1(x_1) - z_1) - \dot{y}_r$$

We construct the Lyapunov function

$$V_1(\xi_1, z_1) = \frac{\xi_1^{p-p_1+2}}{p - p_1 + 2} + \frac{1}{2}\varepsilon_1 z_1^T z_1$$

which is positive-definite and proper. By Lemma 4.2, its derivative is given by

$$\dot{V}_1 \leq \xi_1^{p-p_1+1}(x_2^{p_1} + \varphi_1(x_1)^T(\hat{\theta}_1 + \beta_1(x_1) - z_1) - \dot{y}_r) - \frac{1}{2}(\varphi_1(x_1)^T z_1)^2$$

$$= \xi_1^{p-p_1+1}[x_2^{p_1} + \varphi_1(x_1)^T(\hat{\theta}_1 + \beta_1(x_1)) - \dot{y}_r] - \xi_1^{p-p_1+1}\varphi_1(x_1)^T z_1 - \frac{1}{2}(\varphi_1(x_1)^T z_1)^2$$

$$\leq \xi_1^{p-p_1+1}[x_2^{p_1} + \varphi_1(x_1)^T(\hat{\theta}_1 + \beta_1(x_1)) - \dot{y}_r] + \frac{1}{2}\xi_1^{2(p-p_1+1)}.$$

Since $\dot{y}_r$ is assumed to be bounded, it can be shown that for any real number $\delta > 0$, using Lemma 4.1 by choosing

$$b = \delta, a = \left| \xi_1^{p-p_1+1} [\varphi_1(x_1)^T(\hat{\theta}_1 + \beta_1(x_1)) - \dot{y}_r] \right|, m = \frac{p+1}{p-p_1+1},$$

there always exists a smooth function $\rho_{11}(\xi_1, \hat{\theta}_1) \geq 0$ such that

$$\left| \xi_1^{p-p_1+1} [\varphi_1(x_1)^T(\hat{\theta}_1 + \beta_1(x_1)) - \dot{y}_r] \right| \leq \delta + \xi_1^{p+1} \rho_{11}(\xi_1, \hat{\theta}_1).$$

Hence, one has

$$\dot{V}_1 \leq \xi_1^{p-p_1+1} x_2^{p_1} + \delta + \xi_1^{p+1} \rho_{11}(\xi_1, \hat{\theta}_1) + \frac{1}{2} \xi_1^{2(p-p_1+1)}.$$

Then, the virtual smooth controller

$$x_2^* = -\xi_1 (n + \rho_{11}(\xi_1, \hat{\theta}_1) + \frac{1}{2} \xi_1^{p-2p_1+1})^{\frac{1}{p_1}}$$

$$:= -\xi_1 \alpha_1(\xi_1, \hat{\theta}_1), \quad \alpha_1(\xi_1, \hat{\theta}_1) > 0$$

renders the derivative of the Lyapunov function

$$\dot{V}_1 \leq -n\xi_1^{p+1} + \delta + \xi_1^{p-p_1+1}(x_2^{p_1} - x_2^{*p_1}) \tag{4.25}$$

Step 2 We define $\xi_2 = x_2 - x_2^*$. Since x_2^* is smooth, we have

$$\dot{\xi}_2 = x_3^{p_2} + \varphi_2(x_1, x_2)^T(\hat{\theta}_2 + \beta_2(x_1, x_2) - z_2)$$

$$- \frac{\partial x_2^*}{\partial x_1}[x_2^{p_1} + \varphi_1(x_1)^T(\hat{\theta}_1 + \beta_1(x_1) - z_1)]$$

$$- \frac{\partial x_2^*}{\partial \theta_1}\dot{\hat{\theta}}_1 - \frac{\partial x_2^*}{\partial y_r}\dot{y}_r.$$

We construct the Lyapunov function

$$V_2(\xi_1, \xi_2, z_1, z_2) = V_1 + \frac{\xi_2^{p-p_2+2}}{p-p_2+2} + \frac{1}{2}\sum_{i=1}^{2}\varepsilon_i z_i^{\mathrm{T}} z_i,$$

which is positive-definite and proper. Its derivative is given by

$$
\begin{aligned}
\dot{V}_2 &\leq n\xi_1^{p+1} + \delta + \xi_1^{p-p_1+1}(x_2^{p_1} - x_2^{*p_1}) \\
&\quad + \xi_2^{p-p_2+1}\{x_3^{p_2} + \varphi_2(x_1,x_2)^T(\hat{\theta}_2 + \beta_2(x_1,x_2) - z_2) \\
&\quad - \frac{\partial x_2^*}{\partial x_1}[x_2^{p_1} + \varphi_1(x_1)^T(\hat{\theta}_1 + \beta_1(x_1) - z_1)] \\
&\quad - \frac{\partial x_2^*}{\partial \theta_1}\dot{\hat{\theta}}_1 - \frac{\partial x_2^*}{\partial y_r}\dot{y}_r\} - \sum_{i=1}^{2}\left(\varphi_i(x_1,\cdots,x_i)^{\mathrm{T}} z_i\right)^2 \\
&= n\xi_1^{p+1} + \delta + \xi_1^{p-p_1+1}(x_2^{p_1} - x_2^{*p_1}) \\
&\quad + \xi_2^{p-p_2+1}\{[x_3^{p_2} + \varphi_2(x_1,x_2)^T(\hat{\theta}_2 + \beta_2(x_1,x_2)] \\
&\quad - \frac{\partial x_2^*}{\partial x_1}[x_2^{p_1} + \varphi_1(x_1)^T(\hat{\theta}_1 + \beta_1(x_1)] - \frac{\partial x_2^*}{\partial \theta_1}\dot{\hat{\theta}}_1 - \frac{\partial x_2^*}{\partial y_r}\dot{y}_r\} \\
&\quad - \xi_2^{p-p_2+1}\varphi_2(x_1,x_2)^T z_2 - \xi_2^{p-p_2+1}\frac{\partial x_2^*}{\partial x_1}\varphi_1(x_1)^T z_1 \\
&\quad - \sum_{i=1}^{2}\left(\varphi_i(x_1,\cdots,x_i)^{\mathrm{T}} z_i\right)^2
\end{aligned}
\tag{4.26}
$$

Note that

$$
\begin{aligned}
\left|\xi_1^{p-p_1+1}(x_2^{p_1} - x_2^{*p_1})\right| &\leq p_1\left|\xi_1^{p-p_1+1}\right|\left\|x_2 - x_2^*\right\|\left|x_2^{p_1-1} + x_2^{*p_1-1}\right| \\
&= p_1\left|\xi_1^{p-p_1+1}\right|\left|\xi_2\right| \cdot ((\xi_2 - \xi_1\bar{\alpha}_1(\xi_1,\hat{\theta}_1))^{p_1-1} \\
&\quad + (\xi_1\alpha_1(\xi_1,\hat{\theta}_1))^{p_1-1}).
\end{aligned}
$$

Using $|x+y|^p \leq 2^{p-1}(|x|+|y|)$, we have

$$\left| \xi_1^{p-p_1+1}(x_2^{p_1} - x_2^{*p_1}) \right| \le p_1 \left(\left| \xi_1^{p-p_1+1} \right| \left| \xi_2^{p_1} \right| 2^{p_1-2} \right.$$

$$+ \left| \xi_1^{p} \right| \left| \xi_2 \right| [\alpha_1(\xi_1, \hat{\theta}_1)]^{p_1-1} (1 + 2^{p_1-2})) \quad (4.27)$$

$$\le \xi_1^{p+1} + \xi_2^{p+1} \overline{\rho}_{21}(\xi_1, \xi_2, \hat{\theta}_1)$$

for a smooth non-negative function $\overline{\rho}_{21}(\xi_1, \xi_2, \hat{\theta}_1)$. And this last relation follows from Young's inequality.

Because of the boundedness of the output and its derivative, like in step 1, by using Lemma 4.1, there always exists a smooth function $\rho_{22}(\xi_1, \xi_2, \hat{\theta}_1, \hat{\theta}_2) \ge 0$ such that

$$\left| \xi_2^{p-p_2+1} \{ [\varphi_2(x_1, x_2)^T (\hat{\theta}_2 + \beta_2(x_1, x_2) - \frac{\partial x_2^*}{\partial x_1} [x_2^{p_1} + \varphi_1(x_1)^T (\hat{\theta}_1 + \beta_1(x_1)] - \frac{\partial x_2^*}{\partial \theta_1} \dot{\hat{\theta}}_1 - \frac{\partial x_2^*}{\partial y_r} \dot{y}_r \} \right|$$

$$\le \xi_2^{p+1} \rho_{22}(\xi_1, \xi_2, \hat{\theta}_1, \hat{\theta}_2) + \delta \quad (4.28)$$

Using $a^2 + b^2 \ge 2ab$ for the last three terms in (4.26), and inserting (4.27), and (4.28) into (4.26), yields

$$\dot{V}_2 \le -(n-1)\xi_1^{p+1} + \xi_2^{p-p_2+1} x_3^{p_2} + \xi_2^{p+1} [\overline{\rho}_{21}(\xi_1, \xi_2, \hat{\theta}_1) + \rho_{22}(\xi_1, \xi_2, \hat{\theta}_1, \hat{\theta}_2)]$$

$$+ \frac{1}{2} \xi_2^{2(p-p_2+1)} \left[1 + \left(\frac{\partial x_2^*}{\partial x_1} \right)^2 \right] + 2\delta,$$

Thus, we can select a virtual smooth controller

$$x_3^* = -\xi_2 \left(n - 1 + \overline{\rho}_{21}(\xi_1, \xi_2, \hat{\theta}_1) + \rho_{22}(\xi_1, \xi_2, \hat{\theta}_1, \hat{\theta}_2) + \frac{1}{2} \xi_1^{p-2p_1+1} \left[1 + \left(\frac{\partial x_2^*}{\partial x_1} \right)^2 \right] \right)^{\frac{1}{p_2}}$$

$$= -\xi_2 \alpha_2(\xi_1, \xi_2, \hat{\theta}_1, \hat{\theta}_2), \quad \alpha_2(\xi_1, \xi_2, \hat{\theta}_1, \hat{\theta}_2) > 0$$

to render

$$\dot{V}_2 \leq -(n-1)(\xi_1^{p+1} + \xi_2^{p+1}) + \xi_2^{p-p_2+1}(x_3^{p_2} - x_3^{*p_2}) + 2\delta .$$

Inductive Step:

Suppose at step $k-1$, there are a set of smooth virtual controllers $x_1^*, \cdots, x_k^*$, defined by

$$
\begin{aligned}
x_1^* &= y_r & \xi_1 &= x_1 - x_1^* \\
x_2^* &= -\xi_1 \alpha_1(\xi_1, \theta_1) & \xi_2 &= x_2 - x_2^* \\
&\vdots & &\vdots \\
x_k^* &= -\xi_{k-1}\alpha_{k-1}(\xi_1, \cdots \xi_{k-1}, \theta_1, \cdots \theta_{k-1}) & \xi_k &= x_k - x_k^*
\end{aligned}
\tag{4.29}
$$

with $\alpha_1(\xi_1, \theta_1) > 0, \cdots, \alpha_{k-1}(\xi_1, \cdots \xi_{k-1}, \theta_1, \cdots \theta_{k-1}) > 0$ being smooth, such that

$$
\begin{aligned}
\dot{V}_{k-1} \leq &-(n-k+2)(\xi_1^{p+1} + \cdots + \xi_{k-1}^{p+1}) \\
&+ \xi_{k-1}^{p-p_{k-1}+1}(x_k^{p_{k-1}} - x_k^{*p_{k-1}}) + (k-1)\delta,
\end{aligned}
\tag{4.30}
$$

where

$$V_{k-1} = \sum_{i=1}^{k-1} \frac{\xi_i^{p-p_i+2}}{p-p_i+2} + \sum_{i=1}^{k-1} \frac{k-i}{2} \varepsilon_i z_i^T z_i$$

is a positive definite and proper Lyapunov function.

Using the inequalities

$$\left| \xi_{k-1}^{p-p_{k-1}+1}(x_k^{p_{k-1}} - x_k^{*p_{k-1}}) \right|$$

$$\leq \xi_1^{p+1} + \cdots + \xi_{k-1}^{p+1} + \xi_k^{p+1} \overline{\rho}_{k1}(\xi_1, \cdots, \xi_k, \hat{\theta}_1, \cdots, \hat{\theta}_{k-1})$$

$$\mid \xi_k^{p-p_k+1}\{(\varphi_k(\cdot)^T(\hat{\theta}_k + \beta_k(\cdot)) -$$

$$\sum_{j=1}^{k-1}\frac{\partial x_k^*}{\partial x_j}[x_{j+1}^{p_1} + \varphi_j(\cdot)^T(\hat{\theta}_j + \beta_j(\cdot)] - \sum_{j=1}^{k-1}\frac{\partial x_k^*}{\partial \hat{\theta}_j}\dot{\hat{\theta}}_j - \frac{\partial x_k^*}{\partial y_r}\dot{y}_r \mid \qquad (4.31)$$

$$\leq \delta + \xi_k^{p+1}\rho_{k2}(\xi_1,\cdots,\xi_k,\hat{\theta}_1,\cdots,\hat{\theta}_k)$$

one can claim that inequality (4.31) also holds at step k. To prove this claim, one considers the following Lyapunov function.

$$V_k = V_{k-1} + \frac{\xi_k^{p-p_k+2}}{p-p_k+2} + \frac{1}{2}\sum_{i=1}^{k}\varepsilon_i z_i^{T}z_i . \qquad (4.32)$$

Using (4.30), the dynamics of (4.32) can be given by

$$\dot{V}_k \leq -(n-k+2)(\xi_1^{p+1}+\cdots+\xi_{k-1}^{p+1}) + \xi_{k-1}^{p-p_{k-1}+1}(x_k^{p_{k-1}} - x_k^{*\,p_{k-1}}) + (k-1)\delta$$

$$+ \xi_k^{p-p_k+1}\{x_{k+1}^{p_k} + \varphi_k(x_1,\cdots,x_k)^T(\hat{\theta}_k + \beta_k(x_1,\cdots,x_k) - z_k)$$

$$-\sum_{j=1}^{k-1}\frac{\partial x_k^*}{\partial x_j}[x_{j+1}^{p_1} + \varphi_j(x_1,\cdots,x_j)^T(\hat{\theta}_j + \beta_j(x_1,\cdots,x_j) - z_j)]$$

$$-\sum_{j=1}^{k-1}\frac{\partial x_k^*}{\partial \hat{\theta}_j}\dot{\hat{\theta}}_j - \frac{\partial x_k^*}{\partial y_r}\dot{y}_r\} - \sum_{i=1}^{k}\left(\varphi_i(x_1,\cdots,x_i)^T z_i\right)^2$$

$$= -(n-k+2)(\xi_1^{p+1}+\cdots+\xi_{k-1}^{p+1}) + \xi_{k-1}^{p-p_{k-1}+1}(x_k^{p_{k-1}} - x_k^{*\,p_{k-1}}) + (k-1)\delta$$

$$+ \xi_k^{p-p_k+1}x_{k+1}^{p_k} + \xi_k^{p-p_k+1}\{(\varphi_k(x_1,\cdots,x_k)^T(\hat{\theta}_k + \beta_k(x_1,\cdots,x_k))$$

$$-\sum_{j=1}^{k-1}\frac{\partial x_k^*}{\partial x_j}[x_{j+1}^{p_1} + \varphi_j(x_1,\cdots,x_k)^T(\hat{\theta}_j + \beta_j(x_1,\cdots,x_j)] - \sum_{j=1}^{k-1}\frac{\partial x_k^*}{\partial \hat{\theta}_j}\dot{\hat{\theta}}_j - \frac{\partial x_k^*}{\partial y_r}\dot{y}_r\}$$

$$- \xi_k^{p-p_k+1}\varphi_k(x_1,\cdots,x_k)^T z_k + \xi_k^{p-p_k+1}\left(\sum_{j=1}^{k-1}\frac{\partial x_k^*}{\partial x_j}\varphi_j(x_1,\cdots,x_j)^T z_j\right)$$

$$-\sum_{i=1}^{k}\left(\varphi_i(x_1,\cdots,x_i)^T z_i\right)^2. \qquad (4.33)$$

Similar to the step 2, it is not difficult to prove that the following relations hold.

$$\left| \xi_{k-1}^{p-p_{k-1}+1} (x_k^{p_{k-1}} - x_k^{*p_{k-1}}) \right| \le \xi_1^{p+1} + \cdots + \xi_{k-1}^{p+1} + \xi_k^{p+1} \overline{\rho}_{k1}(\xi_1, \cdots, \xi_k, \hat{\theta}_1, \cdots, \hat{\theta}_{k-1}) \tag{4.34}$$

$$\left| \xi_k^{p-p_k+1} \{ (\varphi_k(\cdot)^T (\hat{\theta}_k + \beta_k(\cdot)) - \sum_{j=1}^{k-1} \frac{\partial x_k^*}{\partial x_j} [x_{j+1}^{p_1} + \varphi_j(\cdot)^T (\hat{\theta}_j + \beta_j(\cdot))] - \sum_{j=1}^{k-1} \frac{\partial x_k^*}{\partial \hat{\theta}_j} \dot{\hat{\theta}}_j - \frac{\partial x_k^*}{\partial y_r} \dot{y}_r \right|$$
$$\le \delta + \xi_k^{p+1} \rho_{k2}(\xi_1, \cdots, \xi_k, \hat{\theta}_1, \cdots, \hat{\theta}_k) \tag{4.35}$$

where $\overline{\rho}_{k1}(\cdot), \rho_{k2}(\cdot)$ are nonnegative smooth functions.

Putting (4.33), (4.34) and (4.35) together, we have

$$\dot{V}_k \le -(n - k + 1)(\xi_1^{p+1} + \cdots + \xi_{k-1}^{p+1})$$
$$+ \xi_k^{p-p_k+1} x_{k+1}^{p_k} + \xi_k^{p+1} [\overline{\rho}_{k1}(\cdot) + \rho_{k2}(\cdot)]$$
$$+ \frac{1}{2} \xi_2^{2(p-p_2+1)} \left[1 + \left(\sum_{j=1}^{k-1} \frac{\partial x_k^*}{\partial x_j} \right)^2 \right] + k\delta.$$

We can select the virtual smooth controller as follows

$$x_{k+1}^* = -\xi_k \left(n - k + 1 + \overline{\rho}_{k1} + \rho_{k2} + \frac{1}{2} \xi_1^{p-2p_1+1} \left[1 + \left(\sum_{j=1}^{k-1} \frac{\partial x_k^*}{\partial x_j} \right)^2 \right] \right)^{\frac{1}{p_2}}$$
$$= -\xi_k \alpha_k(\xi_1, \cdots, \xi_k, \hat{\theta}_1, \cdots, \hat{\theta}_k), \qquad \alpha_k(\xi_1, \cdots, \xi_k, \hat{\theta}_1, \cdots, \hat{\theta}_k) > 0.$$

Hence,

$$\dot{V}_k \le -(n - k + 1)(\xi_1^{p+1} + \cdots + \xi_k^{p+1}) + \xi_k^{p-p_k+1} (x_{k+1}^{p_k} - x_{k+1}^{*p_k}) + k\delta$$

Similarly, it can be shown that the claim holds until $k = n - 1$.

Step n: now, considering the positive-definite function

$$V_n = V_{n-1} + \frac{\xi_n^{p+1}}{p+1} + \frac{1}{2}\sum_{i=1}^{n}\varepsilon_i z_i^{\mathrm{T}} z_i + \frac{p_0}{2\eta}\tilde{\phi}^2 + \frac{1}{2q}\int_0^R \tilde{p}^2(t,r)dr$$

and computing the time derivative, one gets

$$\dot{V}_n \leq -2(\xi_1^{p+1} + \cdots + \xi_{n-1}^{p+1}) + \xi_{n-1}^{p-p_{n-1}+1}(x_n^{p_{n-1}} - x_n^{*p_{n-1}}) + (n-1)\delta$$
$$+ \xi_n^p[w + \varphi_n(x_1,\cdots,x_n)^T\theta_n - \sum_{j=1}^{n-1}\frac{\partial x_n^*}{\partial x_j}(x_{j+1}^{p_j} + (\varphi_j(\cdot)^T\theta_j))$$
$$- \frac{\partial x_n^*}{\partial y_r}\dot{y}_r] - \frac{1}{2}\sum_{i=1}^{n}\left(\varphi_i(x_1,\cdots,x_i)^T z_i\right)^2$$
$$\frac{p_0}{\eta}\tilde{\phi}\dot{\hat{\phi}} + \frac{1}{q}\int_0^R \tilde{p}(t,r)\tfrac{\partial}{\partial t}\tilde{p}(t,r)dr$$

Therefore, the above inequality becomes

$$\dot{V}_n \leq -(\xi_1^{p+1} + \cdots + \xi_n^{p+1}) + n\delta + \xi_n^{p+1}\overline{\rho}_{n1}(\xi_1,\cdots,\xi_n,\hat{\theta}_1,\cdots,\hat{\theta}_{n-1})$$
$$+ \xi_n^{p+1}\rho_{n2}(\xi_1\cdots,\xi_n,\hat{\theta}_1,\cdots,\hat{\theta}_n) + \frac{1}{2}\xi_2^{2p}\left[1 + \left(\sum_{j=1}^{n-1}\frac{\partial x_n^*}{\partial x_j}\right)^2\right]$$
$$+ \xi_n^p w + \frac{p_0}{\eta}\tilde{\phi}\dot{\hat{\phi}} + \frac{1}{q}\int_0^R \tilde{p}(t,r)\tfrac{\partial}{\partial t}\tilde{p}(t,r)dr$$

Since one has $w(t) = p_0 v(t) - d[v](t)$, $p_0 = \dfrac{1}{\phi}$ and the controller of the form $v(t) = \hat{\phi}v_1(t)$ is

proposed, one obtains

$$p_0 v(t) = p_0 \hat{\phi}v_1(t) = v_1(t) - p_0\tilde{\phi}v_1(t)$$

Hence, the derivative of the Lyapunov function satisfies

$$\dot{V}_n \leq -(\xi_1^{p+1} + \cdots + \xi_n^{p+1}) + n\delta + \xi_n^{p+1}\overline{\rho}_{n1}(\xi_1, \cdots, \xi_n, \hat{\theta}_1, \cdots, \hat{\theta}_{n-1})$$

$$+ \xi_n^{p+1}\rho_{n2}(\xi_1 \cdots, \xi_n, \hat{\theta}_1, \cdots, \hat{\theta}_n) + \frac{1}{2}\xi_2^{2p}\left[1 + \left(\sum_{j=1}^{n-1}\frac{\partial x_n^*}{\partial x_j}\right)^2\right]$$

$$+ \xi_n^p(v_1(t) - d[v](t)) + \frac{p_0}{\eta}\tilde{\phi}(\dot{\hat{\phi}} - \eta v_1 \xi_n^p)$$

$$+ \frac{1}{q}\int_0^R \tilde{p}(t,r)\frac{\partial}{\partial t}\tilde{p}(t,r)dr$$

Thus, the control law can be designed by

$$v(t) = \hat{\phi}(t) \cdot v_1(t)$$
$$v_1(t) = (u_p + u_h) \tag{4.36}$$

$$u_p = -\xi_n[1 + \overline{\rho}_{n1}(\cdot) + \rho_{n2}(\cdot)]$$
$$- \frac{1}{2}\xi_n^p \cdot \left[1 + \left(\sum_{j=1}^{n-1}\frac{\partial x_n^*}{\partial x_j}\right)^2\right] \tag{4.37}$$

$$u_h = sign(\xi_n)\hat{C} \tag{4.38}$$

where $\overline{\rho}_{n1}(\cdot), \rho_{n2}(\cdot)$ are the corresponding terms in (4.31) in which $n = k$, and their

updating laws for parameters of the hysteresis model are chosen as:

$$\hat{C}(t) = \int_0^R \hat{p}(r,t)|F_r[v](t)|dr$$

$$\frac{\partial}{\partial t}\hat{p}(t,r) = \begin{cases} 0 & if \hat{p}_c(t,r) = p_{\max} \\ q|F_r[v(t)]|\xi_n^p| & if \hat{p}_c(t,r) = p_{\max} \end{cases} \tag{4.39}$$

$$\dot{\hat{\phi}}(t) = \begin{cases} 0 & \text{if } \hat{\phi} = \dfrac{1}{p_{0\min}} \text{ and } \eta v_1 \xi_n^P < 0 \\[2mm] & \text{if}\,[\dfrac{1}{p_{0\max}} < \hat{\phi} < \dfrac{1}{p_{0\min}}] \\[2mm] -\eta v_1 \xi_n^P & \text{or}\,[\hat{\phi} = \dfrac{1}{p_{0\min}} \text{ and } \eta v_1 \xi_n^P \geq 0] \\[2mm] & \text{or}\,[\hat{\phi} = \dfrac{1}{p_{0\max}} \text{ and } \eta v_1 \xi_n^P \leq 0] \\[2mm] 0 & \text{if } \hat{\phi} = \dfrac{1}{p_{0\max}} \text{ and } \eta v_1 \xi_n^P > 0 \end{cases} \tag{4.40}$$

where $r \in [0, R]$, q is a constant, and ξ_n is the n-th state of the error dynamics.

Hence, one obtains

$$\begin{aligned} \dot{V}_n \leq &-(\xi_1^{p+1} + \cdots + \xi_n^{p+1}) + n\delta \\ &- \xi_n^P sign(\xi_n)\hat{C} + |d[v](t)|\|\xi_n^P| + \frac{p_0}{\eta}\tilde{\phi}(\dot{\hat{\phi}} - \eta v_1 \xi_n^P) \\ &+ \frac{1}{q}\int_0^R \tilde{p}(t,r)\tfrac{\partial}{\partial t}\tilde{p}(t,r)dr \\ =&-(\xi_1^{p+1} + \cdots + \xi_n^{p+1}) + n\delta \\ &-|\xi_n^P|\tilde{C} + \int_0^R \tilde{p}(t,r)q|F_r[v](t)|\|\xi_n^P|dr \\ =&-(\xi_1^{p+1} + \cdots + \xi_n^{p+1}) + n\delta \end{aligned} \tag{4.41}$$

In virtue of Lemma 3, (4.41) immediately implies that all the solutions of the closed-loop systems are globally bounded and well defined over $[0,+\infty)$. This leads to the fact that the states $(x_1, \cdots, x_n)$ are globally bounded, due to the relation (4.29) and the boundedness of y_r.

Moreover, from Lemma 3, for any $\delta > 0$, there exists a finite time T, such that

$$|y - y_r(t)| = |\xi| \le \left[\frac{2(p - p_1 + 2)}{p+1} \left(\sum_{i=1}^{n} \frac{p_i - 1}{p - p_i + 2} + n + \frac{n\lambda}{2} \right) \cdot \delta^{2/(p+1)} \right]^{1/(p - p_1 + 2)}$$

$$\forall t \ge T > 0.$$

Hence, for any $\mu > 0$, there is a $\delta(\mu)$ such that

$$|y - y_r(t)| < \mu \qquad \forall t \ge T > 0.$$

Remark 4.7: The conditions (4.24) are the price paid for the boundedness of $\frac{p_0}{2\eta} \tilde{\phi}^2$

and $\frac{1}{2q} \int_0^R \tilde{p}^2(t,r) dr$ in (4.19), which is required to obtain practical tracking. The conditions

(4.24) imply that (4.34) and (4.35) are locally bounded, which were originally introduced

by the unknown density function of the Prandtl-Ishlinskii model.

Remark 4.8: The function $\hat{C}(t) = \int_0^R \hat{p}(r,t) |F_r[v](t)| dr$ in the implementation can be

computed using numerical techniques by replacing the integration with the

sum $\hat{C}(t) = \sum_{l=0}^{N-1} \hat{p}_r(l\Delta r, t) |F_{l\Delta r}[v](t)| \Delta r$ where N determines the size of the intervals of R

such that $\Delta r = R / N$. The selection of the size of the intervals depends on the required

accuracy requirement.

4.5 Conclusion

This chapter has proposed an adaptive control scheme of inherently nonlinear

systems preceded by an unknown hysteresis, represented by the Prandtl-Ishlinskii model.

The main contributions are twofold: (i) The challenge of how to fuse hysteresis models

with available adaptive control techniques to cope with control problems of inherently

nonlinear systems has been addressed; (ii) The new adaptive mechanism has been

87

combined with the technique of adding a power integrator under the framework of I&I tools. This scheme ensures that all signals of closed-loop systems are bounded, while practically keeping the output tracking error to an arbitrary small neighbourhood around the origin and mitigating the effects of unknown hysteresis, without necessarily constructing a hysteresis inverse operator.

CHAPTER 5

SLIDING MODE CONTROL FOR NONLINEAR SYSTEMS WITH PLAY-LIKE OPERATORS-BASED HYSTERESIS MODEL REPRENSENTATIONS

5.1 Introduction

As mentioned in Chapter 4, those inversion compensation methods may bring mathematical complications, computational costs, and high sensitivity of the model parameters to unknown measurement errors, and difficulties for the stability analysis of systems. Motivated by mitigating the hysteresis nonlinearities without necessarily constructing the inverse operators in the last Chapter, one may ask whether there are other hysteresis models in the literature or whether a new hysteresis can be developed to share the same facilitation as the Prandtl-Ishlinskii hysteresis model representation has. This chapter focuses on this issue by developing a new hysteresis model using play-like operators [17, 18] and thus provides an alternative hysteresis model for this mitigation of the hysteresis nonlinearities.

Thus, a sliding mode based control design is developed for a class of systems preceded by this new class of hysteresis models.

The organization of this chapter is as follows. Section 5.2 gives the problem statement. In Section 5.3, the class of hysteresis models based on play-like operators is constructed and its properties are explored. The details about sliding mode control design for the nonlinear system with the newly developed hysteresis model is presented in

Section 5.4. Simulation results are given in Section 5.5. Section 5.6 concludes this paper with some brief remarks.

5.2 Problem Statement

Consider a nonlinear plant preceded by an actuator with a hysteresis nonlinearity, i.e., the hysteresis is presented as an input for the nonlinear plant. The hysteresis is denoted as an operator

$$w(t) = P[v](t),\tag{5.1}$$

where $v(t)$ is the input and $w(t)$ is the output. The operator $P[v]$ will be constructed in detail in the next section. The nonlinear dynamic system preceded by the above hysteresis is described in canonical form as

$$x^{(n)}(t) + \sum_{i=1}^{k} a_i Y_i(x(t), \dot{x}(t), \cdots, x^{(n-1)}(t)) = bw(t),\tag{5.2}$$

where $X = [x, \dot{x}, \cdots, x^{(n-1)}]^T$ is the plant state vector, $Y_i(i = 1, \cdots, k)$ are known continuous linear or nonlinear functions, and parameters a_i and control gain b are unknown constants. It is commonly assumed that the sign of b is known. Without losing generality, we assume b is greater than zero. It should be noted that more general classes of nonlinear systems can be transformed into this structure [76].

90
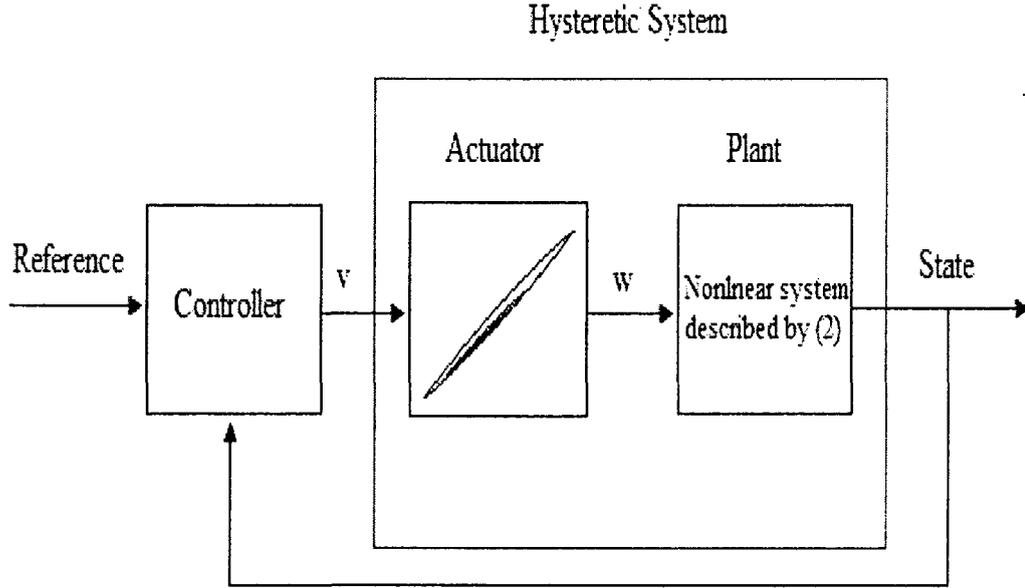
Figure 5.1 Configuration of the hysteretic system

The control objective is to design a controller $v(t)$ in (5.2), as shown in Figure 5.1, to make the plant state $X(t)$ to track a specified desired trajectory $X_d(t)$ with a certain precision, i.e., $\|X(t) \to X_d(t)\| \leq \varsigma$ as $t \to \infty$ with ς being a positive constant.

Throughout this paper the following assumption is made.

Assumption 5.1: The desired trajectory $X_d = [x_d, \dot{x}_d, \cdots, x_d^{(n-1)}]^T$ is continuous. Furthermore, $[X_d^T, x_d^{(n)}]^T \in \Omega_d \subset R^{n+1}$ with Ω_d is a compact set.

5.3 Hysteresis Model Based on Play-like Operators

In this section, we first recall the play-like operator [17, 18] which serves as the elementary hysteresis operator. In other words, the play-like operator plays the role of

91

building blocks. Then, we will show how the hysteresis model is constructed by using the play-like operator and, finally, some useful properties of this model will be explored.

5.3.1 Play-like Operator

Let's assume there is an alternating string of distinct real numbers $\{v_i\}_{i=-2n+2}^{-1}$ such that $\{v_{2i}\}_{i=-n+1}^{-1}$ is strictly decreasing and $\{v_{2i+1}\}_{i=-n+1}^{-1}$ is strictly increasing with $v_{-1} < v_{-2}$. Operator $w(t) = F_{\frac{c}{a_0}}[v;v]$ is defined by

$$w^{(n)} + sign(\dot{v})a_{n-1}w^{(n-1)} + \cdots + (sign(\dot{v}))^{n-1}d(w^{(1)},w,v) = 0,$$

where $d(w^{(1)},w,v) = a_1(w^{(1)} - 1) + sign(\dot{v})a_0(w-v) + c$ and $w^{(k)}$ denotes the $k-th$ derivatives of w with respect to v and $a_m > 0$ for all m. For simplicity, we consider the play-like operator generated from the 1st order differential equation below, namely backlash-like operator

$$\frac{dF}{dt} = \alpha \left|\frac{dv}{dt}\right|(cv - F) + B_1\frac{dv}{dt},$$ (5.3)

where α, c, and B_1 are constants satisfying $c > B_1$ [17].

The solution to (5.3) can be obtained explicitly for piecewise monotone v as follows:

$$F(t) = cv(t) + [F_0 - cv_0]e^{-\alpha(v-v_0)\,\mathrm{sgn}\,\dot{v}} + e^{-\alpha v\,\mathrm{sgn}\,\dot{v}}\int_{v_0}^{v}[B_1 - c]e^{\alpha\zeta\,(\mathrm{sgn}\,\dot{v})}d\zeta$$ (5.4)

for $\dot{v}$ constant and $w(v_0) = w_0$. Equation (5.4) can also be rewritten as

$$F(t) = \begin{cases} cv(t) + [F_0 - cv_0]e^{-\alpha(v-v_0)} + e^{-\alpha v}\dfrac{B_1 - c}{\alpha}(e^{\alpha v} - e^{\alpha v_0}), & \dot{v} > 0, \\[3mm] cv(t) + [F_0 - cv_0]e^{\alpha(v-v_0)} + e^{\alpha v}\dfrac{B_1 - c}{-\alpha}(e^{-\alpha v} - e^{-\alpha v_0}), & \dot{v} < 0. \end{cases} \qquad (5.5)$$

It is worth noting that

$$\lim_{v \to +\infty}(F(v) - cv) = -\frac{c - B_1}{\alpha}$$

$$\lim_{v \to -\infty}(F(v) - cv) = \frac{c - B_1}{\alpha}$$

$$(5.6)$$

Hence, solution $F(t)$ exponentially converges the output of a play operator with

threshold $r = \dfrac{c - B_1}{\alpha}$ and switches between lines $cv + \dfrac{c - B_1}{\alpha}$ and $cv - \dfrac{c - B_1}{\alpha}$. We will

construct a hysteresis model based on the above play-like (i.e., backlash-like) operator in

the next subsection, similar to the construction of the well-known Prandtl-Ishilinskii

model from play operators.

5.3.2 Construction of the Hysteresis Model

We are now ready to construct a class of hysteresis models through a weighted

superposition of the elementary play-like operator $F_r[v](t)$, in a similar way to *L.*

Prandtl's [10] construction of the Prandtl-Ishilinskii model using play operators.

Keeping $r = \dfrac{c - B_1}{\alpha}$ in mind and, without losing generality, setting $F(v(0) = 0) = 0$,

we rewrite equation (5.5) as

$$
F_r(t) = \begin{cases} v(t) - r + re^{\frac{-(c-B_1)}{r}v}, & \dot{v} > 0 \\ v(t) + r - re^{\frac{c-B_1}{r}v}, & \dot{v} < 0 \end{cases} \tag{5.7}
$$

where r is the positive threshold of the backlash-like operator (due to $c > B_1$).

To this end, we construct the hysteresis model as follows:

$$
w(t) = \int_{0+\varepsilon}^{R} p(r) F_r[v](t) dr, \tag{5.8}
$$

where ε is a sufficiently small positive constant, $p(r)$ is a given continuous density function satisfying $p(r) \geq 0$ with $\int_{0+\varepsilon}^{\infty} p(r) dr < +\infty$, and is expected to be identified from experimental data [8, 10]. Since it is reasonable to assume that the density function $p(r)$ vanishes for large values of r [10], the choice of $R = +\infty$ as the upper limit of integration in the literature is just a matter of convenience [10].

Inserting (5.7) into (5.8) yields

$$
w[v](t) = \begin{cases} \int_{0+\varepsilon}^{R} p(r) dr \cdot v(t) + \int_{0+\varepsilon}^{R} p(r)(-r + re^{\frac{-(c-B_1)}{r}v}) dr, & \dot{v} > 0 \\ \int_{0+\varepsilon}^{R} p(r) dr \cdot v(t) + \int_{0+\varepsilon}^{R} p(r)(+r - re^{\frac{c-B_1}{r}v}) dr, & \dot{v} < 0 \end{cases} \tag{5.9}
$$

Also, hysteresis (5.9) can be expressed as

$$
w(t) = p_0 v + \begin{cases} \int_{0+\varepsilon}^{R} p(r)(-r + re^{\frac{-(c-B_1)}{r}v}) dr, & \dot{v} > 0 \\ \int_{0+\varepsilon}^{R} p(r)(r - re^{-\frac{c-B_1}{r}v}) dr, & \dot{v} < 0, \end{cases} \tag{5.10}
$$

where $p_0 = \int_{0+\varepsilon}^{R} p(r) dr$ is a constant which depends on the density function $p(r)$.

94

Property 5.1 Let

$$
d[v](t) = \begin{cases} \displaystyle\int_{0+\varepsilon}^{R} p(r)(-r + re^{\frac{-(c-B_1)}{r}v})dr, & \dot{v} > 0 \\[2ex] \displaystyle\int_{0+\varepsilon}^{R} p(r)(r - re^{\frac{c-B_1}{r}v})dr, & \dot{v} < 0 \end{cases}
\tag{5.11}
$$

where $p(r) \geq 0$ with $\displaystyle\int_{0+\varepsilon}^{\infty} p(r)dr < +\infty$. Then, for any $v(t) \in C_{pm,I}(t_0,\infty)$, there exists a

constant $M \geq 0$ such that $|d[v](t)| \leq M$.

Proof: Since (5.7) can be rewritten as $F_r(t) = v(t) + L(r,v)$, where

$$
L(r,v) = \begin{cases} -r + re^{\frac{-(c-B_1)}{r}v}, & \dot{v} > 0 \\[2ex] r - re^{\frac{c-B_1}{r}v}, & \dot{v} < 0, \end{cases}
$$

$L(r,v)$ has the definition on the domain formed by the variables $r \in [\varepsilon, R]$ and

$v(t) \in C_{pm,I}(t_0,\infty)$ where $C_{pm,I}(t_0,\infty) : C_{pm}(t_0,\infty) \cap C_I(t_0,\infty)$, and I is a closed

sufficiently large interval [74]. Namely, the domain of the variables is bounded and

closed. Hence, it is always possible to partition the domain of the variables into finite

bounded closed sets. Since $L(r,v)$ is continuous on each set, $|L(r,v)|$ has one bound on

each of the sets [78]. Hence, it is always possible to define a positive constant M_1 such

that M_1 is the biggest bound among all the bounds. Thus, for any $r \in [\varepsilon, R]$ and

any $v(t) \in C_{pm,I}(t_0,\infty)$, there exists a positive constant M_1 , such that

$|L(r,v)| \leq M_1$ uniformly holds. Hence, one obtains

$$
d[v](t) = \int_{0+\varepsilon}^{R} p(r)L(r,v)dr \leq \int_{0+\varepsilon}^{R} p(r)|L(r,v)|dr \leq M_1 \int_{0+\varepsilon}^{R} p(r)dr .
$$

With the assumption of $p(r)$, one can conclude that $M = M_1 \int\limits_{0+\varepsilon}^{R} p(r)dr$.

Property 5.2: The hysteresis model constructed by (5.9) is rate-independent.

Proof: Following [10], we let $\sigma : [0,t_E] \to [0,t_E]$ satisfying $\sigma(0) = 0$ and $\sigma(t_E) = t_E$ be a continuous increasing function, i.e. $\sigma(\cdot)$ is an admissible time transformation. We also define $w_f[v_t]$ satisfying $w_f[v_t] = w[v](t), t \in [0,t_E]$ and $v \in M_{pm}[0,t_E]$, where v_t represents the truncation of v at t defined by $v_t(\tau) = v(\tau)$ for $0 \le \tau \le t$ and $v_t(\tau) = v(t)$ for $t \le \tau \le t_E$, and $w[v](t)$ constructed by (5.9). For the model (5.9), we easily have

$$w[v \circ \sigma](t) = w_f[(v \circ \sigma)_t] = w_f[v_{\sigma(t)} \circ \sigma] = w_f[v_{\sigma(t)}] = w[v](\sigma(t)) = w[v](t) \circ \sigma(t).$$

Hence, for all admissible time transformations $\sigma(\cdot)$, according to definition 2.2.1 in [10], the model constructed by (5.9) is rate-independent.

Property 5.3: The hysteresis model constructed by (5.9) has the Volterra property.

Proof: It is obvious that whenever $v, \bar{v} \in M_{pm}[0,t_E]$ and $t \in [0,t_E]$, then $v_t = \bar{v}_t$ implies that $(w[v])_t = (w[\bar{v}])_t$. Therefore, according to [10, page 37], the model (5.8) has the Volterra property.

Lemma 5.1 [10] **(Characterization of a hysteresis operator):** If a functional $w : C_{pm}[0,t_E] \to Map([0,t_E])$ has both rate independence and Volterra properties, w is a hysteresis operator.

Proposition 5.1: the hysteresis model constructed by (5.9) is a hysteresis operator.

Proof: From the Properties 5.1, 5.2 and Lemma 5.1, the hysteresis model constructed by (5.9) is a hysteresis model.

Remark 5.1: It should be mentioned that the Prandtl-Ishilinskii model is a weighted superposition of the play operator, i.e., the play operator is the hysteron [8]. The constructed hysteresis model in this paper is a superposition of play-like operators from a 1st order differential equation [18]. As an illustration, Figure 5.2 shows $w(t)$ generated by (5.9), with $p(r) = e^{-6.7(0.1r-1)^2}$, $r \in [10^{-6}, 50]$, $B_1 = 0.505$ and input $v(t) = 7\sin(4t)/(1+t)$, with $F(v(0) = 0) = 0$.
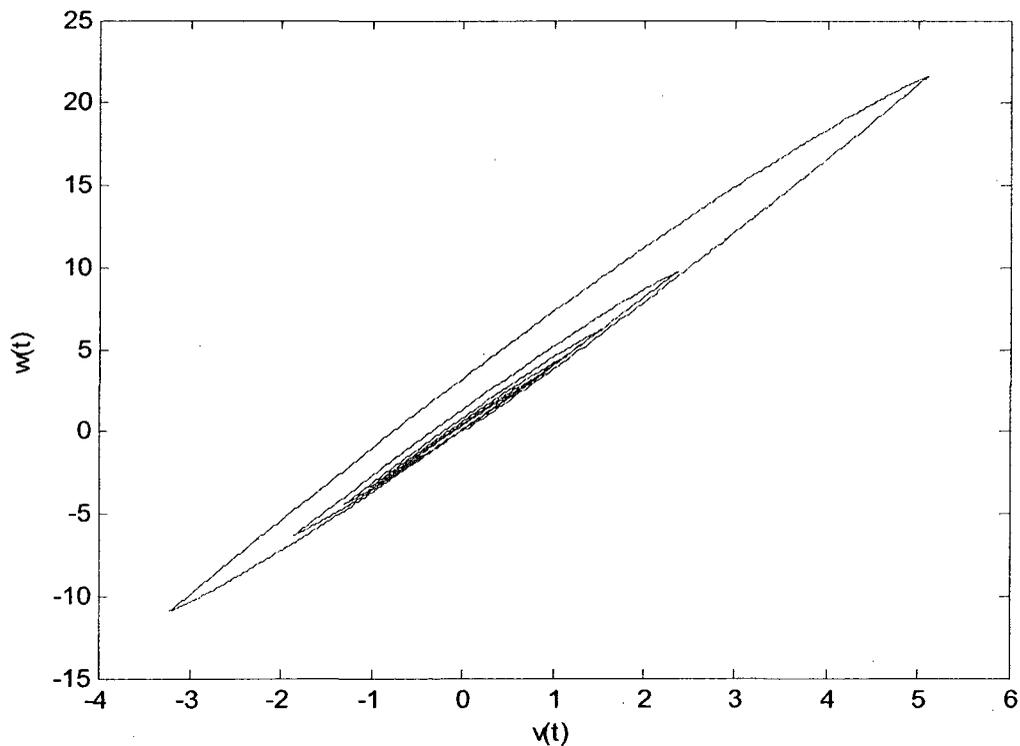
Figure 5.2 Hysteresis loop of the hysteresis model given by (5.10)

Remark 5.2: From the standpoint of the categories of hysteresis models, the constructed hysteresis model is a *subclass* of SSSL-PKP hysteresis models in the literature [18]. However, it provides a possibility to mitigate the effects of hysteresis without necessarily constructing an inverse, which is the unique feature of this subclass

model compared to the SSSL-PKP hysteresis model of the general class. This will be illustrated later in the controller design.

Remark 5.3: From the point of view of an alternative one-parametric representation of the Preisach operator [79], the constructed model mathematically falls into PKP-type operators [18] (which can be easily seen when the density function is independent on the integral variable), as the Prandtl-Ishilinskii model falls into the Preisach model. As a preliminary step, we explore the properties of this model and its potential to facilitate controller design when a system is preceded by this kind of hysteresis model, which will be demonstrated in the next section.

To this end, we can rewrite (5.9) as

$$w(t) = p_0 v + d[v](t), \qquad (5.12)$$

where $p_0 = \int_{0+\varepsilon}^{R} p(r)dr$ and $d[v](t)$ is defined by (5.11).

Remark 5.4: It should be noted that (5.10) decomposes the hysteresis behavior into two terms. The first term describes the linear reversible part, while the second term describes the nonlinear hysteretic behavior. This decomposition is crucial since it facilitates the utilization of the available control techniques for the controller design in the next section. Furthermore, it is worth mentioning that one of advantages of the hysteresis model using differential-equation-based building blocks is the simplicity of implementation [18].

5.4 Sliding Mode Control Design

From (5.10) and Property 5.1, we see that the signal $w(t)$ is expressed as a linear

function of input signal $v(t)$ plus a bounded term. Thus, the available robust adaptive control techniques can be utilized to design the controller.

Using the hysteresis model of (5.10) and the representation of (5.12), the nonlinear system becomes

$$x^{(n)}(t) + \sum_{i=1}^{k} a_i Y_i(x(t), \dot{x}(t), \cdots, x^{(n-1)}(t)) = b\{p_0 v(t) - d[v](t)\} \qquad (5.13)$$

where the input signal $v(t)$ is linear to the bp_0. It is very important to note from the Property 1 that there exists a uniform bound $M \geq 0$ such that $|d[v](t)| \leq M$.

We define the tracking error vector $\tilde{X} = X - X_d$, and a filtered tracking error as in [25]

$$s(t) = \left(\frac{d}{dt} + \lambda\right)^{(n-1)} \tilde{X}(t), \qquad (5.14)$$

where $s(t)$ can be rewritten as $s(t) = \Lambda^T \tilde{X}(t)$ with $\Lambda^T = [\lambda^{(n-1)}, (n-1)\lambda^{(n-2)}, \cdots, 1]$ and a strictly positive constant λ.

Lemma 5.2 [25]: For the definition of the filtered tracking error (5.14), the following statements hold:

i). The equation $s(t) = 0$ defines a time-varying hyperplane in R^n on which the tracking error vector $\tilde{X}$ decays exponentially to zero;

ii). If $\tilde{X}(0) = 0$ and $|s(t)| \leq \varepsilon$, where ε is a constant, then for $\forall t \geq 0$,

$$\tilde{X}(t) \in \Omega_\varepsilon \overset{\Delta}{=} \{\tilde{X}(t) \mid \ |\tilde{X}_i| \leq 2^{i-1} \lambda^{i-n} \varepsilon, i = 1, ..., n\};$$

iii). If $\tilde{X}(0) \neq 0$ and $|s(t)| \leq \varepsilon$, then $\tilde{X}(t)$ will converge to Ω_ε within a time constant $(n-1)/\lambda$.

In sliding mode control design, the controller contains the discontinuous nonlinearity $\text{sgn}(\cdot)$. It will cause chattering due to practical imperfections in switching devices and delays. In order to eliminate chattering, rather than using the filtered error $s(t)$ to derive the adaptive law, a tuning error s_ε is introduced as

$$s_\varepsilon = s - \varepsilon sat(s/\varepsilon) \,, \tag{5.15}$$

where ε is an arbitrary positive constant and $sat(\cdot)$ is the saturation function. Please note that the tuning error $s_\varepsilon = 0$ when the filtered error $s \leq \varepsilon$.

For the controller design, we need to make the following assumptions.

Assumption 5.1: The desired trajectory $X_d = [x_d, \dot{x}_d, \ldots, x_d^{(n-1)}]^T$ is continuous and available. And, $[X_d^T, x_d^n]^T \in \Omega_d \subset R^{n+1}$ with Ω_d being a compact set.

Assumption 5.2: There exist known constants $0 < b_{\min} \leq b_{\max}$ such that the control gain b in (1) satisfies $b \in [b_{\min}, b_{\max}]$.

Assumption 5.3: Defining a vector $\theta = [a_1/bp_0, \cdots, a_k/bp_0]^T \in R^k$, then the vector $\theta \in \Omega_\theta$ and $\Omega_\theta \overset{\Delta}{=} \{\theta | \ \theta_{i\min} \leq \theta_i \leq \theta_{i\max}, i = 1, \ldots k\}$, where $\theta_{i\min}$ and $\theta_{i\max}$ are some known real numbers.

Assumption 5.4: The bound M for $|d[v](t)| \leq M$ is known.

Assumption 5.5: There exist known constants $p_{0\min}, p_{0\max}$ such that the slope p_0 is

bounded, i.e., $p_0 \in [p_{0\min}, p_{0\max}]$.

Remark 5.5: Assumption 5.1 is generally adopted for the design of a tracking controller. Assumption 5.2 is common for nonlinear controller designs [25]. In Assumption 5.3 a new parameter vector θ has been defined for the convenience of the following development. This assumption implies that the range of the plant parameters, $a_i, i = 1,..., K$ are known in advance. This is a reasonable assumption regarding the prior knowledge of the plant. Assumption 5.4 requires knowledge concerning the boundedness of the hysteresis, which is again quite reasonable and practical from a physical point of view. Assumption 5.5 assumes the slope range of the hysteresis, which is reasonable [17].

In presenting the sliding mode control law, we define that

$$\tilde{\theta}(t) = \hat{\theta}(t) - \theta$$

$$\tilde{\phi}(t) = \hat{\phi}(t) - \phi \tag{5.16}$$

where $\hat{\theta}(t)$ is an estimate of θ and $\hat{\phi}(t)$ is an estimate of $\phi = 1/(bp_0)$.

Given the plant and hysteresis model subjected to the assumptions described above, a control law is designed as follows:

$$v = -k_d s(t) + \hat{\phi} v_{fd}(t) + \hat{\theta}^T Y(X) + v_h \tag{5.17}$$

$$\dot{\hat{\phi}}(t) = proj(\hat{\phi}, -\eta v_{fd} s_\varepsilon) \tag{5.18}$$

$$\dot{\hat{\theta}}(t) = proj(\hat{\theta}, -\gamma Y s_\varepsilon) \tag{5.19}$$

where $k_d > 0$ is a design parameter;

$$v_{fd}(t) = X_d^{(n)} - \dot{s}(t)$$
$$= X_d^{(n)} - [0, \lambda^{(n-1)}, (n-1)\lambda^{(n-2)}, ..., (n-1)\lambda]^T \tilde{X};$$

$$Y = [Y_1, \cdots, Y_k]^T \in R^k \, ;$$

$$v_h = -sat(\frac{s}{\varepsilon})k^* \text{ s.t. } k^* \geq M / p_{0\min}$$

and the parameters η and γ are positive design parameters determining the rates of the adaptations, and the projection operators $proj(\cdot)$ are formulated as:

$$proj\,(\hat{\phi}, -\eta\,v_{fd}s_\varepsilon)$$

$$= \begin{cases} 0 & if \quad \hat{\phi} = \phi_{\max}, and \quad \eta v_{fd}s_\varepsilon > 0 \\[1em] -\eta\,v_{fd}s_\varepsilon & if \quad \hat{\phi} \in [\phi_{\min}, \phi_{\max}] \\ & or \quad [\hat{\phi} = \phi_{\min}, and \quad \eta v_{fd}s_\varepsilon \leq 0] \\ & or \quad [\hat{\phi} = \phi_{\max}, and \quad \eta v_{fd}s_\varepsilon \geq 0] \\[1em] 0 & if \quad \hat{\phi} = \phi_{\min}, and \quad \eta v_{fd}s_\varepsilon > 0 \end{cases} \qquad (5.20)$$

$$\{proj(\hat{\theta}, -\gamma Ys_\varepsilon)\}_i$$

$$= \begin{cases} 0 & if \quad \hat{\theta}_i = \theta_{i\max}, and \quad \gamma(Ys_\varepsilon) < 0 \\[1em] -\gamma(Ys_\varepsilon)_i & if \quad \hat{\theta}_i \in [\theta_{i\min}, \theta_{i\max}] \\ & or \quad [\hat{\theta}_i = \theta_{i\min}, and \quad \gamma(Ys_\varepsilon)_i \leq 0] \\ & or \quad [\hat{\theta}_i = \theta_{i\max}, and \quad \gamma(Ys_\varepsilon)_i \geq 0] \\[1em] 0 & if \quad \hat{\theta}_i = \theta_{i\min}, and \quad \gamma(Ys_\varepsilon)_i > 0 \end{cases} \qquad (5.21)$$

Remark 5.6:

(1) The projection operators used in the above control law have the following properties [26]:

(i). $\hat{\Theta}(t) \in \Omega_\Theta$ if $\hat{\Theta}(t_0) \in \Omega_\Theta$ where Ω_Θ is a compact set;

(ii). $\| proj(\varpi, y) \| \leq \| y \|$;

(iii). $-(\hat{\varpi} - \varpi)^T \Lambda \, proj(\hat{\varpi}, z) \geq -(\hat{\varpi} - \varpi)^T \Lambda z$ where Λ is a positive definite symmetric matrix.

(2) The projection operators require the upper and lower bounds of the parameters ϕ and θ. Assumption 2, Assumption 3 and Assumption 5 are fundamental to these bounds. However, these parameters are only used to specify the variable ranges of the parameter for the projection operator. These ranges are not restricted as long as the estimated parameters are bounded.

The stability of the closed-loop system is established in the following theorem:

Theorem: For the plant (5.2) with the hysteresis (5.10), subject to Assumptions (1)-(5), the robust adaptive controller specified by equations (5.17)-(5.21) ensures that for:

$$\Omega_\theta = \{ \theta | \ \theta_{i\min} \leq \theta_i \leq \theta_{i\max}, i = 1,...k \};$$

$$\Omega_\phi = \{ \phi | \ 1/(b_{\max} p_{0\max}) \leq \phi \leq 1/(b_{\min} p_{0\min}) \};$$

$$\Omega_\varepsilon = \{ \tilde{X}(t) \| \ \tilde{X}_i | \leq 2^{i-1} \lambda^{i-n} \varepsilon, i = 1,..., n \},$$

if $\hat{\theta}(t_0) \in \Omega_\theta$ and $\hat{\phi}(t_0) \in \Omega_\phi$, all the signals of the closed-loop system are bounded and the error between the state vector and the reference trajectory $\tilde{X}(t)$ converges to Ω_ε as time goes to infinity.

Proof: For the system (5.13), after applying the control laws (5.17)-(5.21), the time derivative of the filtered error (5.14) is:

$$\dot{s}(t) = -v_{fd} - \sum_{i=1}^{k} a_i Y_i$$

$$+ \frac{1}{\phi}[-k_d s(t) + \hat{\phi} v_{fd}(t) + Y^T \hat{\theta} - sat(\frac{s}{\varepsilon})k^*] \qquad (5.22)$$

$$+ bd(v)$$

To establish the global boundedness of the close-loop system, a candidate Lyapunov function is defined:

$$V(t) = \frac{1}{2}[\phi s_\varepsilon^2 + \frac{1}{\gamma}(\hat{\theta} - \theta)^T(\hat{\theta} - \theta)^T + \frac{1}{\eta}(\hat{\phi} - \phi)^2] . \qquad (5.23)$$

Since the discontinuity at $|s| = \varepsilon$ is of the first kind, and $s_\varepsilon = 0$ when $|s| \le \varepsilon$, the derivative $\dot{V}(t)$ exists for all s. Especially $\dot{V}(t) = 0, \forall |s| \le \varepsilon$, when $|s| > \varepsilon$ from (5.22) and noticing the fact $s_\varepsilon \dot{s}_\varepsilon = s_\varepsilon \dot{s}$, one has

$$\dot{V}(t) \le -k_d s_\varepsilon^2 + s_\varepsilon[\hat{\phi} v_{fd}(t) + Y^T \hat{\theta} - sat(\frac{s}{\varepsilon})k^*]$$

$$+ s_\varepsilon[-\phi v_{fd}(t) + Y^T \theta + 1/p_0 \cdot d[v](t)]$$

$$+ \frac{1}{\lambda}(\hat{\theta} - \theta)^T \dot{\hat{\theta}} + \frac{1}{\eta}(\hat{\phi} - \phi) \dot{\hat{\phi}}.$$

Applying the adaptive laws (5.18)-(5.21) and the properties of the projection operators as

$$(\hat{\theta} - \theta)^T proj(\hat{\theta}, -\gamma Y s_\varepsilon) \le -\gamma(\hat{\theta} - \theta)^T Y s_\varepsilon,$$

$$(\hat{\phi} - \phi) proj(\hat{\phi}, -\eta v_{fd} s_\varepsilon) \le -\eta(\hat{\phi} - \phi) v_{fd} s_\varepsilon,$$

one has

$$\dot{V}(t) \le -k_d s_\varepsilon{}^2 + s_\varepsilon [\hat{\phi} v_{fd}(t) + Y^T \hat{\theta} - sat(\frac{s}{\varepsilon})k^*]$$

$$+ s_\varepsilon [-\phi v_{fd}(t) + Y^T \theta + 1/p_0 \cdot d[v](t)]$$

$$-(\hat{\theta} - \theta)^T Y s_\varepsilon - (\hat{\phi} - \phi) \ v_{fd}(t)s_\varepsilon$$

$$= -k_d s_\varepsilon{}^2 - sat(\frac{s}{\varepsilon})k^* + 1/p_0 \cdot d[v](t) \qquad (5.24)$$

$$\le -k_d s_\varepsilon{}^2$$

Noticing $\dot{V}(t) = 0, \forall |s| \le \varepsilon$ and Equation (5.24), we conclude that $V(t)$ is a Lyapunov function which leads to a global boundedness of $s_\varepsilon, \tilde{\theta} = \hat{\theta} - \theta$ and $\tilde{\phi} = \hat{\phi} - \phi$. From the definition of s_ε, $s(t)$ is bounded. It can be shown that if $\tilde{X}(0)$ is bounded, then $\tilde{X}(t)$ is also bounded for all t, and since $X_d(t)$ is bounded by design, $X(t)$ must also be bounded. To complete the proof and establish an asymptotic convergence of the tracking error, it is necessary to show that $s_\varepsilon \to 0$ as $t \to \infty$. This is accomplished by applying Barbalat's lemma [80] to the continuous, nonnegative function

$$V_1(t) = V(t) - \int_0^t (\dot{V}(\tau) + k_d s_\varepsilon{}^2(\tau))d\tau \ge 0$$

with $\dot{V}_1(t) = -k_d s_\varepsilon{}^2(\tau) \le 0$. Since every term in (5.23) is bounded, $\dot{s}(t)$ and $\dot{s}_\varepsilon(t)$ are bounded. This implies that $V_1(t)$ is a uniformly continuous function of time. Since $V_1(t) \ge 0$ and $\dot{V}_1(t) \le 0$ for all t, applying Barbalat's lemma proves that $\dot{V}_1(t) \to 0$ as $t \to \infty$. Therefore, from the derivative of $V_1(t)$, it can be demonstrated that $s_\varepsilon(t) \to 0$ as $t \to \infty$. The Lemma indicates that $\tilde{X}(t)$ will converge to Ω_ε.

Remark 5.7: It is now clear that the sliding mode control scheme to mitigate the hysteresis nonlinearities can be applied to many systems and may not necessarily be

limited to the system (5.2). However, we should emphasize that our goal is to show the fusion of the hysteresis model with available control techniques in a simpler setting that reveals its essential features.

5.5 Simulation Studies

In this section, we illustrate the methodologies presented in the previous sections using a simple nonlinear system described by

$$\dot{x} = a\frac{1-e^{-x(t)}}{1+e^{-x(t)}} + bw(t) , \qquad (5.25)$$

where w represents the output of the hysteresis nonlinearity. The actual parameter values are $a = 1$, and $b = 1$. Without applying the control signal, i.e., $w(t) = 0$, one notices that (5.25) is unstable, because for $x > 0$, $\dot{x} = (1-e^{-x(t)})/(1+e^{-x(t)}) > 0$, and for $x < 0$, $\dot{x} = (1-e^{-x(t)})/(1+e^{-x(t)}) < 0$. The objective is to control the system state x to follow the desired trajectory $x_d = 2.5\sin(2.3t) + \cos(t)$.

In the simulations, the parameters are chosen as: $\eta = 0.5$, $\gamma = 0.5$, $k_d = 10$, $\varepsilon = 0.2$, $\Gamma = 0.1$, $k^* = 25$ $\hat{\phi}(0) = 0.5$, $\hat{\theta}(0) = 0.6$, $\hat{x}(0) = 1.05$, $v(0) = 0$, $p_{0\min} = 1$, $p_{0\max} = 10$, $c = 1$, $B_1 = 0.505$, $p(r) = e^{-6.7(0.1r-1)^2}$ for $r \in [10^{-6}, 50]$. The simulation results are shown in Figures 5.3-5.5. Figures 5.3 and 5.4 show the tracking error for the desired trajectory, Figure 5.5 shows the control signal of the hysteretic system. From figures 5.3-5.4 we see that the proposed control scheme demonstrates the good tracking with an acceptable precision. Please note that it is desirable to compare the control performance with and without considering the effects of hysteresis. However, this comparison is not possible in this case since the control law is designed for the entire cascaded hysteretic system [17].

106
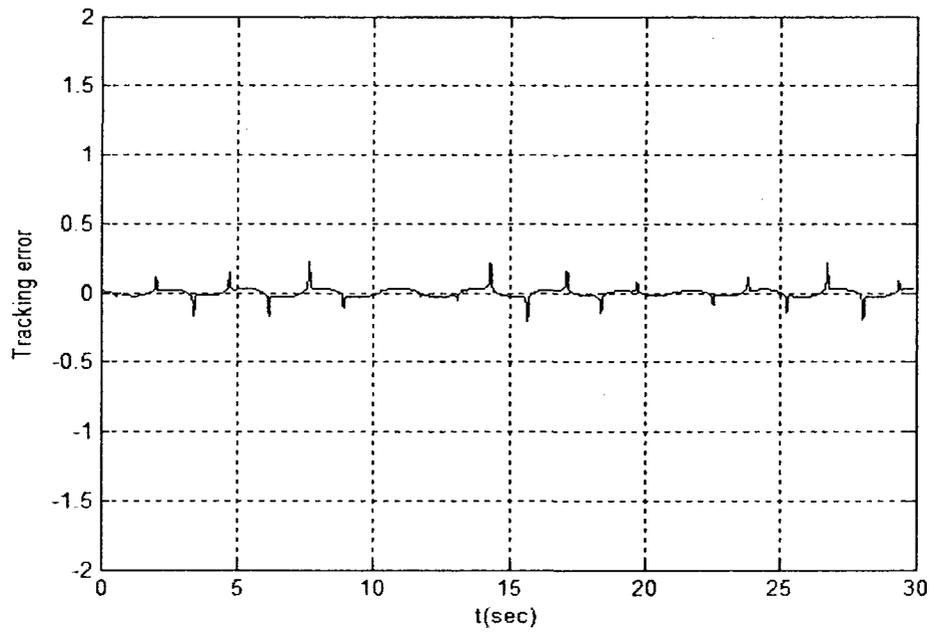
Figure 5.3 Tracking error under the control scheme
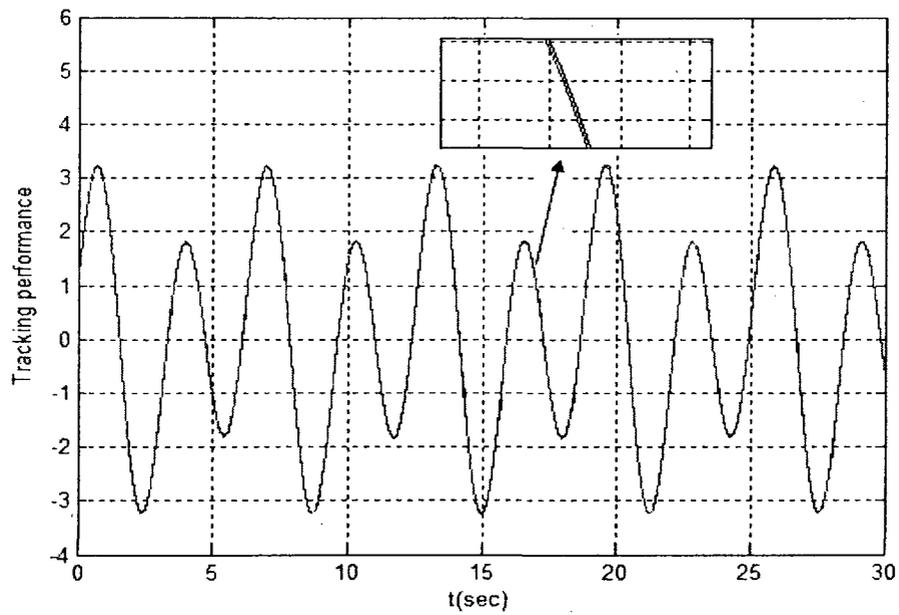
Figure 5.4 Tracking performances--Reference signal (dashed line); under the control

scheme (solid line)

107
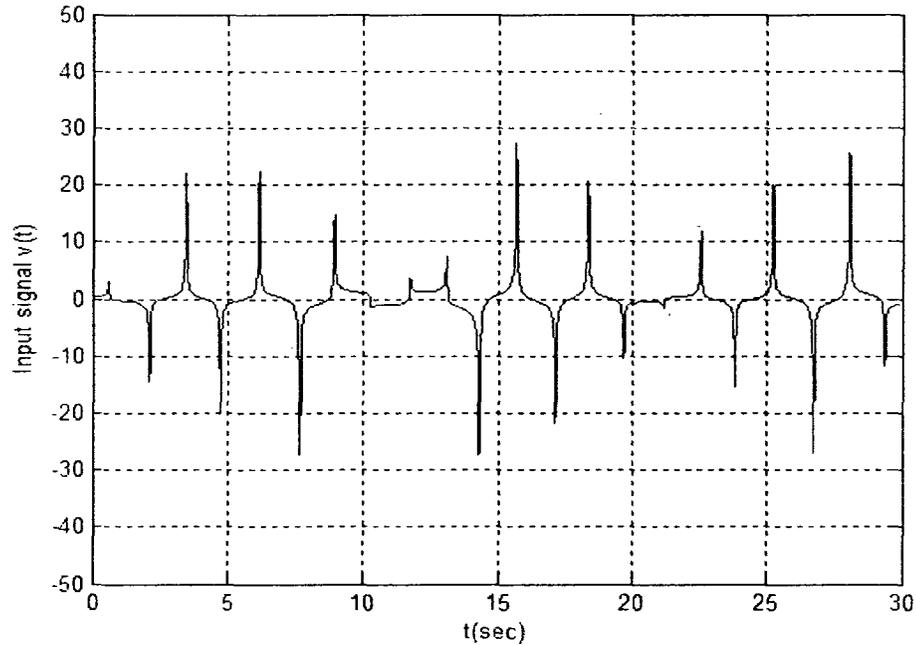
Figure 5.5 Control signal $v(t)$ of the hysteretic system

5.6 Conclusion

We have for the first time constructed a class of hysteresis models based on play-like operator, which facilitates the application of available control techniques to systems preceded with hysteresis to mitigate the effects of hysteresis, without necessarily constructing an inverse. Our main contributions in this paper are highlighted as follows:

(i)   A new class of hysteresis models is constructed, where the play-like operators play the role of building blocks. From the standpoint of categories of hysteresis models, this class is a subclass of SSSL-PKP hysteresis models. It allows the mitigation of the effects of hysteresis without necessarily constructing an inverse, which is the unique feature of this subclass model identified from the SSSL-PKP hysteresis model of general class in the literature;

108

(ii)   The paper addresses the challenge of fusing a suitable hysteresis model with available robust adaptive techniques to mitigate the effects of hysteresis, while avoiding the construction of a complicated inverse operator of the hysteresis model;

(iii)   A sliding mode based control scheme is proposed to accomplish robust adaptive control tasks for a class of hysteretic nonlinear systems. The control scheme ensures stabilization and acceptable tracking performances of the hysteretic dynamic nonlinear systems.

CHAPTER 6

BACKSTEPPING CONTROL FOR NONLINEAR SYSTEMS WITH PLAY-LIKE OPERATOR-BASED HYSTERESIS MODEL REPRENSENTATIONS

6.1 Introduction

Backstepping is a very popular control technique in control theory since it provides a systematic way to simultaneously construct Lyapunov functions and controllers for nonlinear systems in lower triangular structures [76, 80]. With the same motivation as in the last chapter, this chapter proposes two backstepping based adaptive control schemes for the same class of nonlinear systems, with the same hysteresis model representation discussed in the last chapter, to mitigate the hysteresis without necessarily constructing a traditional hysteresis inverse operator. The new methods not only can perform global stabilization and tracking tasks of dynamic nonlinear systems, but can also derive transient performance in terms of L_2 norm of tracking error as an explicit function of design parameters, which allows designers to meet the desired performance requirements by tuning the design parameters in an explicit way.

The layout of this chapter is as follows. Section 6.2 gives the problem statement. The details of backstepping based control schemes for the nonlinear systems with play-like operators based hysteresis model representation are presented in Section 6.3. Simulation results are given in Section 6.4. Section 6.5 concludes this paper with some

brief remarks.

6.2 Problem Statement

In this chapter, for the same class of nonlinear hysteretic systems discussed in Chapter 5, the robust adaptive control design can also be developed using backstepping technique and the new hysteresis model.

Considering the hysteresis model based on play-like operators given in (5.10), the hysteresis output can be expressed as

$$w(t) = p_0 v + d[v](t), \tag{6.1}$$

where

$$d[v](t) = \begin{cases} \int_{0+\varepsilon}^{R} p(r)(-r + re^{\frac{-(c-B_1)}{r}v})dr, & \dot{v} > 0 \\ \int_{0+\varepsilon}^{R} p(r)(r - re^{\frac{c-B_1}{r}v})dr, & \dot{v} < 0 \end{cases}$$

with $p_0 = \int_{0+\varepsilon}^{R} p(r)dr$, and the other variables and notions can be seen in section 5.3.

The nonlinear dynamic system in the presence of the above hysteresis nonlinearities is described in canonical form as

$$x^{(n)}(t) + \sum_{i=1}^{k} a_i Y_i(x(t), \dot{x}(t), \cdots, x^{(n-1)}(t)) = bw(t) , \tag{6.2}$$

where $X = [x, \dot{x}, \cdots, x^{(n-1)}]^T$ is the plant state vector, Y_i (i=1, ..k) are known continuous linear or nonlinear functions, parameters a_i and control gain b are unknown constants. It

is a common assumption that the sign of b is known. Without losing generality, we assume b is greater than zero. It should be noted that more general classes of nonlinear systems can be transformed into this structure [76, 80].

The control objective is to design backstepping based controller $v(t)$ in (6.1) to drive the plant state $X(t)$ to track a specified desired trajectory $X_d(t)$, i.e., $X(t) \to X_d(t)$ as $t \to \infty$ and all the other signals of the overall systems are bounded.

Throughout this chapter the following assumption is made.

Assumption 6.1: The desired trajectory $X_d = [x_d, \dot{x}_d, \cdots, x_d^{(n-1)}]^T$ is continuous. Furthermore, $[X_d^T, x_d^{(n)}]^T \in \Omega_d \subset R^{n+1}$ with Ω_d is a compact set.

6.3 Backstepping Control Design

From (6.1) and Property 5.1, the signal $w(t)$ is expressed as a linear function of input signal $v(t)$ plus a bounded term. Hence, the nonlinear system dynamics can be re-expressed as

$$
\begin{aligned}
\dot{x}_1 &= x_2 \\
&\vdots \\
\dot{x}_{n-1} &= x_n \\
\dot{x}_n &= -\sum_{i=1}^{k} a_i Y_i(x_1(t), x_2(t), \cdots, x_n(t)) \\
&\quad + b\{p_0 v(t) - d[v](t)\} \\
&= \mathbf{a}^T Y + b_p v(t) - d_b[v],
\end{aligned}
\tag{6.3}
$$

where $x_1(t) = x(t)$, $x_2(t) = \dot{x}(t), \cdots, x_n(t) = x^{(n-1)}(t)$, $\mathbf{a} = [-a_1, -a_2, \cdots, -a_k]^T$, and $Y = [Y_1, Y_2, \cdots, Y_k]^T$, $b_p = bp_0$, and $d_b[v](t) = bd[v](t)$.

Before presenting the adaptive control design using the standard backstepping technique in [76, 82] to achieve the control objectives, we make the following change of coordinates:

$$z_1 = x_1 - x_d$$
$$z_i = x_i - x_d^{(i-1)} - \alpha_{i-1}, \qquad i = 2,3,\cdots,n \tag{6.4}$$

where α_{i-1} is the virtual controller in the i th step and will be determined later. In the following two subsections, we give two control schemes. In Scheme I, the controller is discontinuous; and in Scheme II, it is continuous, for the implantation issue.

6.3.1 Scheme I

In what follows, the robust adaptive control law is developed for Scheme I.

First, we give the following definitions

$$\tilde{\mathbf{a}}(t) = \mathbf{a} - \hat{\mathbf{a}}(t)$$
$$\tilde{\phi}(t) = \phi - \hat{\phi}(t) \tag{6.5}$$
$$\tilde{M}(t) = M - \hat{M}(t),$$

where $\hat{\mathbf{a}}$ is an estimate of the vector $\mathbf{a}$, $\hat{\phi}$ is an estimate of ϕ, which is defined as $\phi := \dfrac{1}{b_p}$, and $\hat{M}$ is an estimate of M.

Given the plant and the hysteresis model subject to the assumption above, we propose the following control law

$$v(t) = \hat{\phi}(t)v_1(t)$$

$$v_1(t) = -c_n z_n - z_{n-1} - \hat{\mathbf{a}}^T Y - \text{sgn}(z_n)\hat{D} + x_d^{(n)} + \dot{\alpha}_{n-1}$$

$$\dot{\hat{\phi}}(t) = -\eta v_1(t)z_n \tag{6.6}$$

$$\dot{\hat{\mathbf{a}}}(t) = \Gamma Y z_n$$

$$\dot{\hat{M}}(t) = \gamma |z_n|$$

where c_n, η, and γ are positive design parameters, and Γ is a positive-definite matrix. These parameters can provide a certain degree of freedom to determine the rates of the adaptations. Also, α_{n-1} and the implicit α_{i-1}, $i = 2,3,\cdots,n-1$ in (6.6) will be designed in the proof of the following theorem for stability analysis.

The stability of the closed-loop system is established as:

Theorem 6.1: For the plant given in (6.2) with the hysteresis (6.1), subject to Assumption 6.1, the robust adaptive controller specified by (6.6) ensures that the following statements hold.

(i) The resulting closed-loop system (6.2), (6.1) and (6.6) is globally stable in the sense that all the signals of the closed-loop system are ultimately bounded;

(ii) Asymptotic tracking is achieved, i.e., $\lim_{t\to\infty}[x(t) - x_d(t)] = 0$;

(iii) The transient tracking error can be explicitly specified by

$$\|x(t) - x_d(t)\|_2 \leq \sqrt{\frac{\left(\frac{1}{2}\tilde{\mathbf{a}}(0)^T\Gamma^{-1}\tilde{\mathbf{a}}(0) + \frac{b_p}{2\eta}\tilde{\phi}(0)^2 + \frac{1}{2\gamma}\tilde{M}(0)^2\right)}{c_1}}$$

Proof: We will use the standard backstepping technique from [76, 82] to prove the statements in a systematic way as follows:

Step 1: The time derivative of z_1 can be computed as

$$\dot{z}_1 = z_2 + \alpha_1. \tag{6.7}$$

The virtual control α_1 can be designed as

$$\alpha_1 = -c_1 z_1,$$

where c_1 is a positive design parameter.

Hence, we can get the first equation of tracking error:

$$\dot{z}_1 = z_2 - c_1 z_1$$

Step 2: Differentiating z_2 gives

$$\dot{z}_2 = z_3 + \alpha_2 - \dot{\alpha}_1.$$

The virtual control α_2 can be designed as

$$\alpha_2 = -c_2 z_2 - z_1 + \dot{\alpha}_1,$$

Hence, the dynamics is

$$\dot{z}_2 = -c_2 z_2 - z_1 + z_3.$$

Following this procedure step by step, we can derive the dynamics of the rest of the states, until the real control appears.

Step n: The *n-th* dynamics is given by

115

$$\dot{z}_n = b_p v(t) + a^T Y - x_d^{(n)} - \dot{\alpha}_{n-1} + d_b[v](t). \tag{6.8}$$

We design the real control as follows:

$$v(t) = \hat{\phi}(t) v_1(t)$$
$$v_1(t) = -c_n z_n - z_{n-1} - \hat{\mathbf{a}}^T Y - \text{sgn}(z_n)\hat{M} + x_d^{(n)} + \dot{\alpha}_{n-1}$$
$$\dot{\hat{\phi}}(t) = -\eta v_1(t) z_n$$

$$\dot{\hat{\mathbf{a}}}(t) = \Gamma Y z_n$$
$$\dot{\hat{M}}(t) = \gamma |z_n| \tag{6.9}$$

Note that $b_p v(t)$ in (6.9) can be expressed as

$$b_p v(t) = b_p \hat{\phi}(t) v_1(t) = v_1(t) - b_p \tilde{\phi}(t) v_1(t). \tag{6.10}$$

Hence, we obtain

$$\dot{z}_n = -c_n z_n - z_{n-1} - \hat{\mathbf{a}}^T Y - \text{sgn}(z_n)\hat{M} + d_b[v](t) - b_p \tilde{\phi}(t) v_1(t). \tag{6.11}$$

To this end, we define the candidate Lyapunov function as

$$V = \sum_{i=1}^{n} \frac{1}{2} z_i^2 + \frac{1}{2} \tilde{\mathbf{a}}^T \Gamma^{-1} \tilde{\mathbf{a}} + \frac{b_p}{2\eta} \tilde{\phi}^2 + \frac{1}{2\gamma} \tilde{M}^2. \tag{6.12}$$

The derivative $\dot{V}$ is given by

$$\dot{V} = \sum_{i=1}^{n} z_i \dot{z}_i + \tilde{\mathbf{a}}^T \Gamma^{-1} \dot{\tilde{\mathbf{a}}} + \frac{b_p}{\eta} \tilde{\phi} \dot{\tilde{\phi}} + \frac{1}{\gamma} \tilde{M} \dot{\tilde{M}}$$

$$\leq \sum_{i=1}^{n} c_i z_i^2 + \tilde{\mathbf{a}}^T \Gamma^{-1} (\Gamma Y z_n - \dot{\hat{\mathbf{a}}}) - \frac{b_p}{\eta} \tilde{\phi} (\eta \nu_1 z_n + \dot{\hat{\phi}})$$

$$-|z_n| \hat{M} + |z_n| |d_b[\nu](t)| + \frac{1}{\gamma} \tilde{M} \dot{\tilde{M}}$$

$$\leq -\sum_{i=1}^{n} c_i z_i^2 + \tilde{\mathbf{a}}^T \Gamma^{-1} (\Gamma Y z_n - \dot{\hat{\mathbf{a}}}) - \frac{b_p}{\eta} \tilde{\phi} (\eta \nu_1 z_n + \dot{\hat{\phi}})$$

$$+ \frac{1}{\gamma} \tilde{M} (\gamma |z_n| - \dot{\hat{M}})$$

$$= -\sum_{i=1}^{n} c_i z_i^2$$

(6.13)

Equations (6.12) and (6.13) imply that V is nonincreasing. Hence, the boundedness of the variables $z_1, z_2, \cdots, z_n$, $\hat{\phi}$, $\hat{\mathbf{a}}$ and $\hat{M}$ is ensured. By applying the LaSalle-Yoshizawa Theorem [81, Theorem 2.1], it further follows that $z_i \to 0$, $i = 1, 2, \cdots, n$ as time goes to infinity, which implies $\lim_{t \to \infty} [x(t) - x_d(t)] = 0$.

We can prove the third statement of Theorem 6.1 in the following way. From (6.13), we know

$$\|z_1\|_2^2 = \int_0^{\infty} |z_1(s)|^2 ds \leq \frac{V(0) - V(\infty)}{c_1} \leq \frac{V(0)}{c_1}.$$

Noticing $V(0) = \frac{1}{2} \tilde{\mathbf{a}}(0)^T \Gamma^{-1} \tilde{\mathbf{a}}(0) + \frac{b_p}{2\eta} \tilde{\phi}(0)^2 + \frac{1}{2\gamma} \tilde{M}(0)^2$ after setting $z_i(0) = 0, i = 1, 2, \cdots, n$,

one obtains

$$\left\| x(t) - x_d(t) \right\|_2 \le \sqrt{\frac{\left(\dfrac{1}{2} \widetilde{\mathbf{a}}(0)^T \Gamma^{-1} \widetilde{\mathbf{a}}(0) + \dfrac{b_p}{2\eta} \widetilde{\phi}(0)^2 + \dfrac{1}{2\gamma} \widetilde{M}(0)^2 \right)}{c_1}} \ . \qquad (6.14)$$

Remark 6.1: From (6.14), we know that the transient performance in a computable explicit form depends on the design parameters η, γ, c_1 and the initial estimate errors $\widetilde{\mathbf{a}}(0), \widetilde{\phi}(0)$ $\widetilde{M}(0)$, which gives designers enough freedom to tune transient performance.

6.3.2 Scheme II

In the control scheme above, we notice that in the controller, $\mathrm{sgn}(z_n)$ is introduced in the design process, which makes the controller discontinuous and this may cause undesirable chattering. An alternative smooth scheme is proposed to avoid possible chattering by using the definition of the continuous sign function below, as defined in [82].

First, the definition of $sg_i(z_i)$ is introduced as follows:

$$sg_i(z_i) = \begin{cases} \dfrac{z_i}{|z_i|}, & |z_i| \ge \delta_i, \\[4mm] \dfrac{z_i}{|z_i| + (\delta_i^2 - z_i^2)^{n-i+2}} & |z_i| < \delta_i, \end{cases} \qquad (6.15)$$

where the design parameters $\delta_i (i = 1, \cdots, n)$ are positive. It is known that $sg_i(z_i)$ has $(n - i + 2)$-th order derivatives.

Hence, we have

$$sg_i(z_i)f_i(z_i) = \begin{cases} 1, & z_i \geq \delta_i \\ 0, & |z_i| < \delta_i \\ -1, & z_i \leq -\delta_i \end{cases}$$

where

$$f_i(z_i) = \begin{cases} 1, & |z_i| \geq \delta_i, \\ 0, & |z_i| < \delta_i. \end{cases}$$

Given the plant and hysteresis model subject to the assumption above, we propose the continuous controller as follows:

$$
\begin{aligned}
v(t) &= \hat{\phi}(t)v_1(t) \\
v_1(t) &= -(c_n + 1)(|z_n| - \delta_n)sg_n(z_n) - \hat{\mathbf{a}}^T Y \\
&\quad - sg_n(z_n)\hat{M} + x_d^{(n)} + \dot{\alpha}_{n-1} \\
\dot{\hat{\phi}}(t) &= -\eta v_1(t)(|z_n| - \delta_n)f_n sg_n(z_n) \\
\dot{\hat{\mathbf{a}}}(t) &= \Gamma Y(|z_n| - \delta_n)f_n sg_n(z_n) \\
\dot{\hat{M}}(t) &= \gamma(|z_n| - \delta_n)f_n
\end{aligned}
\tag{6.16}
$$

where, similar to Control Scheme 1, c_n, η, and γ are positive design parameters, and Γ is a positive-definite matrix, and α_{n-1} and the implicit α_{i-1}, $i = 2, 3, \cdots, n-1$ in (6.16) will be designed in the proof of the following theorem for stability analysis.

Theorem 6.2: For the plant given in (6.2) with hysteresis (6.1), subject to Assumption 1, the robust adaptive controller specified by (6.16) ensures that the following statements hold.

(i) The resulting closed-loop system (6.2), (6.1) and (6.16) is globally stable in the sense that all the signals of the closed-loop system are ultimately bounded;

(ii) The tracking error can asymptotically reach δ_1, i.e., $\lim\limits_{t \to \infty}[x(t) - x_d(t)] = \delta_1$;

(iii) The transient tracking error can be explicitly specified by

$$\left\| x(t) - x_d(t) \right\|_2 \leq \delta_1 + \frac{1}{c_1^{2n}} \left(\frac{1}{2} \tilde{\mathbf{a}}(0)^T \Gamma^{-1} \tilde{\mathbf{a}}(0) + \frac{b_p}{2\eta} \tilde{\phi}(0)^2 + \frac{1}{2\gamma} \tilde{M}(0)^2 \right)^{1/2n} \qquad (6.17)$$

Proof: To guarantee the differentiability of the resultant functions, z_i^2 in the Lyapunov functions is replaced by $(|z_i| - \delta_i)^{n-i+2} f_i$ in Scheme I and z_i in the design procedure detailed below is replaced by $(|z_i| - \delta_i)^{n-i+1} sg_i$, as in [82].

Step 1: We consider the positive-definition function V_1 in [82]:

$$V_1 = \frac{1}{n+1} (|z_1| - \delta_1)^{n+1} f_1(z_1),$$

and we design a virtual controller α_1 as in [82]

$$\alpha_1 = -(c_1 + k)(|z_1| - \delta_1)^n sg_1(z_1) - (\delta_2 + 1)sg_1(z_1), \qquad (6.18)$$

with constant k satisfying $0 < k \leq \frac{1}{4}$ and a positive design parameter c_1. Its time derivative is computed by using (6.7) and (6.18),

$$\dot{V}_1 = (|z_1| - \delta_1)^n f_1(z_1) sg_1(z_1) \dot{z}_1$$
$$\leq -(c_1 + k)(|z_1| - \delta_1)^{2n} f_1(z_1) \tag{6.19}$$
$$+ (|z_1| - \delta_1)^n (|z_2| - \delta_2 - 1) f_1(z_1).$$

Step 2: We choose a positive-definition function V_2 as in [82]:

$$V_2 = V_1 + \frac{1}{n}(|z_2| - \delta_2)^n f_2(z_2),$$

and design virtual controller α_2 as

$$\alpha_2 = -(c_2 + k + 1)(|z_2| - \delta_2)^{n-1} sg_2(z_2)$$
$$+ \dot{\alpha}_1 - (\delta_3 + 1) sg_2(z_2), \tag{6.20}$$

with a positive design parameter c_2, then compute its time derivative,

$$\dot{V}_2 \leq -\sum_{i=1}^{2} c_i (|z_i| - \delta_i)^{2(n-i+1)} f_i(z_i) - k(|z_1| - \delta_1)^{2n} f_1(z_1)$$
$$+ (|z_1| - \delta_1)^n (|z_2| - \delta_2 - 1) f_1(z_1) - (|z_2| - \delta_2)^{2(n-1)} f_2(z_2)$$
$$+ (|z_2| - \delta_2)^{n-1} (|z_3| - \delta_3 - 1) f_2(z_2).$$

By using inequality $2ab \leq a^2 + b^2$, we have

$$\dot{V}_2 \leq -\sum_{i=1}^{2} c_i (|z_i| - \delta_i)^{2(n-i+1)} f_i(z_i) + \frac{1}{4k}(|z_2| - \delta_2 - 1)^2$$
$$- (|z_2| - \delta_2)^{2(n-1)} f_2(z_2) + (|z_2| - \delta_2)^{n-1} (|z_3| - \delta_3 - 1) f_2(z_2)$$

for both cases $|z_2| \geq \delta_2 + 1$ and $|z_2| < \delta_2 + 1$, we can conclude that

$$\dot{V}_2 \le -\sum_{i=1}^{2} c_i (|z_i| - \delta_i)^{2(n-i+1)} f_i(z_i) + (|z_2| - \delta_2)^{n-1} (|z_3| - \delta_3 - 1) f_2(z_2). \qquad (6.21)$$

Step n: Following this procedure step by step, we can derive the real control

$$
\begin{aligned}
v(t) &= \hat{\phi}(t) v_1(t) \\
v_1(t) &= -(c_n + 1)(|z_n| - \delta_n) sg_n(z_n) - \hat{\mathbf{a}}^T Y \\
&\quad - sg_n(z_n) \hat{M} + x_d^{(n)} + \dot{\alpha}_{n-1} \\
\dot{\hat{\phi}}(t) &= -\eta v_1(t)(|z_n| - \delta_n) f_n sg_n(z_n) \\
\dot{\hat{\mathbf{a}}}(t) &= \Gamma Y (|z_n| - \delta_n) f_n sg_n(z_n) \\
\dot{\hat{M}}(t) &= \gamma (|z_n| - \delta_n) f_n
\end{aligned}
\qquad (6.22)
$$

where α_{n-1} can be obtained from the common form of virtual controllers

$$\alpha_i = -(c_i + k + 1)(|z_i| - \delta_i)^{n-i+1} sg_i(z_i) + \dot{\alpha}_{i-1} - (\delta_{i+1} + 1) sg_i(z_i), \quad (i = 3, \cdots, n-1) \text{ with positive}$$

design parameters c_i.

We define a positive-definite function V_n as

$$V_n = \sum_{i=1}^{n} \frac{1}{n-i+2} (|z_i| - \delta_i)^{(n-i+2)} f_i(z_i) + \frac{1}{2} \tilde{\mathbf{a}}^T \Gamma^{-1} \tilde{\mathbf{a}} + \frac{b_p}{2\eta} \tilde{\phi}^2 + \frac{1}{2\gamma} \tilde{M}^2$$

and compute its time derivative by using (6.3), (6.18), (6.20) and (6.22),

$$\dot{V}_n = \dot{V}_{n-1} + \left(\left|z_n\right| - \delta_n\right)^2 f_n(z_n) sg_n(z_n)\dot{z}_n + \tilde{a}^T \Gamma^{-1}\dot{\tilde{a}} + \frac{b_p}{\eta}\tilde{\phi}\dot{\tilde{\phi}} + \frac{1}{\gamma}\tilde{M}\dot{\tilde{M}}$$

$$\leq -\sum_{i=1}^{n} c_i\left(\left|z_i\right| - \delta_i\right)^{2(n-i+1)} f_i(z_i) + \tilde{a}^T\Gamma^{-1}(\Gamma Y z_n - \dot{\hat{a}})$$

$$-\frac{b_p}{\eta}\tilde{\phi}(\eta v_1 z_n + \dot{\hat{\phi}}) - \left|z_n\right|\hat{M} + \left|z_n\right|\left|d_b[v](t)\right| + \frac{1}{\gamma}\tilde{M}\dot{\tilde{M}}$$

$$\leq -\sum_{i=1}^{n} c_i\left(\left|z_i\right| - \delta_i\right)^{2(n-i+1)} f_i(z_i) + \tilde{a}^T\Gamma^{-1}(\Gamma Y z_n - \dot{\hat{a}})$$

$$-\frac{b_p}{\eta}\tilde{\phi}(\eta v_1 z_n + \dot{\hat{\phi}}) + \frac{1}{\gamma}\tilde{M}(\gamma\left|z_n\right| - \dot{\hat{M}})$$

$$= -\sum_{i=1}^{n} c_i\left(\left|z_i\right| - \delta_i\right)^{2(n-i+1)} f_i(z_i)$$

Thus, we proved the first statement of the theorem. The rest of the statements can be easily proven by following those of the proof of theorem 1, which is omitted here for space saving.

Remark 6.2: It is now clear that the two proposed control schemes to mitigate the hysteresis nonlinearities can be applied to many systems and may not necessarily be limited to the system (6.2). However, we should emphasize that our goal is to show the fusion of the hysteresis model with available control techniques in a simpler setting, which reveals its essential features.

6.4 Simulation Results

In this section, we illustrate the methodologies presented in the previous sections by using a simple nonlinear system described by

$$\dot{x} = a\frac{1-e^{-x(t)}}{1+e^{-x(t)}} + bw(t) \tag{6.23}$$

where w represents the output of the hysteresis nonlinearity. The actual parameter values are $a = 1$ and $b = 1$. Without control, i.e., $w(t) = 0$, (6.23) is unstable, because $\dot{x} = (1 - e^{-x(t)})/(1 + e^{-x(t)}) > 0$ for $x > 0$, and $\dot{x} = (1 - e^{-x(t)})/(1 + e^{-x(t)}) < 0$ for $x < 0$. The objective is to make the system state x follow the desired trajectory $x_d = 12.5\sin(2.3t)$.

In the simulations, the robust adaptive control law (6.9) of Scheme I was used, taking $c_1 = 0.9$, $\gamma = 0.2$, $\eta = 0.1$, $\Gamma = 0.1$, $\hat{\phi}(0) = 0.8/3$, $\hat{M}(0) = 2$, $\hat{x}(0) = 3.05$, $v(0) = 0$, $B_1 = 0.505$, $p(r) = e^{-6.7(0.1r-1)^2}$ for $r \in [10^{-6}, 50]$. The simulation results presented in Figures 6.1, 6.2 and 6.3 are comparisons of the system tracking errors, tracking performances and input signals, respectively, for the proposed control Scheme I and without considering the effects of hysteresis. For Scheme II, we chose the same initial values and $\delta = 0.35$. The simulation results presented in Figures 6.4, 6.5 and 6.6 are comparisons of the system tracking errors, tracking performances and input signals, respectively, for the proposed control Scheme II and without considering the effects of the hysteresis. Finally, comparing the solid blue curves in Figures 6.3 and 6.6, the possible chattering phenomenon is avoided in Figure 6.6. Clearly, all simulation results verify the proposed schemes and show their effectiveness.
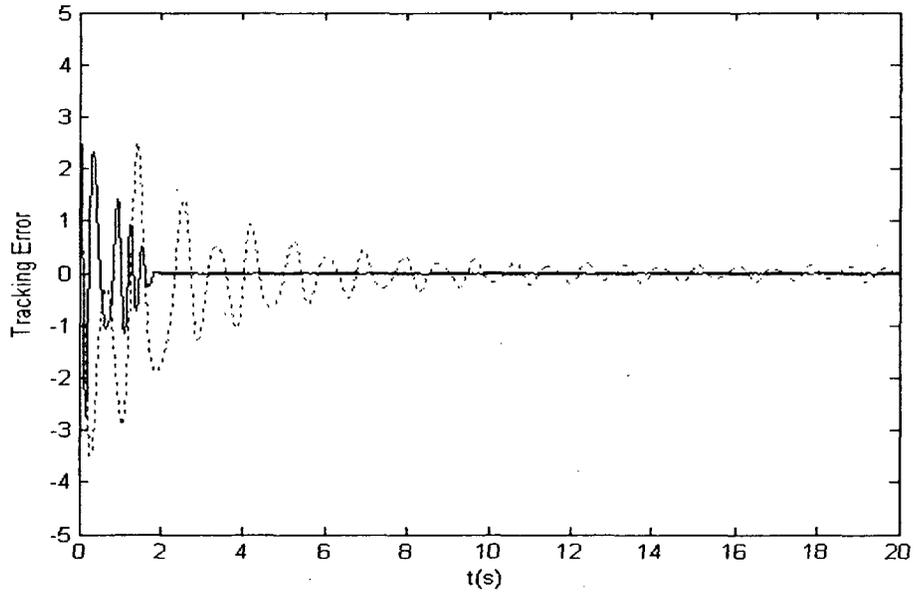
Figure 6.1 Tracking errors -- control Scheme I (solid line) and the scenario without

considering hysteresis effects (dotted line)
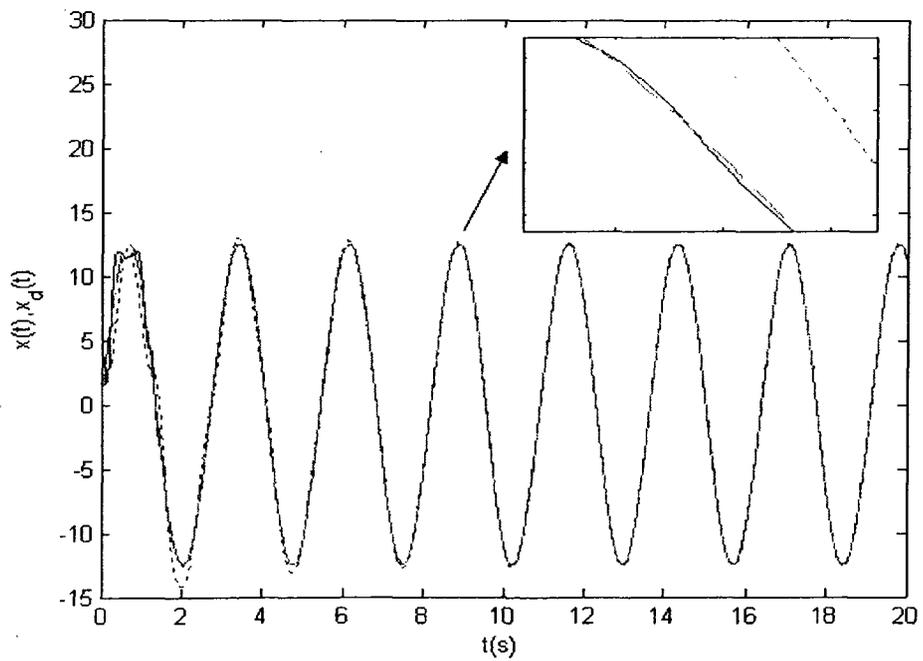
Figure 6.2 Tracking performances--Reference signal (dashed line); control Scheme I

(solid line) and the scenario without considering hysteresis effects (dotted line)
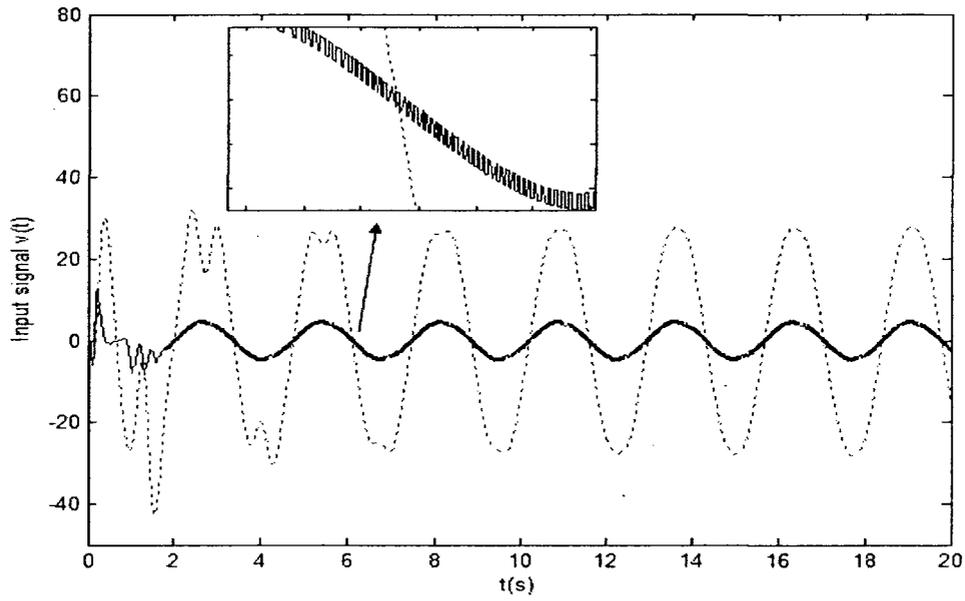
Figure 6.3 Input signals-- control Scheme I (solid line) and the scenario without

considering hysteresis effects (dotted line)
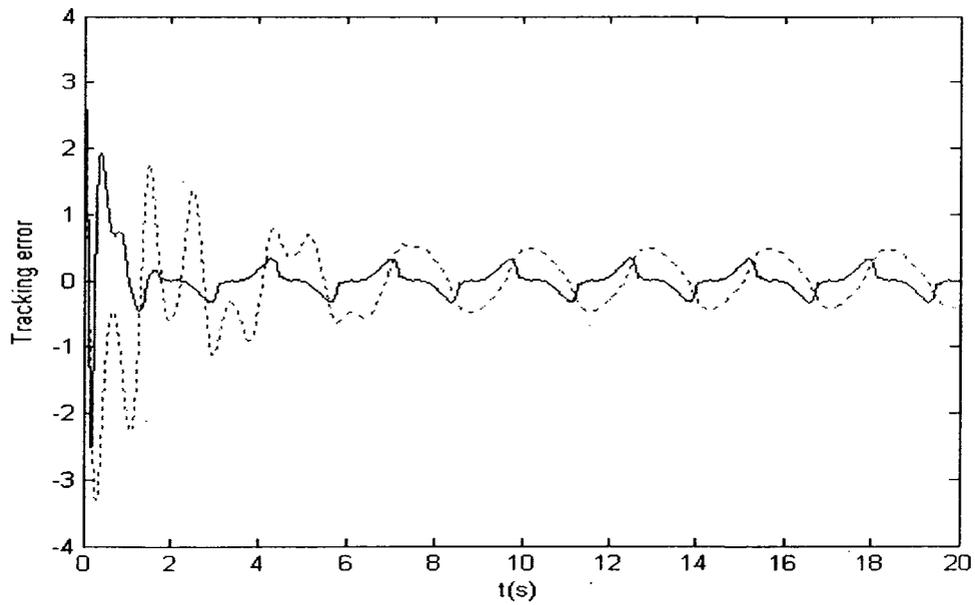
Figure 6.4 Tracking errors -- control Scheme II (solid line) and the scenario without

considering hysteresis effects (dotted line)
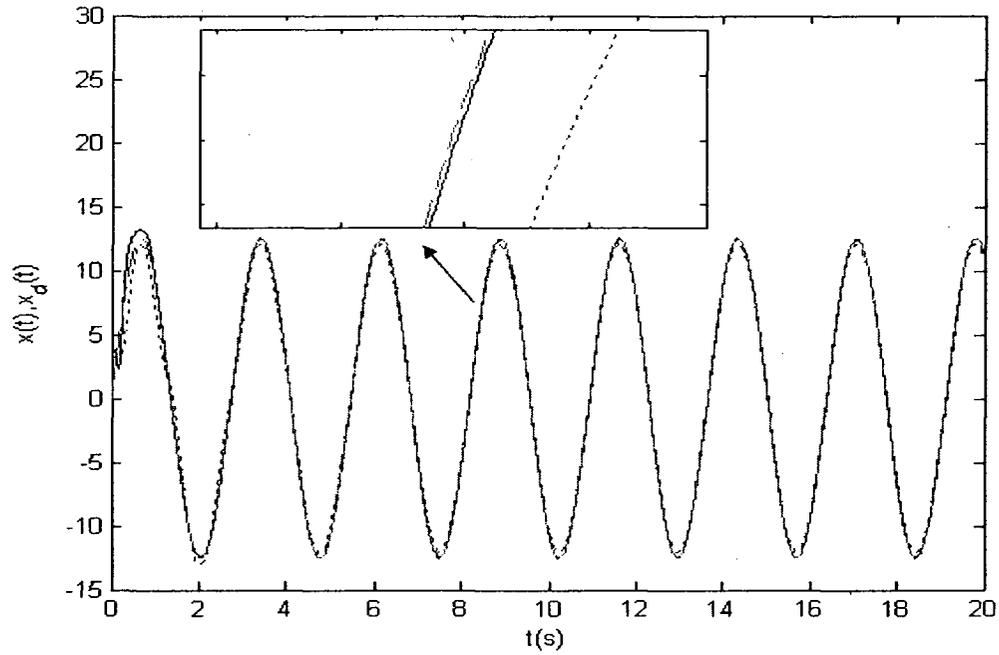
Figure 6.5 Tracking performances--Reference signal (dashed line); control Scheme II

(solid line) and the scenario without considering hysteresis effects (dotted line)
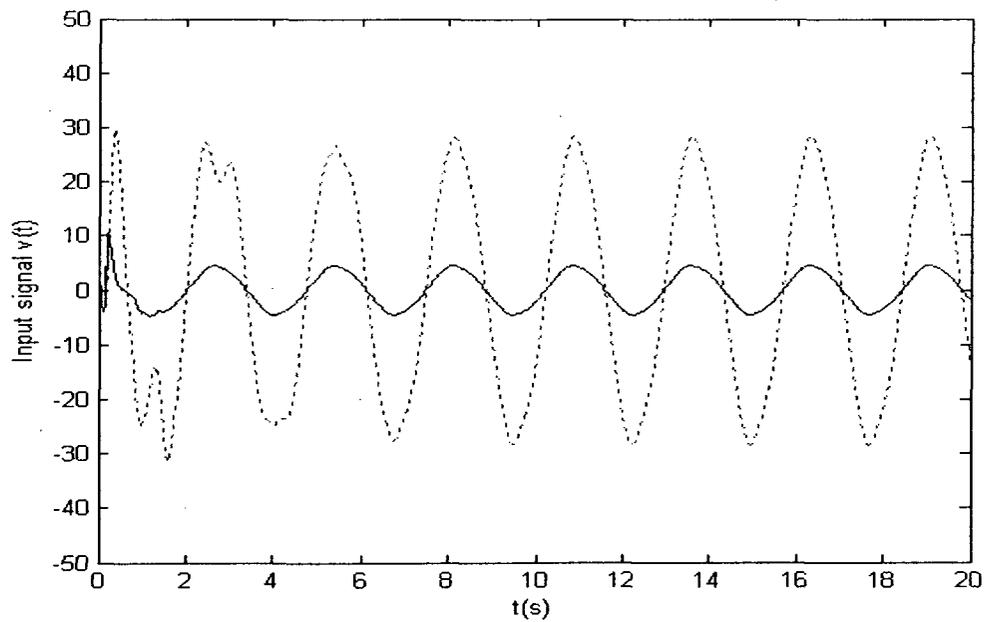
Figure 6.6 Input signals-- control Scheme II (solid line) and the scenario without

considering hysteresis effects (dotted line)

127

6.5 Conclusion

With the newly constructed hysteresis model, two backstepping control schemes were proposed to accomplish robust adaptive control tasks for a class of hysteretic nonlinear systems. The control schemes not only ensure stabilization and tracking of the hysteretic dynamic nonlinear systems, but also derive the transient performance in terms of L_2 norm of tracking error as an explicit function of design parameters. By constructing this class of hysteresis based on play-like operators and using the backstepping technique, this paper has addressed the challenge of how to fuse a suitable hysteresis model with available robust adaptive techniques to mitigate the effects of hysteresis, without constructing a complicated inverse operator for the hysteresis model.

CHAPTER 7

CONCLUSIONS AND RECOMMENDATIONS

7.1 Concluding Remarks

This dissertation research has extensively addressed fusing available adaptive control techniques with suitable hysteresis models to mitigate the effects of hysteresis preceding nonlinear systems, while guaranteeing the basic requirement of system stability and ensuring tracking precision. This has potential applications for smart material actuated systems, such as the SMA actuated robotic joint.

In this research, several adaptive control strategies have been developed for systems with different hysteresis model representations. Based upon the studies carried out in this dissertation, the following major conclusions are drawn:

- With the classical Duhem model, an observer-based adaptive control scheme for nonlinear systems has been proposed. The explicit solution to the Duhem model has been explored and a new formulation of the Duhem model has been presented as a linear model in series with a piecewise continuous nonlinear function. Due to the unavailability of hysteresis output, an observer-based adaptive controller incorporating a pre-inversion neural network compensator for the purpose of mitigating the hysteretic effects has been designed to guarantee the stability of the adaptive system and to track the error between the

129

position of the piezoelectric actuator and the desired trajectory with a desired precision.

- With the Prandtl-Ishlinskii model, an adaptive tracking control approach has been developed for a class of nonlinear systems in p-normal form by using the technique of adding a power integrator to address the challenge of how to fuse this hysteresis model with the control techniques to mitigate hysteresis, without necessarily constructing a hysteresis inverse;

- A class of hysteresis models based on play-like operators has been constructed. The play-like operators play the role of building blocks. From the point of view of an alternative one-parametric representation of the Preisach operator, the constructed model mathematically falls into PKP-type operators, as the Prandtl-Ishilinskii model falls into Preisach model. The new model has provided a possibility to mitigate the effects of hysteresis without necessarily constructing an inverse, which is the unique feature of this subclass model identified from the SSSL-PKP hysteresis model of the general class in the literature.

- With newly proposed hysteresis model using play-like operators, a sliding mode control strategy has been developed for nonlinear systems for tracking and stabilization purposes for the first time. An attempt has been made to fuse this hysteresis model with the available control techniques without necessarily constructing a complicated hysteresis inverse to guarantee the stability of the adaptive system and to track the desired trajectory with a desired precision.

- For the same hysteretic nonlinear system, two backstepping schemes have been proposed to accomplish robust adaptive control tasks. Such control schemes not

only ensure the stabilization and tracking of the hysteretic dynamic nonlinear systems, but also derive the transient performance in terms of the L_2 norm of tracking error as an explicit function of design parameters.

7.2 Recommendations for Future Studies

The following particular topics for future research in this area will be of academic and practical interests and can be conducted to extend the research work presented in this dissertation:

- For the systems considered in this thesis, it is possible and useful to further develop and extend the current adaptive control strategies to rate-dependent hysteresis exhibited in the systems.

- Experimental data will be used to verify the newly constructed model with play-like operators.

- Since this research focuses on the theoretical results of exploring how the advanced control techniques can be fused into the hysteretic systems to lay a foundation for the potential applications, applying the results presented in this work to smart material actuated systems and the experimental validations will be interesting and promising.

7.3 Publication list

The following papers have been published, accepted, or submitted. These papers were written under the guidance of my supervisors, Dr. W. F. Xie and Dr. C. -Y. Su. Some of the papers have co-authors who contributed through extensive discussions with

important recommendations, initial computer codes and simulations, or combinations of the above.

These papers are listed as follows:

1. Wen-Fang Xie, Jun Fu, Han Yao and, Chun-Yi Su, Adaptive Control of Piezoelectric Actuators with Unknown Hysteresis, in the book: *Adaptive Control*, I-Tech publisher, Vienna, 2009. (Chapter 12, pp257-276), ISBN: 978-953-7619-47-3.

2. Wen-Fang Xie, Jun Fu, Han Yao and Chun-Yi Su, Neural network-based adaptive control of piezoelectric actuators with unknown hysteresis, *International Journal of Adaptive Control and Signal Processing*, Vol. 23, 30-54, 2009.

3. Jun Fu, Ying Jin, Jun Zhao and G. M. Dimirovski, Robust Stabilization of a Class of Non-minimum-phase Nonlinear Systems in a Generalized Output Feedback Canonical Form, *International Journal of Adaptive Control and Signal Processing*, Vol. 23, 260-277, 2009.

4. Jun Fu, Wen-Fang Xie, Robust Adaptive Control of a Class of Nonlinear Systems Including Actuator Hysteresis Nonlinearities, Submitted to *International Journal of Dynamic Systems, Measurement and Control, Transactions of ASME*, 2009.

5. Jun Fu, Ying Jin, and Jun Zhao, Nonlinear Control of Power Converters: A New Adaptive Backstepping Approach, *Asian Journal of Control*, Vol.11, No.6, 2009 (To appear).

6. Jun Fu, Wen-Fang Xie, Robust Adaptive Control of a Class of Nonlinear Systems preceded hysteresis based on Play-like Operators, Submitted to *Information Sciences*, 2009.

7. Wen-Fang Xie, Jun Fu, Han Yao and Chun-Yi Su, Observer Based Control of Piezoelectric Actuators with Classical Duhem Modeled Hysteresis, *American Control Conference*, pp. 4221-4226, St-Louis, USA, 2009.

8. Jun Fu, Wen-Fang Xie, and Chun-Yi Su, Practically Adaptive Output Tracking Control of Inherently Nonlinear Systems Proceeded by Unknown Hysteresis, *Proc. of the 46th IEEE Conference on Decision and Control*, pp: 1326-1331, New Orleans, LA, USA, Dec. 12-14, 2007.

9. Jun Fu, Wen-Fang Xie, Chun-Yi Su and Jun Zhao, A new approach to practically adaptive output tracking control of nonlinear systems with uncontrollable unstable linearization, *American Control Conference*, 504-509, New York, USA, 2007.

10. Han Yao, Jun Fu, Wen-Fang Xie, and Chun-Yi Su, Neural Network Based Adaptive Control of Actuator with Unknown Hysteresis, 4297-4302, *American Control Conference*, New York, USA, 2007.

11. Jun Fu, Sining Liu, Wen-Fang Xie, Robust Invariance Control of a Class of Cascade Systems, *IEEE System, Man and Cybernetics*, 2820-2824, Montreal, Canada, 2007.

12. Jun Fu, Wen-Fang Xie, Robust Adaptive Control of Nonlinear Systems with Unknown Hysteresis Based on Play-like Operators, *Proc. of the 48th IEEE Conference on Decision and Control*, Shanghai, China, 2009 (Accepted).

REFERENCES

[1] R. C. Smith, *Smart Material Systems: Model Development*, SIAM, Philadelphia, 2005.

[2] D. J. Leo, *Engineering Analysis of Smart Material Systems*, John Wiley & Sons, Inc. 2007.

[3] B. P. Kramer and M. Fussenegger, Hysteresis in a Synthetic Mammalian Gene Network, *Proceedings of National Academy of Science of the United States of America (PNAS)*, Vol. 102, No. 27, pp. 9517-9522, 2005.

[4] H. T. Banks and R. C. Smith, Hysteresis Modeling in Smart Material Systems, *J. Appl. Mech. Eng*, Vol. 5, pp. 31-45, 2000.

[5] X. Tan and R. Iyer, Modeling and Control of Hysteresis, *IEEE Control Systems Magazine*, Vol. 29, No. 1, pp. 26-29, 2009.

[6] X. Tan, *Control of Smart Actuator*, Ph. D. dissertation, University Maryland, College Park, MD, 2002.

[7] D. C. Jiles, and D. L. Atherton, Theory of Ferromagnetic Hysteresis, *J. Magnet. Magn. Mater*, Vol. 61, pp. 48-60, 1986.

[8] M. A. Krasnosel skii and A. V. Pokrovskii, *Systems with Hysteresis*, New York: Springer-Verlag, 1980.

[9] I. D. Mayergoyz. *Mathematical Models of Hysteresis*, Spring-Verlag, New York, 1991.

[10] M. Brokate and J. Sprekels, *Hysteresis and Phase Transitions*, Spring-Verlag, New York, 1996.

[11]   K. Kuhnen and P. Krejci, Compensation of Complex Hysteresis and Creep Effects in Piezoelectrically Actuated Systems-A New Preisach Modeling Approach, *IEEE Transactions on Automatic Control*, Vol. 54, No. 3, pp. 537-550, 2009.

[12]   R. Iyer and X. Tan, Control of Hysteretic Systems through Inverse Compensation: Inversion Algorithms, Adaptation, and Embedded Implementation, *IEEE Control Systems Magazine*, Vol. 29, No.1, pp. 83-99, 2009.

[13]   A. Visintin, *Differential Models of Hysteresis*. New York: Springer-Verlag, 1994.

[14]   J. W. Macki, P. Nistri, and P. Zecca, Mathematical Models for Hysteresis, *SIAM Review*, Vol. 35, No. 1, pp. 94-123, 1993.

[15]   B. D. Coleman and M. L. Hodgdon, On a Class of Constitutive Relations for Ferromagnetic Hysteresis, *Arch. Rational Mech. Anal.*, Vol. 99, No. 4, pp. 375-396, 1987.

[16]   R. Banning, W. L. Koning, J. J. Adriaens, and R. K. Koops, State-space Analysis and Identification for a Class of Hysteretic Systems, *Automatica*, Vol. 37, No. 12, pp. 1883-1892, 2001.

[17]   C.-Y. Su, Y. Stepanenko, J. Svoboda, and T. P. Leung, Robust Adaptive Control of a Class of Nonlinear Systems with Unknown Backlash-Like Hysteresis, *IEEE Transactions on Automatic Control*, Vo. 45, No. 12, pp. 2427-2432, 2000.

[18]   D. B. Ekanayake and R. V. Iyer, Study of a Play-like Operator, *Physica B: Condensed Matter*, Vol. 403, No. 2-3, pp. 456-459, 2008.

[19]   Y. K. Wen, Method for Random Vibration of Hysteretic Systems. *Journal of the Engineering Mechanics Division*, Vo. 102, No. 2, pp. 49-106, 1976.

[20] B. P. Spencer, Reliability of Randomly Excited Hysteresis Structures. *Lecture Notes in Engineering*, New York: Springer-Verlag, 1986.

[21] P. M. Sain, M.K. Sain, and B. F. Spencer, Models for Hysteresis and Application to Structural Control, *Proc. American Control Conf.*, Albuquerque, USA, pp. 16-20, 1997.

[22] L. O. Chua and K. A. Stromsmoe, Mathematical Model for Dynamic Hysteresis Loops, *International Journal of Engineering Science*, Vol. 9, pp. 435-450, 1971.

[23] L. O. Chua and S. C. Bass. A Generalized Hysteresis Model. *IEEE Transactions on Circuit Theory*, Vol. 19, No. 1, pp. 36-48, 1972.

[24] D. C. Jiles and J. B. Thoelke, Theory of Ferromagnetic Hysteresis: Determination of Model Parameters from Experimental Hysteresis Loops Magnetics, *IEEE Transactions on Magnetics*, Vol. 25, No. 5, pp. 3928 – 3930, 1989.

[25] Q. Q. Wang, *Robust Adaptive Control of a Class of Nonlinear Systems including Actuator Hysteresis with Prandtl-Ishlinskii Presentations*, PhD thesis, Concordia University, 2006.

[26] P. Weiss, J. de Freundereich, Etude de l'aimantation initiale en function de la temperature, *Arch. Sci. Phys. Nat.* , Vol. 42, pp. 449, 1916.

[27] P. Preisach, Uber die magnetische Nachwirkung, *Zeit. fur Physik*, vol. 94, pp. 277-302, 1935.

[28] S. Mittal and C.H Menq, Hysteresis Compensation in Electromagnetic Actuators through Preisach Model Inversion, *IEEE Transactions on Mechatronics*, Vol. 5, No. 4, pp. 394-409, 2000.

[29] Y. F. Wang, *Methods for Modeling and Control for Systems with Shape Memory Alloys Actuators*. PhD thesis, Concordia University, 2007.

[30] T. Banks, A.J. Kurdila, and G.Webb, Identification of Hysteretic Control Influence Operators Representing Smart Actuators, Part I: Formulation, *Mathematical Problems in Engineering*, Vol. 3, No. 4, pp. 287–328, 1997.

[31] W. Galinaities, *Two Methods for Modeling Scalar Hysteresis and Their Using in Controlling Actuators with Hysteresis*, PhD thesis, Blacksburg, Virginia, USA, 1999.

[32] G. Tao and P.V. Kokotovic, Adaptive Control of Plants with Unknown Hysteresis, *IEEE Trans. on Automatic Control*, Vol. 40, No. 2, pp. 200-212, 1995.

[33] P. Ge, and M. Jouaneh, Tracking Control of a Piezoceramic Actuator, *IEEE Trans. on Control Systems Technology*, Vol. 4, No. 3, pp. 209-216, 1996.

[34] S. Mittal and C-H. Meng, Hysteresis Compensation in Electromagnetic Actuators through Preisach Model Inverse, *IEEE/ASME Trans. Mechatron.*, Vol. 5, No. 4, pp. 394-409, 2000.

[35] D. Croft, G. Shed, and S. Devasia, Creep, Hysteresis, and Vibration Compensation for Piezoactuators: Atomic Force Microscopy Application, *J. of Dynamic Systems, Measurement, and Control*, Vol. 123, pp. 35-43, 2001.

[36] G. Webb, A. Kurdila, and D. Lagoudas, Adaptive Hysteresis Model for Model Reference Control with Actuator Hysteresis, *J. Guidance, Control and Dynamics*, Vol. 23, No. 3, pp. 459-465, 2000.

[37] P. Krejci and K. Kuhnen, Inverse Control of Systems with Hysteresis and Creep, *IEE Proc.-Control Theory Appl.*, Vol. 148, pp. 185-192, 2001.

[38] J. D. Wei and C. T. Sun, Constructing Hysteresis Memory in Neural Networks, *IEEE Trans. System, Man, and Cybernetics-part B: Cybernetics*, Vol. 30, No. 4, pp. 601-609, 2000.

[39] R. R. Selmic and F. L. Lewis, Backlash Compensation in Nonlinear Systems Using Dynamics Inversion by Neural Networks, *Proc. IEEE Int. conf. Control Appliccations*, pp. 1163-1168, 1999.

[40] C-L. Hwang, C. Jan, and Y-H. Chen, Piezomechanics Using Intelligent Variable-Structure Control, *IEEE Trans. Industrial Electronics*, Vol.48, pp. 47-59, 2001.

[41] C-L. Hwang and C. Jan, A Reinforcement Discrete Neuro-adaptive Control for Unknown Piezoelectric Actuator Systems with Dominant Hysteresis, *IEEE Trans. Neural Networks*, Vol. 14, No.1, pp. 66-78, 2001.

[42] T. Lu, Y. H. Tan, and C.-Y. Su, Pole Placement Control of Discrete Time Systems Proceeded with Hysteresis via Dynamic Neural Network Compensator Intelligent Control, *Proc. of the IEEE international symposium*, pp. 228-233, 2002.

[43] T. Nakaguchi, S. Isome, K. Jin'no, and M. Tanaka, Box Puzzling Problem Solver by Hysteresis Neural Networks, *IEICE Trans. Fundamentals*, Vol.E84-A, No.9, pp. 2173-2181, 2001.

[44] M. Tsai and J. Chen, Robust Tracking Control of a Piezoactuator Using a New Approximate Hysteresis Model, *Tran. of ASME*, Vol. 125, pp. 96-102, 2003.

[45] T. E. Pare, Robust Stability and Performance Analysis of Systems with Hysteresis Nonlinearities, *Proc. of American Control Conference*, Philadolphia, Pennsylvania, pp.1904-1908, 1998.

[46] R. B. Gorbet, *Control of Hysteresis Systems with Preisach Representations*, Ph. D Thesis, Waterloo, Ontario, Canada, 1997.

[47] F. Ikhouane and J. Rodellar, *Systems with Hysteresis-Analysis, Identification and Control using the Bouc-Wen Model*, John Wiley, 2007.

[48] C. -Y. Su, Q. Wang, X. Chen, and S. Rakheja, Adaptive Variable Structure Control of a Class of Nonlinear Systems with Unknown Prandtl-Ishlinskii Hysteresis, *IEEE Trans. Automat. Contr.*, Vol. 50, No. 12, pp. 2069-2074, 2005.

[49] Q. Wang and C. -Y. Su, Robust Adaptive Control of a Class of Nonlinear Systems Including Actuator Hysteresis with Prandtl-Ishlinskii Presentations, *Automatica*, Vol. 42, No. 5, pp. 859-867, 2006.

[50] R. Bouc, Model Mathematical Hysteresis, *Acoustica*, Vol. 24, No. 1, pp. 16-25, 1971.

[51] P. Dahl, Solid Friction Damping of Mechanical Vibrations, *AIAA Journal*, Vol. 14, pp. 1675-1682, 1976.

[52] C. C. de Wit, H. Olsson, K. J. Astrom, and P. Lischinsky, A New Model for Control of Systems with Friction, *IEEE Transactions on Automatic Control*, Vol. 40, No. 3, pp. 419-425, 1995.

[53] J. Swevers, F. Al-Bender, C. G. Ganseman, and T. Prajogo, An Integrated Friction Model Structure with Improved Presliding Behavior for Accurate Friction Compensation, *IEEE Transactions on Automatic Control*, Vol. 45, No. 4, pp. 675-686, 2000.

[54] C. Jan, and C. L. Hwang, Robust Control Design for a Piezoelectric Actuator System with Dominant Hysteresis, *IECON*, Vol. 3, pp. 1515-1520, 2000.

[55] S. S. Ge, and C. Wang, Direct Adaptive NN Control of a Class of Nonlinear Systems, *IEEE Transactions on Neural Networks,* Vol. 13, No. 1, pp. 214-221, 2002.

[56] H. Yao, W.F. Xie, and C. Ye, A Composite Approach to Adaptive Neural Networks Control of Unknown Flexible Joint Robots, *2006 International Conference on Dynamics, Instrumentation and Control (CDIC'06)*, Queretaro, Mexico, August 13-16, 2006.

[57] D. Makaveev, L. Dupre, and J. Melkebeek, Neural-Network-Based Approach to Dynamic Hysteresis for Circular and Elliptical Magnetization in Electrical Steel Sheet, *IEEE Transactions on Magnetics,* Vol. 38, No.5, pp. 3189-3191, 2002.

[58] A. J. K rener, and A. Isidori, Linearization by Output Injection and Nonlinear Observer, *System & Control Letter,* Vol. 3, pp. 47-52, 1983.

[59] A.J. Krener, and W. Kang, Locally Convergent Nonlinear Observers, *SIAM J. Control Optim,* Vol. 42, No. 1, pp. 157-177, 2003.

[60] W. F. Xie, Sliding-Mode-Observer-Based Adaptive Control for Servo Actuator with Friction, *IEEE Transactions on Industrial Electronics,* Vol. 54, No. 3, pp. 1517-1528, 2007.

[61] K. Hornik, M. Stinchcombe, et al, Multilayer Feedforward Networks Are Universal Approximators, *Neural Networks*, Vol. 2, pp. 359-366, 1989.

[62] M. Kuczmann and A. Ivanyi, A New Neural-Network-Based Scalar Hysteresis Model, *IEEE Transactions on Magnetics*, Vol. 38, No. 2, pp. 857-860, 2002.

[63] C.-Y. Su, and Y. Stepanenko, Redesign of Hybrid Adaptive/Robust Motion Control of Rigid-Link Electrically-Driven Robot Manipulators, *IEEE Transactions on Robotics and Automation,* Vol. 14, No. 4, pp. 651-655, 1998.

[64] W. Lin and C. J. Qian, Adding One Power Integrator: A Tool for Global Stabilization of High-Order Cascade Nonlinear Systems. *Systems & Control Letters*, Vol. 39, No. 5, pp. 339-351, 2000.

[65] W. Lin and C. J. Qian, Adaptive Regulation of High-Order Lower-Triangular Systems: an Adding a Power Integrator Technique, *Systems & Control Letters*, Vol. 39, No. 5, pp. 353-364, 2000.

[66] C. J. Qian and W. Lin, Practical Output Tracking of Nonlinear Systems with Uncontrollable Unstable Linearization, *IEEE Transactions on Automatic Control*, Vol. 47, No. 1, pp. 21-36, 2002.

[67] W. Lin and C. J. Qian, Adaptive Control of Nonlinearly Parameterized Systems: A Nonsmooth Feedback Framework, *IEEE Transactions on Automatic control*, Vol. 47, No. 5, pp. 757-774, 2002.

[68] W. Lin and C. J. Qian, Adaptive Control of Nonlinearly Parameterized Systems: the Smooth Feedback Case. *IEEE Transactions on Automatic control*, Vol. 47, No. 8, pp. 1249-1266, 2002.

[69] W. Lin and R. Pongvuthithum, Adaptive Output Tracking of Inherently Nonlinear Systems with Nonlinear Parameterization, *IEEE Transactions on Automatic control*, Vol. 48, No. 10, pp. 1737-1749, 2003.

[70] D. B. Dicic, P. V. Kokotovic, A Scaled Feedback Stabilization of Power Integrator Triangular Systems, *Systems & Control Letters*, Vol. 54, pp. 645-653, 2005.

[71] D. Z. Cheng and W. Lin. On p-normal Forms of Nonlinear Systems. *IEEE Transactions on Automatic control*, Vol. 48, No. 7, pp. 1242-1248, 2003.

[72] A. Astolfi and R. Ortega, Immersion and Invariance: a New Tool for Stabilization and Adaptive Control of Nonlinear Systems, *IEEE Transactions on Automatic Control*, Vol. 48, No. 4, pp. 590-606, 2003.

[73] D. Karagiannis and A. Astolfi, Nonlinear Adaptive Control of Systems in Feedback Form: an Alternative to Adaptive Backstepping, *IFAC Symposium on Large Scale Systems*, Osaka, pp. 71-76, 2004.

[74] R. V. Iyer, X. Tan, and P. S. Krishnaprasad, Approximate Inversion of the Preisach Hysteresis Operator with Application to Control of Smart Actuators, *IEEE Transactions on Automatic Control*, Vol. 50, No. 6, pp. 798-810, 2005.

[75] J. Fu, W. F. Xie, and C.-Y. Su, Practically Adaptive Output Tracking Control of Inherently Nonlinear Systems Proceeded by Unknown Hysteresis, *Proc. of the 46th IEEE Conference on Decision and Control*, pp. 1326-1331, New Orleans, LA, USA, 2007.

[76] A. Isidori, *Nonlienar Control Systems: an Introduction*, 2nd ed. Berlin, Germany: Springer-Verlag, 1989.

[77] H. Janocha, D. Pesotski, and K. Kuhnen, FPGA-Based Compensator of Hysteretic Actuator Nonlinearities for Highly Dynamic Applications, *IEEE/ASME Transactions on Mechatronics*, Vol. 13, No. 1, pp. 112-116, 2008.

[78] V. A. Zorich, *Mathematical Analysis*, New York, Springer-Verlag, 2004.

[79] P. Krejci, *Hysteresis, Convexity and Dissipation in Hyperbolic Equations*, Gakuto Int. Series Math. Sci. & Appl. Vol. 8, Gakkotosho, Tokyo, 1996.

[80]   V. Popov, *Hyperstability of Control Systems*, Berlin, Germany: Springer-Verlag, 1973.

[81]   M. Kristi, I. Kanellakopoulos and P. V. Kokotovic, *Nonlinear and Adaptive Control Design*. New York: Wiley, 1995.

[82]   J. Zhou, C. Y. Wen and Y. Zhang, Adaptive Backstepping Control of a Class of Uncertain Nonlinear Systems with Unknown Backlash-like Hysteresis, *IEEE Transactions on Automatic Control*, Vol. 49, No. 10, pp. 1751-1757, 2004.

[83]   W.-F. Xie, J. Fu, H. Yao, and C. -Y. Su, Neural network-based adaptive control of piezoelectric actuators with unknown hysteresis, *International Journal of Adaptive Control and Signal Processing*, Vol. 23, pp. 30-54, 2009.

[84]   A. Ivanyi, *Hysteresis Models in Electromagnetic Computation*, Akademiai Kiado, Budapest, 1997.